

# Biological treatment of process water of an amine based CO<sub>2</sub> - capture plant

Master thesis

**Ingrid Hauser**

Supervisor:

Prof. Kjetill Østgaard

Co-Supervisor:

Prof. Dr. Georg Gübitz



Department of Biotechnology  
Norwegian University for Science and Technology  
Institute of Environmental Biotechnology  
Graz University of Technology

Graz, June 2011

# Statutory Declaration

I declare that I have authored this thesis independently, that I have not used other than the declared sources / resources, and that I have explicitly marked all material which has been quoted either literally or by content from the used sources.

Date \_\_\_\_\_ Signature \_\_\_\_\_



# Acknowledgement

I would like to thank Professor Kjetill Østgaard and Aslak Einbu for giving me the opportunity to work on this project, and for their supportive guidance throughout this work. It was a great experience working under such enthusiastic scientific dedication and needless to say it was also a personal enrichment living in Norway during this time.

I also want to thank my colleagues at the Biotechnology Department at NTNU for their wonderful hospitality, and for the fruitful discussions. I especially want to thank Julie Anita Skjæran and Anna Synnøve Ødegaard Røstad for their kind assistance when settling in both in the lab and privately - Takk for meg!

In Graz, I would like to thank Professor Gübitz for his assistance and feedback. For combating my numerous computational issues I have to give thanks to Harald Dermutz, as well as to Bettina Halwachs. I also want to thank both of them and especially my mother for proof-reading this work.

Besides those colleagues and friends directly contributing to this work, I also want to thank my family at home, Andreas, Martin, Michael and Andrea for visiting me during my stay in Norway. This was literally very refreshing and helpful in distracting me when necessary, although I also met many new friends from all over the world for equally pleasant distractions. Apart from being grateful for discovering Norwegian culture with Anja, Anne Bente and Marie, I also want to thank Pierre-Yves for inspiring me and lighting up my days, especially during the dark wintertime in Norway - Merci beaucoup!

Last, but definitely not least, I want to express my gratitude to my parents. Their continuous moral support and their unconditional back-up are invaluable to me, as well as their financial support - Thank you!

I would like to dedicate this master thesis to my grandparents.

# Kurzfassung

Die Menschheit wird sich in naher Zukunft zahlreichen Herausforderungen stellen müssen, darunter auch der globalen Erderwärmung. Der weltweite Temperaturanstieg ist größtenteils auf anthropogene Aktivitäten zurückzuführen, die seit der industriellen Revolution zu einer steten Erhöhung der Treibhausgase, allen voran  $\text{CO}_2$ , in der Atmosphäre beigetragen haben. Noch dazu ist  $\text{CO}_2$  in der Atmosphäre nur schwer abbaubar, daher ist es notwendig die globale  $\text{CO}_2$  Emission so rasch wie möglich einzudämmen. Mit der  $\text{CO}_2$ -Abscheidungs und -Lagerungs Technologie wird  $\text{CO}_2$  von erhöhten Belastungspunkten, wie Kohlekraftwerken, abgeschieden und in tiefen unterirdischen Gesteinsschichten gelagert. In einer auf Aminabsorption basierten  $\text{CO}_2$ -Abscheidung wird meist MEA (Monoethanolamin) als Absorptionsmittel eingesetzt, aber auch die Amine AMP (2-Amino-2-methylpropan-1-ol), MDEA (N-Methyldiethanolamin), DEA (Diethanolamin) und Piperazin finden Anwendung. Durch den Absorptionsprozess entstehen jedoch Abfallprodukte der Amine, die üblicherweise in einem Rückgewinner (Reclaimer) abgetrennt werden und in folge als gefährliche Abfälle dementsprechend behandelt werden müssen. Eine alternative Abfallbehandlung bietet der biologische Abbau, beziehungsweise die biologische Stickstoffentfernung.

Zu Beginn wurden die toxischen Wirkungen des Rückgewinnungsabfalles und der oben angeführten Amine mit nitrifizierenden und denitrifizierenden Bakterienkulturen in Laborversuchsanlagen einzeln bestimmt. Dabei stellte sich heraus, dass die nitrifizierende Bakterienkultur eine unterschiedliche Sensitivität aufwies und die denitrifizierende Bakterienkultur relativ unbeeinflusst war. In beiden Kulturen wurde jedoch eine verminderte Aktivität nach Erholung von der Piperazin-Exponierung gemessen.

Der biologische Abbau des Rückgewinnungsabfalles als einzige Kohlenstoffquelle im Vor-Denitrifikationssystem war erfolgreich. Nach zweiwöchiger Adaptionszeit war die Denitrifikationskultur imstande sämtliches MEA zu Ammonium abzubauen, und durch externe Zufuhr von Nitrat wurde vollständige Denitrifikation erreicht. Die Nitrifikationskultur benötigte etwa 1 Woche länger um sich zu adaptieren. Abgesehen vom MEA Abbau wurde auch weiterer chemischer Sauerstoffbedarf (CSB) des Rückgewinnungsabfalles abgebaut. Ausgewählte Abbauprodukte wurden mittels Flüssigchromatographie - Massenspektrometrie (LC-MS) quantifiziert, wobei sich herausstellte, dass ein Großteil bereits im Denitrifikationsreaktor abgebaut wurde, aber auch im Nitrifikationsreaktor. Insgesamt belief sich die Effizienz der Stickstoffentfernung bei MEA auf 97%, beim Gesamtstickstoff auf

76% und die Effizienz der Entfernung von organischen Stoffen auf 73%. Daher scheint es durchaus möglich zu sein den Rückgewinnungsabfall biologisch, unter Nitratzufuhr zu behandeln, oder auch die Richtung der partiellen Nitrifikation zu Nitrit und anschließender Nitritdenitrifikation anzustreben.

## Abstract

Mankind is facing major challenges in this century, the most adverse being the global warming. Despite worldwide concern, this rise in temperature is due to an increased amount of anthropogenic greenhouse gases, especially of CO<sub>2</sub> since the industrial revolution - a man-made sword of Damocles. CO<sub>2</sub> has a long persistence in the atmosphere and therefore it is of significant importance to set actions to minimize the global CO<sub>2</sub> emission. In the CO<sub>2</sub> capture and storage technology, CO<sub>2</sub> is captured from large point sources and safely stored in the underground. In an amine based CO<sub>2</sub> capture facility MEA (monoethanolamine) is most commonly used as an absorbent, although other amines, such as AMP (2-amino-2-methylpropan-1-ol), MDEA (N-methyldiethanolamine), DEA (diethanolamine) and piperazine are also used. During the process amine waste is generated, whereas these degradation products are commonly separated in an evaporative reclaimer and treated as hazardous chemical waste. An alternative method to treat this waste is by biological degradation, respectively biological nitrogen removal.

Initially, the reclaimer waste and the abovementioned amines were tested for toxicity on both nitrifying and denitrifying biofilms in separate lab bench scale bioreactors. The results revealed varying sensitivity of the nitrifying culture and an almost unaffected response from the denitrifying culture.

The biological degradation of reclaimer waste as a sole carbon source in the pre-denitrification system was successful. After 2 weeks adaptation, the denitrifying reactor was able to degrade all MEA to ammonium and with external addition of nitrate the denitrifying culture achieved total denitrification. The nitrifying reactor needed approximately 1 week longer for adaptation. Besides the degradation of MEA, also further chemical oxygen demand (COD) could successfully be removed from the reclaimer waste. Selected degradation products were quantified by liquid chromatography - mass spectrometry (LC-MS), whereas the majority was readily degraded in the denitrifying reactor, whilst others were further degraded in the nitrifying reactor. Overall, the nitrogen removal efficiency of MEA achieved 97%, of total nitrogen 76% and the removal efficiency of organic matter 73%. Thus, it generally appears feasible to apply biological treatment on the reclaimer waste by adding nitrate or considering the process of partial nitrification to nitrite and nitrite denitrification.

# Contents

<b>Abbreviations</b>	<b>viii</b>
<b>1 Introduction</b>	<b>1</b>
1.1 The Carbon Dioxide Problem . . . . .	1
1.2 Carbon Dioxide Capture . . . . .	3
1.2.1 Reclaimer waste . . . . .	5
1.2.2 Amines used in CCS . . . . .	6
1.3 Environmental impact of amines . . . . .	7
1.4 Biodegradation of xenobiotics . . . . .	9
1.4.1 Nitrification . . . . .	12
1.4.2 Denitrification . . . . .	18
1.4.3 Combined Nitrification and Denitrification in Pre-Denitrification configuration . . . . .	21
1.5 Moving Bed Biofilm reactors . . . . .	22
1.6 Previous studies . . . . .	23
1.7 Scope of this work . . . . .	25
<b>2 Materials and Methods</b>	<b>26</b>
2.1 Chemical analysis . . . . .	26
2.1.1 Hach-Lange assays . . . . .	26
2.1.2 Fluorescamine assay . . . . .	30
2.1.3 LC-MS . . . . .	30
2.2 Reclaimer waste analysis . . . . .	31
2.3 Biofilm development . . . . .	32
2.3.1 Inoculum . . . . .	32
2.3.2 Medium . . . . .	32
2.3.3 Reactor . . . . .	32
2.3.4 Monitoring . . . . .	35
2.4 Nitrification . . . . .	35
2.4.1 Inoculum . . . . .	35

---

2.4.2	Medium . . . . .	35
2.4.3	Reactor . . . . .	36
2.4.4	Monitoring . . . . .	37
2.4.5	Acute Toxicity Test . . . . .	38
2.5	Denitrification . . . . .	40
2.5.1	Inoculum . . . . .	40
2.5.2	Medium . . . . .	41
2.5.3	Reactor . . . . .	42
2.5.4	Monitoring . . . . .	43
2.5.5	Acute Toxicity Test . . . . .	43
2.6	Pre-Denitrification System . . . . .	45
2.6.1	Inoculum . . . . .	45
2.6.2	Medium . . . . .	46
2.6.3	Reactors . . . . .	47
2.6.4	Monitoring . . . . .	50
2.6.5	Reclaimer waste as a sole carbon source . . . . .	51
2.6.6	Acute Toxicity Test . . . . .	52
2.7	Waste handling . . . . .	53
<b>3</b>	<b>Results and Discussion</b>	<b>54</b>
3.1	Reclaimer waste analysis . . . . .	54
3.1.1	LC-MS analysis . . . . .	54
3.1.2	Hach-Lange analysis . . . . .	55
3.2	Biofilm development . . . . .	55
3.3	Inhibition of nitrification . . . . .	56
3.3.1	Biofilm history . . . . .	56
3.3.2	Acute Toxicity Test . . . . .	57
3.3.3	Discussion . . . . .	67
3.4	Inhibition of denitrification . . . . .	71
3.4.1	Acute Toxicity Test . . . . .	71
3.4.2	Discussion . . . . .	77
3.5	Total pre-Denitrification System . . . . .	77
3.5.1	Reclaimer waste as a sole carbon source . . . . .	77
3.5.2	Summation . . . . .	94
3.6	Summary and Outlook . . . . .	96
<b>4</b>	<b>Conclusions</b>	<b>99</b>

---

<b>Bibliography</b>	<b>101</b>
<b>Appendices</b>	<b>107</b>
<b>A Biofilm development - Nitrifying activity</b>	<b>108</b>
<b>B Reclaimer waste analysis - LC-MS</b>	<b>109</b>
<b>C Acute toxicity test - Nitrifying culture</b>	<b>111</b>
<b>D Pre-Denitrification</b>	<b>116</b>
D.1 Rawdata . . . . .	116
D.2 Removal efficiency . . . . .	118
D.3 Calculation of COD . . . . .	120

# List of Figures

1.1	Atmospheric concentrations of carbon dioxide over the last 10 000 years . . .	1
1.2	Global average radiative forcing estimates and ranges in 2005 . . . . .	2
1.3	CO <sub>2</sub> capture and storage (CCS) . . . . .	3
1.4	Post-combustion CO <sub>2</sub> capture by amine absorption . . . . .	4
1.5	Process flow diagram for a typical MEA CO <sub>2</sub> capture process . . . . .	6
1.6	Main sources of possible amine emissions of an amine based CO <sub>2</sub> capture process . . . . .	8
1.7	Microbial community composition of the autotrophic nitrifying biofilm . . .	15
1.8	Fluorescence in situ hybridization combined with microsensor measurements of a vertical biofilm . . . . .	16
1.9	Inhibition of the nitrification process as a function of NH <sub>3</sub> , HNO <sub>2</sub> and pH .	17
1.10	Modular organization of denitrification . . . . .	19
1.11	Set-up and flow scheme of the pre-denitrification system . . . . .	21
1.12	Enlarged Kaldnes K1 carriers . . . . .	22
2.1	Ammonium-N recordings according to the LCK 303 Ammonium-Nitrogen assay as a function of ammonium-N concentration . . . . .	29
2.2	Nitrite-N recordings according to the LCK 341 Nitrite-Nitrogen assay as a function of nitrite-N concentration . . . . .	29
2.3	Experimental set-up of the nitrification reactor . . . . .	34
2.4	Set-up of the aeration for the nitrification reactor . . . . .	34
2.5	Experimental set-up of the nitrification reactor . . . . .	37
2.6	Set-up of the aeration for the nitrification reactor . . . . .	38
2.7	Flow schema of the acute toxicity assay . . . . .	39
2.8	Set-up of the deaeration for the denitrification water . . . . .	42
2.9	Experimental set-up of the denitrification reactor . . . . .	43
2.10	Flow schema of the acute toxicity assay . . . . .	44
2.11	Experimental set-up of the pre-denitrification system . . . . .	47
2.12	Set-up of the aeration for the nitrification reactor . . . . .	48
2.13	Flow scheme of the pre-denitrification system . . . . .	50

---

2.14	Operational timeline of the pre-denitrification system in days . . . . .	51
2.15	Flow schema of the acute toxicity assay . . . . .	52
3.1	Gained COD during the development of nitrifying biofilm on Kaldnes K1 carriers . . . . .	56
3.2	Experiment 1: Acute toxicity of reclaimer waste . . . . .	58
3.3	Experiment 2: Acute toxicity of reclaimer waste . . . . .	59
3.4	Experiment 2: Acute toxicity of MEA on the nitrifying culture . . . . .	60
3.5	EC <sub>50</sub> of reclaimer waste, as well as MEA on the nitrifying culture . . . . .	61
3.6	Experiment 3: Acute toxicity of piperazine on the nitrifying culture . . . . .	62
3.7	Experiment 3: Acute toxicity of AMP on the nitrifying culture . . . . .	64
3.8	Experiment 3: Acute toxicity of DEA on the nitrifying culture . . . . .	65
3.9	Experiment 3: Acute toxicity of aMDEA on the nitrifying culture . . . . .	66
3.10	Experiment 3: EC <sub>50</sub> of piperazine, AMP, DEA, as well as aMDEA on the nitrifying culture . . . . .	67
3.11	EC <sub>50</sub> of AMP on the nitrifying culture, calculated with data from Skjæran [47] . . . . .	69
3.12	Acute toxicity of piperazine on the denitrifying culture . . . . .	72
3.13	Acute toxicity of AMP on the denitrifying culture . . . . .	73
3.14	Acute toxicity of DEA on the denitrifying culture . . . . .	74
3.15	Acute toxicity of aMDEA on the denitrifying culture . . . . .	75
3.16	Comparison of the acute toxicity test of the 4 selected amines run on the denitrifying culture . . . . .	76
3.17	Ammonium balance of the denitrifying reactor with reclaimer waste as sole carbon source . . . . .	78
3.18	Primary amine balance of the denitrifying reactor with reclaimer waste as sole carbon source . . . . .	79
3.19	Amine degradation and formed NH <sub>4</sub> -N in the denitrifying reactor with reclaimer waste as sole carbon source . . . . .	80
3.20	Nitrate and nitrite balance of the denitrifying reactor with reclaimer waste as sole carbons source . . . . .	81
3.21	Nitrate and nitrite consumption in the denitrifying reactor with reclaimer waste as sole carbon source . . . . .	82
3.22	COD balance of the denitrifying reactor with reclaimer waste as sole carbon source . . . . .	83
3.23	COD consumed in the denitrifying reactor with reclaimer waste as sole carbon source . . . . .	84
3.24	Ammonium balance of the nitrifying reactor with reclaimer waste as sole carbon source . . . . .	85



---

3.25	Primary amine balance of the nitrifying reactor with reclaimer waste as sole carbon source . . . . .	86
3.26	Nitrate and nitrite balance of the nitrifying reactor with reclaimer waste as sole carbon source . . . . .	87
3.27	Nitrate and nitrite production of the nitrifying reactor with reclaimer waste as sole carbon source . . . . .	88
3.28	COD balance of the nitrifying reactor with reclaimer waste as sole carbon source . . . . .	89
3.29	Consumed COD in the nitrifying reactor with reclaimer waste as sole carbon source . . . . .	90
3.30	LC-MS positive and negative scan of the pre-denitrification system . . . . .	92
3.31	LC-MS quantification of selected degradation products of MEA . . . . .	93
A.1	Nitrifying activity during the biofilm development . . . . .	108
B.1	LC-MS analyses of reclaimer waste . . . . .	110
C.1	Experiment 1: EC <sub>50</sub> of the reclaimer waste on the nitrifying culture . . . . .	111
C.2	Experiment 2: EC <sub>50</sub> of the reclaimer waste on the nitrifying culture . . . . .	112
C.3	Experiment 2: EC <sub>50</sub> of MEA on the nitrifying culture . . . . .	113
C.4	Experiment 3: EC <sub>50</sub> of piperazine on the nitrifying culture . . . . .	113
C.5	Experiment 3: EC <sub>50</sub> of AMP on the nitrifying culture . . . . .	114
C.6	Experiment 3: EC <sub>50</sub> of DEA on the nitrifying culture . . . . .	115
C.7	Experiment 3: EC <sub>50</sub> of aMDEA on the nitrifying culture . . . . .	115
D.1	Measured values of ammonium, nitrate, nitrite and pH of the denitrifying reactor . . . . .	116
D.2	Measured values of COD and amine (MEA) of the denitrifying reactor . . . . .	117
D.3	Measured values of ammonium, nitrate, nitrite, pH and DO of the nitrifying reactor . . . . .	117
D.4	Measured values of COD and amine (MEA) of the nitrifying reactor . . . . .	118

# List of Tables

1.1	Reaction rate constants of nitrifying bacteria at 20°C . . . . .	13
1.2	Reaction rate constants for denitrification at 20°C . . . . .	19
2.1	Hach-Lange assays used for nitrogen determination . . . . .	27
2.2	Hach-Lange assays used for determining the chemical oxygen demand . . . . .	28
2.3	Dilutions of the reclaimer waste for various assays . . . . .	31
2.4	Media composition for the nitrification reactor . . . . .	32
2.5	Composition of the trace metal stock solution (100-fold) . . . . .	33
2.6	Media composition for the nitrification reactor . . . . .	36
2.7	Composition of the trace metal stock solution (100-fold) . . . . .	36
2.8	Chemicals tested for acute toxicity on the nitrifying culture . . . . .	40
2.9	Media composition for the denitrification reactor . . . . .	41
2.10	Composition of the trace metal stock solution (100-fold) . . . . .	41
2.11	Chemicals tested for acute toxicity on the denitrifying culture . . . . .	45
2.12	Media composition for the pre-denitrification reactor . . . . .	46
2.13	Composition of the trace metal stock solution (100-fold) . . . . .	46
3.1	Quantification of the reclaimer waste by LC-MS . . . . .	54
3.2	Quantification of reclaimer waste by Hach-Lange and fluorescamine assay . . . . .	55
3.3	Acute Toxicity experiments on nitrifying culture . . . . .	57
3.4	Summary of the acute toxicity on the nitrifying culture . . . . .	63
3.5	Acute toxicity and recovery of selected amines on the denitrifying culture . . . . .	76
3.6	Consumption, respectively formation of NH <sub>4</sub> -N in the denitrification reactor with reclaimer waste as sole carbon source . . . . .	84
3.7	Quantification of MEA by LC-MS and Fluorescamine assay . . . . .	91
3.8	Total nitrogen removal efficiency of the pre-denitrification system . . . . .	94
D.1	Average total nitrogen removal efficiency of the pre-denitrification system . . . . .	118
D.2	Average MEA nitrogen removal efficiency of the pre-denitrification system . . . . .	119
D.3	Average COD removal efficiency of the pre-denitrification system . . . . .	119

# Abbreviations

AMP	AMP Regular [2-amino-2-methylpropan-1-ol]
AOB	ammonia oxidizing bacteria
CCS	CO <sub>2</sub> capture and storage
COD	chemical oxygen demand
DEA	diethanolamine [2-(2-hydroxyethylamino)ethanol]
DO	dissolved oxygen
EC <sub>50</sub>	median effective concentration
LC-MS	liquid chromatography - mass spectrometry
MBBR	moving bed biofilm reactor
MDEA	N-methyldiethanolamine [2-[2-hydroxyethyl(methyl)amino]ethanol]
MEA	monoethanolamine [2-aminoethanol]
MF	molecular formula
MW	molecular weight
NOB	nitrite oxidizing bacteria
RW	reclaimer waste

# Chapter 1

## Introduction

### 1.1 The Carbon Dioxide Problem

Since the beginning of the 18<sup>th</sup> century, when the industrial revolution set in, an increased atmospheric concentration of carbon dioxide has been recorded, as shown in Figure 1.1. According to the IPCC (Intergovernmental Panel on Climate Change), the primary source of the increased atmospheric concentration of CO<sub>2</sub> since the pre-industrial period results from fossil fuel use, with land-use change providing another significant but smaller contribution [48].

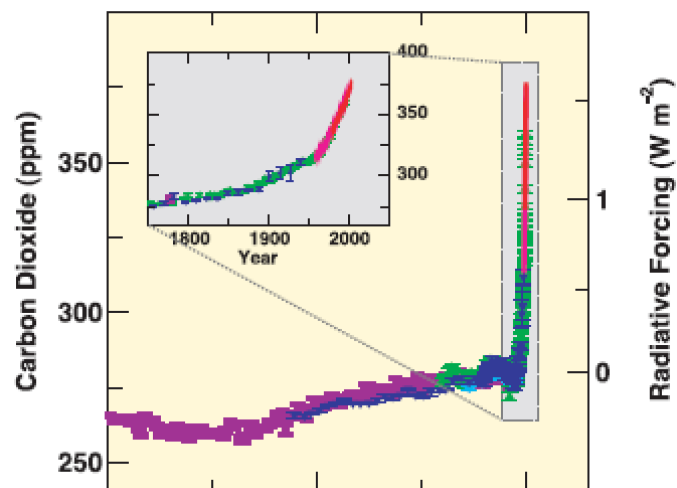


**Figure 1.1:** Atmospheric concentrations of carbon dioxide over the last 10 000 years (large panel) and since 1750 (inset panel) (IPCC, 2007 [48]).

Apart from CO<sub>2</sub>, also methane, nitrous oxide, and other greenhouse gases have increased due to human activities, visualized in Figure 1.2, highlighting the anthropogenic contribution versus the minor natural radiative forcing<sup>1</sup>.

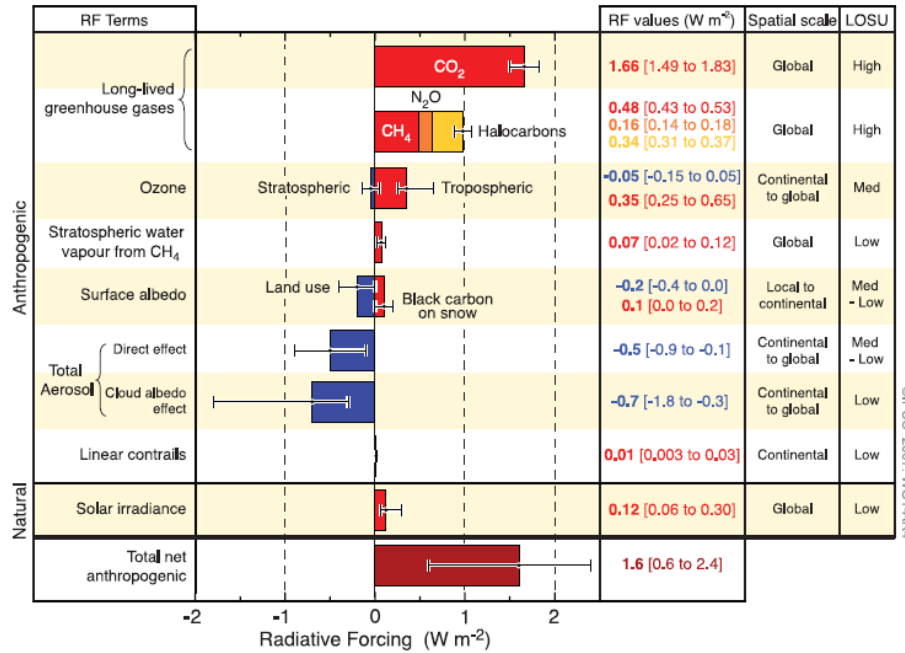


**Figure 1.2:** Global average radiative forcing estimates and ranges in 2005 for anthropogenic carbon dioxide, methane, nitrous oxide and other important agents and mechanisms, together with the typical geographical extent (spatial scale) of the forcing and the assessed level of scientific understanding (LOSU). The net anthropogenic radiative forcing and its range are also shown (IPPC, 2007 [48]).

The human-caused increases in the greenhouse gases are a driving force of the global warming, with carbon dioxide being the most important single radiative forcing agent [49]. The global temperature is already 0.7°C above the pre-industrial level, and 2°C increase is generally considered as the threshold above which dramatic and irreversible impact will occur. Ecosystems may collapse and 15 to 40% of all species may become extinct. Extreme weather events, such as draughts, floods and other can be expected and will furthermore increase the pressure on decreasing food and water resources for the world population, which is growing towards nine billion humans by 2050 [45]. All published studies to date, show largely irreversible warming due to future carbon dioxide increases on a timescale of at least 1000 years. In other words, zero emission does

<sup>1</sup>Radiative forcing is a measure of the influence that a factor has in altering the balance of incoming and outgoing energy in the earth-atmosphere system and is an index of the importance of the factor as a potential climate change mechanism. Positive forcing warms the surface while negative forcing tends to cool it [48].

not lead to zero concentration for thousands of years [49]. Therefore it is of significant importance, to set actions to minimize the global CO<sub>2</sub> emission as soon as possible.

The Bellona Foundation [45] reported the IPCC has recommended a 50 to 85% reduction of global greenhouse gas emissions from 2000 to 2050 and a peak in emissions no later than 2015. Furthermore, that it is possible to reduce global emissions by as much as 85% by 2050: Energy can be generated from renewable sources and used more efficiently; fossil power can be de-carbonized by CO<sub>2</sub> capture and storage (CCS); and forestation management can be improved [45].

## 1.2 Carbon Dioxide Capture

CO<sub>2</sub> capture and storage (CCS) is a technology being developed to reduce green house gas emissions to the atmosphere while allowing continued use of fossil fuel. The principle of this technology is to capture the CO<sub>2</sub> arising from large point sources, such as fossil fuel-fired power plants, to transport it and finally store it safely in an underground geological formation, as illustrated in Figure 1.3 [45].

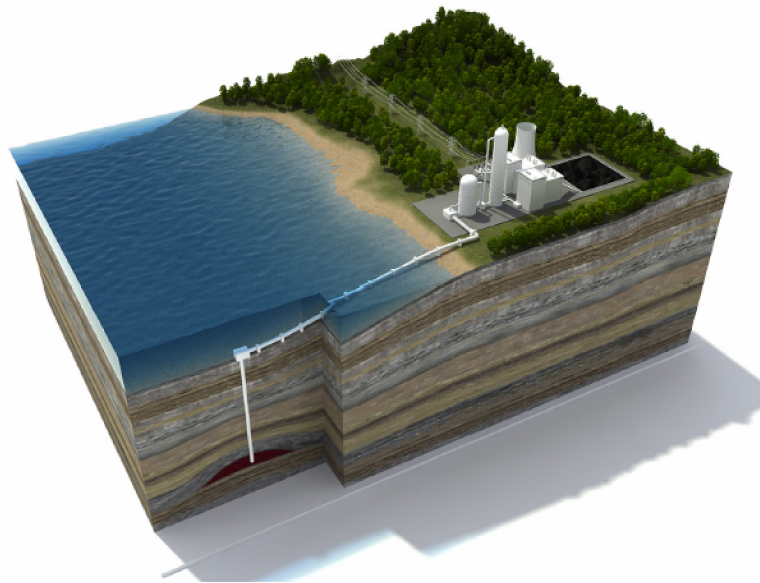


**Figure 1.3:** CO<sub>2</sub> capture and storage (CCS) [45].

CO<sub>2</sub> can be captured by applying a post-combustion, pre-combustion or oxyfuel CO<sub>2</sub> capture. In post-combustion CO<sub>2</sub> capture, which seems to be highly beneficial, because it can be implemented in already existing power plants, the CO<sub>2</sub> is most commonly separated from the flue gas by means of reversible physical or chemical absorption, such as carbonates or amines.

In an amine based post-combustion  $\text{CO}_2$  capture plant, the  $\text{CO}_2$  is removed by a chemical absorption process that involves exposing a flue gas stream to an aqueous amine solution [45]. The general set-up of an amine based post-combustion capture plant is shown in Figure 1.4. In this type of process, the flue gas is counter-currently contacted with the aqueous amine solution in the absorber column. The  $\text{CO}_2$  reacts reversibly with the amine to form a soluble carbonate salt, being either a bicarbonate or a carbamate. The rich amine solution, loaded with  $\text{CO}_2$ , is then sent through a counter-current heat exchanger, where it is preheated by the lean amine solution before entering the stripper column. In the stripper heat is provided in the reboiler by steam and is used to reverse the chemical equilibrium between the amine and its carbonate salt, thus liberating the  $\text{CO}_2$ . The gas leaving the stripper contains  $\text{CO}_2$  and water and can be dehydrated and compressed before being sequestered. The hot lean amine solution passes through the counter-current heat exchanger where it is cooled before being recycled to the absorber [19, 45].

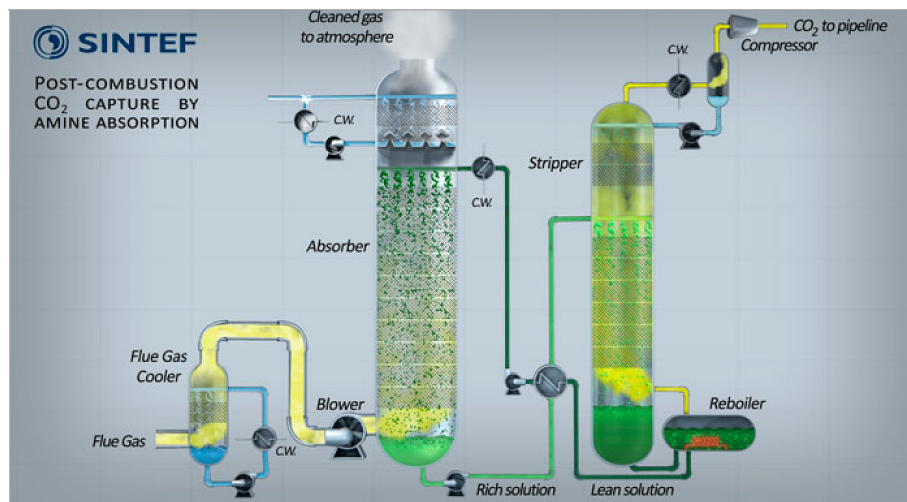
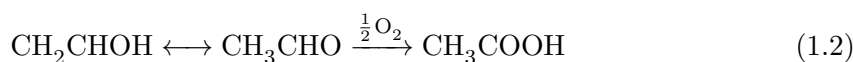
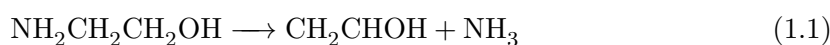


**Figure 1.4:** Post-combustion  $\text{CO}_2$  capture by amine absorption [2].

The process flow diagram implies that in an ideal post-combustion system the solvent is continuously recycled and reused. However, amine solvents in these processes are subject to three types of degradation: thermal, carbamate polymerization, and oxidative. Thermal degradation only occurs at temperatures in excess of  $200^\circ\text{C}$  and should not be a problem in flue gas applications. Carbamate polymerization results in the formation of high molecular weight degradation products and occurs at stripper conditions in the presence of  $\text{CO}_2$ . Oxidative degradation occurs in the presence of oxygen, results in fragmentation of the amine solvent, and is catalyzed by the presence of dissolved metals such as iron or copper [19].

A most widely used solvent for chemical absorption is an aqueous solution of monoethanolamine (MEA), which has been used on an industrial scale [50]. Nevertheless, CCS is not yet commercially viable and many challenges need to be solved before it can be applied in a large scale. A major problem associated with chemical absorption using MEA is the degradation of the solvent through irreversible side reactions with  $\text{CO}_2$  and other flue gas components leading to several problems in the process. Firstly, the degradation of MEA results principally in solvent loss, as for example the oxygen induced MEA degradation will produce ammonia and acetic acid, as given by Equations 1.2 and 1.1, respectively [50].



In order to prevent volatile degradation products to be emitted to the air, the exhaust gas goes through sections of water wash, located at the top of the absorber column (denoted as C.W. in Figure 1.4). These water wash sections after the  $\text{CO}_2$  capture will remove ammonia from the gas, but over time the circulating water will become saturated, thus losing its capacity and subsequently ammonia will be emitted to the atmosphere. Therefore, the circulating wash water must be monitored and exchanged when necessary [14].

Secondly, the occurrence of solvent degradation requires replacement to maintain the  $\text{CO}_2$  capture capacity, since the chemical properties of the degraded amine also change, leading to foaming, corrosion, fouling and increased viscosity of the amine. In existing  $\text{CO}_2$  capture facilities that use MEA, the degradation products are commonly separated in an evaporative reclaimer and treated as hazardous chemical waste, leading to increased disposal costs. Last, but not least, MEA degradation may result in increased environmental impacts, as volatile degradation products can be emitted to the atmosphere with the flue gas exhaust [50, 52].

### 1.2.1 Reclaimer waste

In the reclaiming operation of the CCS, a slip stream from the stripper is taken to remove high molecular weight degradation products and heat stable salts via distillation [8, 50]. Thus, the main goal of this unit is to separate the useful amine from its degradation products. A process flow diagram is shown in Figure 1.5, indicating the location of the reclaimer unit within the process and showing an enlarged picture of the reclaimer waste taken from an eprouvette.



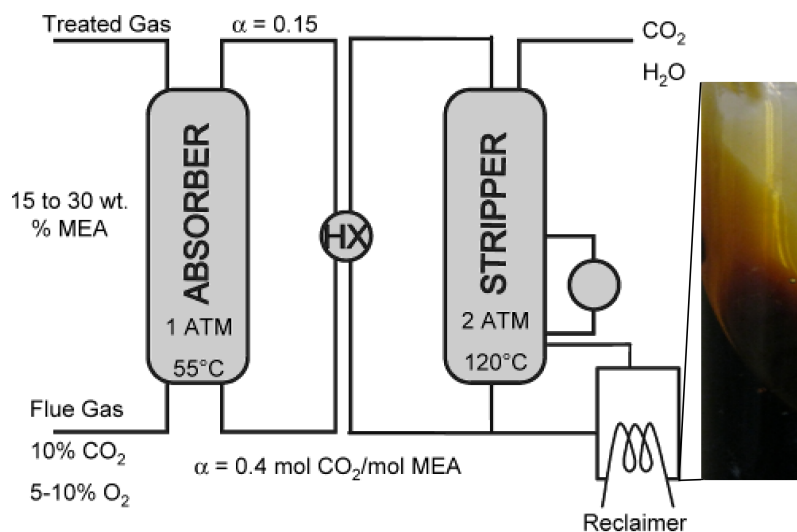


**Figure 1.5:** Process flow diagram for a typical MEA CO<sub>2</sub> capture process [19]. The reclaimer waste is shown in the right panel.

The resulting reclaimer waste is a dark brown solution with high viscosity and high pH, due to the amine content (see right panel of Figure 1.5). In a recent study of Strazisar, 2003 [50], the reclaimer waste of a CO<sub>2</sub> capture plant using MEA as a solvent was analyzed. In the reclaimer, the degradation products are concentrated and temperatures are higher than anywhere else in the process. Therefore some degradation products might be formed in the reclaimer unit itself, rather than in the stripper. However, the composition of the analyzed substances revealed roughly 30% monoethanolamine, 22% 3-hydroxyethylamino-N-hydroxy-ethyl propanamide, 12% ammonia, 12% 2-hydroxyethylamino-N-hydroxy-ethyl acetamide, 9% N-acetyethanolamine, 3% N-formylethanolamine, 1.3% 2-oxazolidone and other. There was no detectable amount of nitrosamines in the reclaimer waste, possibly because of their low boiling point [50].

### 1.2.2 Amines used in CCS

According to the scientific review of NILU [3] and the report from the Bellona Foundation [45], MEA, AMP, MDEA, DEA and piperazine are among the most commonly used amines in the capture process. The solvent often is a mixture of several different amines, also including blends of MEA-piperazine and MDEA-piperazine.

These aqueous amine solutions show different properties such as reaction kinetics in context of CO<sub>2</sub> absorption, depending on the respective reaction mechanism as recently

reviewed by da Silva, 2007 [15]. However, the final reaction of CO<sub>2</sub> will be to form either bicarbonate or carbamate. Fast reaction kinetics alone is preferable, as a given degree of CO<sub>2</sub> separation can be achieved with a smaller absorption column compared to slower kinetics [15].

#### *Monoethanolamine - MEA*

Alkanolamine systems are the current technology of choice for CO<sub>2</sub> capture from flue gas, with monoethanolamine (MEA) being the most widely used solvent [19, 16]. The amino group is responsible for the absorption of the acid gas, whereas the hydroxyl group contributes by reducing the vapour pressure of the alkanolamine MEA, thereby increasing the solubility of CO<sub>2</sub> in water. This rapid reaction even with low concentrations of CO<sub>2</sub> gives MEA the highest separation rate, and additionally it can be easily reclaimed from contaminated solutions. Despite the general efficiency, MEA degrades most rapidly in the presence of oxygen, has the highest corrosivity and a substantially higher vapor pressure than other alkanolamines, resulting in significant vaporisation and solvent loss. Because of these negative properties, both degradation and corrosivity, the use of low concentrations of MEA is required, leading to larger overall equipment size, higher solvent circulation rates, and thus an increased energy requirement for CO<sub>2</sub> regeneration [8].

### 1.3 Environmental impact of amines

As discussed above, the amines are subject to various degradation mechanisms within the CO<sub>2</sub> capturing process. The main sources of possible amine emissions during the process are pointed out in Figure 1.6, whereas the produced amine waste will be mainly concentrated in the reclaimer unit. A typical CO<sub>2</sub> capture plant with the capacity of 1 million tonnes CO<sub>2</sub> annually is expected to produce from 300 to 3000 tonnes amine waste annually. Of course, the volume of amine waste depends on type of fuel, other cleaning processes before CO<sub>2</sub> capture, the type of amine used, and operational conditions, but in most cases the volume of amine waste will be less than 1000 tonnes per year [45].

The biodegradability and ecotoxicity of amines commonly used in the CCS process vary substantially. Eide-Haugmo et al. [17] studied both factors in respect to the marine environment and showed that AMP, MDEA and piperazine would have long persistence due to their low biodegradability, whereas DEA and MEA were found to be higher degradable. In terms of ecotoxicity, all five amines were above the lowest acceptable value (10mg/L) for a chemical to be released in the marine environment [17].

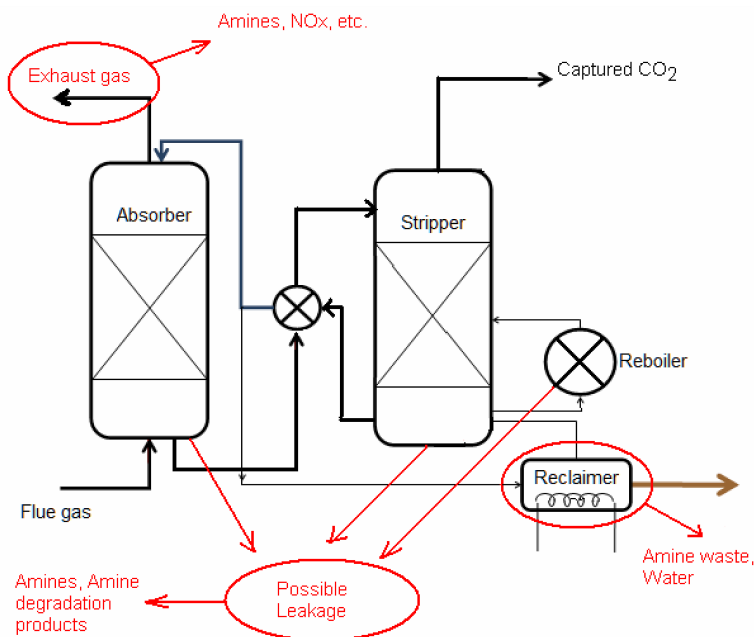


**Figure 1.6:** Main sources of possible amine emissions of an amine based CO<sub>2</sub> capture process [45].

The Bellona Foundation [45] recently reviewed the possible environmental impact of amines in context with CCS. They conclude that the impact will strongly depend on the type of amine used, especially in regard to degradation products and biodegradability. One point of concern might be the airborne emissions of nitrogen and ammonia generated from amine decomposition. If these compounds are emitted in high concentrations, this could cause eutrophication and acidification. Furthermore, there is a variety of degradation products and most of them will not have negative environmental effects. However, as the environmental impact is still uncertain, the amine waste products produced in the CO<sub>2</sub> capture process represent an environmental risk and should be handled thereafter. The most apparent manner for handling amine waste products will be to burn the waste at officially approved hazardous waste incineration facilities [45].

## 1.4 Biodegradation of xenobiotics

*(i) the microorganism is always right, your friend, and a sensitive partner; (ii) there are no stupid microorganisms; (iii) microorganisms can and will do anything; (iv) microorganisms are smarter, wiser, more energetic than chemists, engineers, and others; and (v) if you take care of your microbial friends, they will take care of your future - David Perlman, 1980.*

This quotation of Perlman [39] might be the key to success when facing the existent environmental challenges of this century. The word 'Xenobiotic' derives from the greek, meaning literally 'foreign to life'. Xenobiotic compounds are man-made chemicals, but although foreign to the biosphere this does not imply that they necessarily form an environmental problem. The biosphere has been changing throughout the history of earth, and the huge variety in microbial energy metabolisms can be lead back to adaption. The proven ability to evolve in a changing world, and the extraordinary evolutionary potential of microorganisms, gave reason to hope that new degradative capabilities for xenobiotic compounds could readily be developed [27].

For organisms to grow, electron donors and acceptors, a carbon source and nutrients need to be present. In addition to the naturally occurring organic substrates, many anthropogenic compounds can fulfill the growth requirements of microorganisms. Many aliphatic and aromatic contaminants serve as electron donors, thereby undergoing substantial transformation or even mineralization to inorganic end products such as carbon dioxide, water and inorganic ions [7]. Some compounds are biotransformed into nonhazardous products that may then enter a particular metabolic pathway and be degraded. Other compounds form daughter products which may be more or less toxic than the parent, whilst others may prove to be generally recalcitrant under the prevailing conditions and persist in one or more phases within the treatment plant [11].

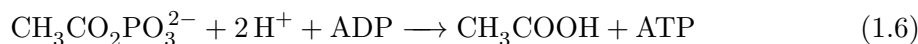
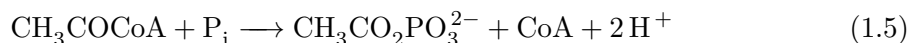
The increase of xenobiotic amines in industrial applications encouraged researchers years ago to investigate their fate in the environment, with emphasis on biological degradation. Rothkopf and Bartha, 1984 [42], studied the biodegradation of xenobiotic industrial amines in acclimated sewage sludge. Their results showed that unbranched monoamines were readily utilized, whereas the branched monoamines were a less suitable substrate. Diamine analogs of biodegradable monoamines were readily utilized, and tertiary polyamines were recalcitrant unless the tertiary amine was a heteroatom. Amino alcohols, such as ethanolamines and N-substituted ethanolamines, were also easily metabolized. Another interesting result of this work is that the biodegradability of the amine was unrelated to the inhibitory properties [42].

The general process of deamination is known to be performed by 4 enzyme classes,

such as oxidases, monooxygenases, dehydrogenases and transaminases. The latter 2 systems also operate under anaerobic conditions, whereas the initial product of amine degradation by procaryotes is an aldehyde or a ketone. Deaminating enzymes generally exhibit broad substrate ranges [42]. Furthermore, the range of substrates utilized under denitrifying conditions includes toluene, xylene, phenols, cresols, phthalate, cyclohexanol, benzoate and other aromatic acids, alcohols, and aldehydes. From the broad substrate spectrum utilized and the variety of bacteria catalyzing these degradative processes, one must conclude that the role of denitrification in anaerobic mineralization is significant [57].

*Biodegradation of Monoethanolamine - MEA*

The biodegradation of MEA has been studied by various researchers in the past decades. Norrod and Jakoby, 1964 [32] postulated the initial aerobic utilization step in form of deamination is catalyzed by the ethanolamine oxidase. Ohtaguchi and Yokoyama [34] extended this research on regenerated MEA from a CCS and suggest the following degradation pathway in *E.coli* (Equation 1.3 to Equation 1.6).



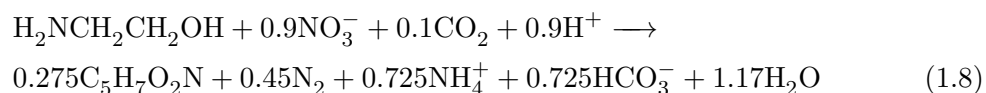
The first products will be ammonium ion and acetaldehyde, whereas the biomass assimilates ammonium ion as a nitrogen source and transforms acetaldehyde to acetic acid. Furthermore, they also observed that the biodegradation activity was positively influenced by unknown nitrogenous compounds of the waste solution, providing additional nitrogen source, thus increasing the cell mass production [34].

Nevertheless, the fate of alkanolamines in the environment has so far not been studied very well. Hawthorne et al. [21] showed that MEA can persist on contaminated soil for decades at high (hundreds of mg/kg) concentrations, without significant migration into groundwater, despite the fact that MEA is miscible in water and that it is easily degradable. The persistence apparently results from strong binding to the soil, as well as inhibition of natural bioremediation in highly contaminated field soils [21]. This is consistent with results from Mrklas et al. [30], showing that MEA biodegraded faster in the water phase than MEA sorbed on the soil phase. Furthermore, they observed that phosphate limitations played a significant role in aerobic, but not in anaerobic biodegradation of MEA.

Recent studies of Kim et al. [24] investigated the biodegradation of MEA in aerobic, as well as anoxic conditions by activated sludge. For the complete degradation of MEA, the ammonium hydrolyzed from MEA needs to be nitrified and denitrified to nitrogen gas ( $N_2$ ) with the help of electron donors. Therefore, they also tested the denitrification characteristics of nitrate and nitrite, with MEA as the electron donor. Nitrification occurred after several weeks of adaptation during MEA degradation, whereas the overall reaction for nitrification of MEA, including the prior aerobic biodegradation to ammonium and acetaldehyd, is shown in Equation 1.7.



In the case of denitrification, the adaption phase to MEA was much shorter, showing activity within a few days. The results from Kim et al. proved that MEA can be regarded as a competitive electron donor for denitrification, whereas it is thought that the ethanol group of MEA is utilized as the electron donor for the denitrification process. The overall denitrification reaction, including energy reaction and cell synthesis by MEA as the electron donor and nitrate as the electron acceptor, is postulated as shown below in Equation 1.8. It should be pointed out that MEA leaves  $NH_4^+$  when utilized as electron donor for denitrification.



However, the authors claim that 28% of MEA nitrogen goes to biomass and 73% goes to nitrogen gas by sequential nitrification and denitrification. Therefore, it can be said that MEA has sufficient electrons for the complete removal of its nitrogen by nitrification and denitrification [24].

In combination with biological nitrogen removal, a well established process in the field of wastewater treatment, this ability of biological degradation of xenobiotics inevitably offers a powerful tool to treat industrial process water containing multiple compounds. Biological nitrogen removal, recently reviewed by Zhu et al. [56] is a two-step process of nitrification and denitrification, described in the following sections.

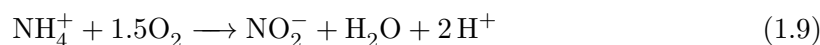
### 1.4.1 Nitrification

Nitrification is the biologically mediated oxidation of reduced forms of nitrogen to nitrite and nitrate. This strictly aerobic process can be facilitated by either autotrophic or heterotrophic nitrifiers, whereas the latter contribute to overall nitrate production only to a minor extent, since no energy is gained by nitrate formation. [9].

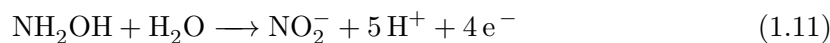
Autotrophic nitrification is a two-step process, carried out by chemolithoautotrophs, and obligate aerobic bacteria. The sequential oxidation of ammonia via nitrite to nitrate is catalyzed by two phylogenetically unrelated groups of bacteria, the ammonia oxidizing bacteria (AOB) and the nitrite oxidizing bacteria (NOB) [53].

#### *Ammonia Oxidizing Bacteria - AOB*

The AOB gain energy from oxidation of ammonia to nitrite, which is commonly summarized by Equation 1.9.



However, the more likely mechanism is based on the investigations of Suzuki et al. [51], suggesting that the actual substrate for the ammonia oxidizing bacteria is ammonia and not ammonium, supported by the fact that cell membranes are highly permeable to  $\text{NH}_3$  and not to  $\text{NH}_4^+$  [25]. Thus, the overall process of ammonia oxidation to nitrite may be characterized as a two-stage process as suggested in recent literature [6, 9], and is given by Equation 1.10 and 1.11.

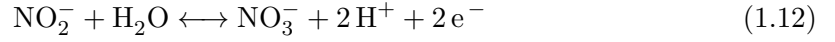


The key enzymes to catalyze the reactions of AOB are the membrane-bound ammonia monooxygenase and the hydroxylamine oxidoreductase, which is located in the periplasmic space [9].

#### *Nitrite Oxidizing Bacteria - NOB*

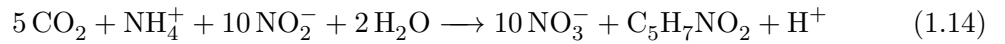
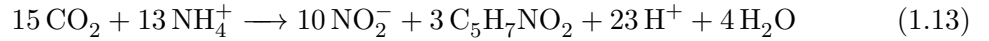
The NOB perform the second step of the nitrification reaction, which is the oxidation of nitrite to nitrate, given by Equation 1.12. The key enzyme of the nitrite-oxidizing bacteria

is the membrane-bound nitrite oxidoreductase generating energy in form of NADH for growth of the NOB [9].



#### *Nitrifying Bacteria*

Both AOB and NOB use molecular oxygen as an electron acceptor, while carbon dioxide serves as the main carbon source [4]. Being autotrophs, the nitrifiers must reduce the carbon dioxide in order to build up biomass. This reduction takes place through the oxidation of the nitrogen source of the organism concerned, shown in Equation 1.13 for the AOB and Equation 1.14 for the NOB [22], whereas the molecular formula  $\text{C}_5\text{H}_7\text{NO}_2$  represents the average composition of cell mass. This is an energy-expensive process, resulting in slow growth.



The reaction rate constants for the nitrifying bacteria were summarized by Henze et al. [22] and are shown in Table 1.1.

**Table 1.1:** Reaction rate constants of nitrifying bacteria at 20°C, adopted from Henze et al. 2002 [22].

Parameter	Unit	AOB	NOB	Total process
Maximum specific growth rate	$\text{d}^{-1}$	0.6-0.8	0.6-1.0	0.6-0.8
Saturation constant	$\text{g NH}_4\text{-N}/\text{m}^3$	0.3-0.7	0.8-1.2	0.3-0.7
Saturation constant	$\text{g O}_2/\text{m}^3$	0.5-1.0	0.5-1.5	0.5-1.0
Maximum yield constant	$\text{g VSS}^1/\text{m}^3$	0.10-0.12	0.05-0.07	0.15-0.20
Decay constant	$\text{d}^{-1}$	0.03-0.06	0.03-0.06	0.03-0.06

Under normal conditions, the reaction of ammonia oxidation to nitrite is a velocity-limiting step; in contrast, nitrite is oxidized rapidly to nitrate, so nitrite seldom accumulates in nitrifying reactors [38]. However, when considering the difference in the oxygen saturation constant (see Table 1.1), the NOB are more susceptible towards low dissolved oxygen (DO) concentrations than AOB [37]. Therefore, nitrite accumulation will occur when the oxidation of ammonium exceeds the velocity of nitrite oxidation, meaning the AOB work faster than the NOB. The localization of both AOB and NOB



communities, shown below in Figure 1.8 also suggests that since the NOB are situated in the deeper parts of the oxic biofilm, oxygen diffusion becomes a more limiting factor than for the AOB with an homogeneous spatial distribution.

The most commonly recognized genus of bacteria that carries out the first step by oxidizing ammonia, is *Nitrosomonas*; however, *Nitrosococcus*, *Nitrospira*, *Nitrosovibrio*, and *Nitrosolobus* are also able to oxidize  $\text{NH}_4^+$  to  $\text{NO}_2^-$ . These AOB, which all have the genus prefix Nitroso, are genetically diverse, but related to each other in the beta subdivision of the *Proteobacteria* [41]. In the second group, the NOB, several genera such as *Nitrospira*, *Nitrospina*, *Nitrococcus*, and *Nitrocystis* are known to be involved. However, the most prominent nitrite oxidizer genus is *Nitrobacter*, which is closely related genetically within the alpha subdivision of the *Proteobacteria* [4]. Thus, the diversity of populations involved in the process of nitrification is obvious and has recently attracted great attention in many studies.

#### *Microbial community of nitrifying biofilms*

The composition of a biofilm in wastewater treatment is complex and consists of multiple species. Especially the coexistence of nitrifying bacteria with heterotrophic bacteria is a well-known situation, whereas it is assumed that the heterotrophic bacteria consume the soluble microbial products produced by the nitrifiers [41]. Recent studies of Okabe et al. determined which phylogenetic groups of heterotrophic bacteria could directly utilize microbial products derived from nitrifying bacteria in an autotrophic nitrifying biofilm. To achieve this, biofilm samples were first incubated with [ $^{14}\text{C}$ ] bicarbonate to radiolabel only nitrifying bacteria, and after this the fate (transfer) of the radiolabelled [ $^{14}\text{C}$ ] atoms incorporated into nitrifying bacteria was traced and visualized by using the MAR-FISH approach. Finally, it was concluded that most phylogenetic groups of heterotrophic bacteria, except the  $\beta$ -Proteobacteria showed uptake of [ $^{14}\text{C}$ ]-labelled microbial products [35]. Figure 1.7 shows their result of the biofilm composition analyzed by FISH, indicating that the amount of AOB is twice as high as the NOB present, accompanied by approximately 30% heterotrophic bacteria.

The spatial distribution of AOB and NOB within the autotrophic nitrifying biofilm was previously also explored by Okabe et al. [36], based on FISH technique and microelectrodes. Their results revealed that spherical clusters of AOB were detected throughout the oxic biofilm strata, indicating more or less a homogeneous spatial distribution of  $\text{NH}_4^+$ -oxidizing bacteria, whereas clusters of *Nitrospira*-like cells, a member of the NOB community, were found in the deeper parts of the oxic region [36].

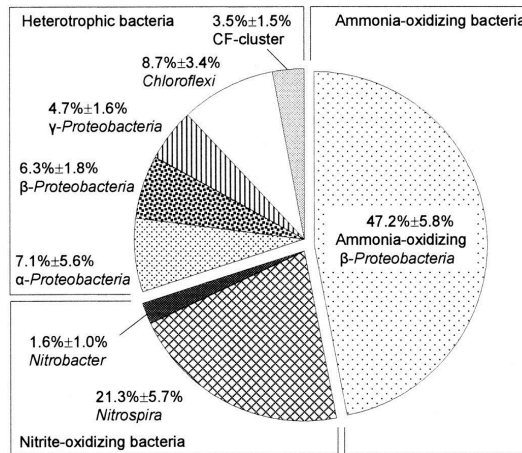


**Figure 1.7:** Microbial community composition of the autotrophic nitrifying biofilm (Okabe et al., 2005 [35]).

Furthermore, they measured the steady-state concentration profiles of  $O_2$ ,  $NH_4^+$ ,  $NO_2^-$ , and  $NO_3^-$  within the nitrifying biofilm by microelectrodes. Based on these results, Okabe et al. demonstrate the sequential oxidation of  $NH_4^+$  and  $NO_2^-$  in the oxic biofilm strata, that is, that active  $NH_4^+$ -oxidizing zone is located in the outer part of the oxic biofilm, whereas the active  $NO_2^-$ -oxidizing zone is located just below the  $NH_4^+$ -oxidizing zone [36].

The spacial distribution, as well as the concentration profiles and activity zones are illustrated in Figure 1.8.

The close spacial organization of AOB and NOB is beneficial for energetic reasons - NOB are able to efficiently capture the nitrite as a substrate produced by the AOB, helping to cope with the poor energy yield of nitrite oxidation. On the other hand, AOB favour the presence of the NOB, as the latter relieve them from the toxic nitrite [38].

#### *Key aspects of the nitrifying process*

The composition of the nitrifying microbial community can result in a competition within the mixed-culture biofilm, with the faster-growing heterotrophs being localized in the outer layers and the slow-growing nitrifiers staying in the deeper parts of the biofilm. This stratification may create a disadvantage for the nitrifiers when the bulk liquid oxygen concentration is low. However, the outer layer of heterotrophs can at the same time also protect them from detachment [6, 41].

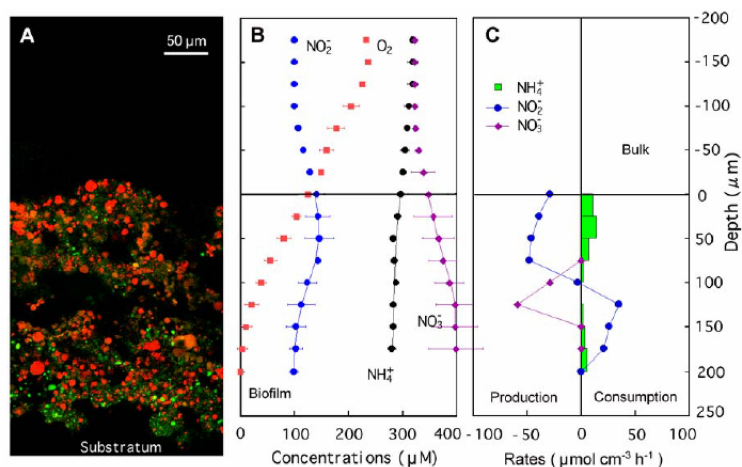


**Figure 1.8:** Fluorescence in situ hybridization result combined with microsensor measurements. In situ hybridization of a vertical biofilm thin section with labelled probes specific for AOB of the beta subclass of the *Proteobacteria* (red stain clusters) and specific for *Nitrospira moscoviensis* and some environmental clones (green stain clusters) (A). Corresponding steady-state microprofiles in the autotrophic nitrifying biofilm (B). The distribution and magnitude of the estimated specific rates of net consumption and production (C). The solid lines are the best fits from the model to calculate the specific consumption and production rates of  $\text{NH}_4^+$ ,  $\text{NO}_2^-$ , and  $\text{NO}_3^-$ . The biofilm surface was at a depth of zero (Okabe et al., 2004 [36]).

Nitrifiers suffer both from substrate (ammonia and nitrite) and product inhibition (nitrite and nitrate). If the concentration of either the substrate or the product is too high, the rate of nitrification will decrease [6].

Furthermore, nitrifiers are sensitive to inhibition from a range of organic and inorganic compounds. Among the most relevant ones are: unionized  $\text{NH}_3$  (at higher pH), undissociated  $\text{HNO}_2$  (usually at low pH), anionic surfactants, heavy metals, chlorinated organic chemicals, and low pH [41].

In fact, the pH plays a major role in the nitrification process, the optimum pH for metabolism and growth of the autotrophic nitrifiers is in the range of pH 7.5-8 [6]. It is possible that the pH dependency is linked to the inhibition phenomena from the substrate, as free ammonia ( $\text{NH}_3$ ) and free nitrous acid ( $\text{HNO}_2$ ) can inhibit both ammonia and nitrite oxidation [22]. Both dissociation equilibria of  $\text{NH}_3 \leftrightarrow \text{NH}_4^+$  ( $\text{pK}_a = 9.3$ ) and  $\text{HNO}_2 \leftrightarrow \text{NO}_2^-$  ( $\text{pK}_a = 3.4$ ) are a function of the pH and therefore attribute to the pH dependent nitrification activity. Anthonisen et al. [5] postulated the relationship of free ammonia ( $\text{NH}_3$ ) and free nitrous acid ( $\text{HNO}_2$ ) inhibition to nitrifying bacteria. A simplified graph of the relationship is shown in Figure 1.9.

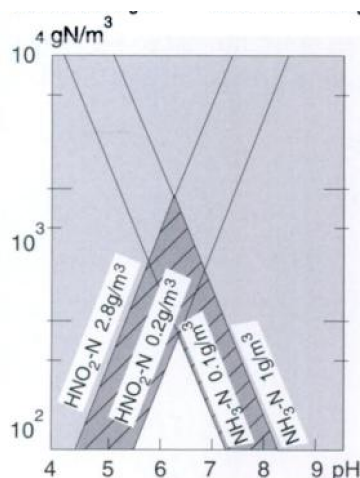


**Figure 1.9:** Inhibition of the nitrification process as a function of  $\text{NH}_3$ ,  $\text{HNO}_2$  and pH. The grey area represents total inhibition, and the dashed area marks partial inhibition (Henze et al. 2002 [22]).

Since severe pH depression can occur when the alkalinity in the wastewater approaches depletion by the acid produced in the nitrification process, the appropriate range of pH must be stabilized by chemical addition, such as lime [4].

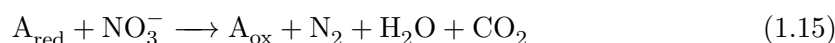
As all biological systems depend on the temperature, this is also true for the nitrification process. The optimum temperature has been reported in the range of  $20^\circ\text{C}$  to  $30^\circ\text{C}$ , although the optimum for the NOB might be lower. Between 5 and  $30^\circ\text{C}$  the temperature affects nitrifying bacteria according to the Arrhenius relation, meaning that their biological activity doubles with every  $10^\circ\text{C}$  water temperature increase [6].

Nitrification is a strict aerobic process, as molecular oxygen is needed for the oxidation of ammonia to nitrate and equally important for respiration of AOB and NOB. Thus, the kinetics of this process is strongly influenced by the dissolved oxygen (DO) concentration. Calculating the stoichiometric amount required for full biological oxidation of ammonium, a minimum of 4.57g of  $\text{O}_2$  per g of  $\text{NH}_4^+$  is required [6, 20]. The DO concentration is usually kept at a low level of approximately 2mg/L  $\text{O}_2$ , whereas the oxygen limitation is known to have more influence on nitrification than on the heterotrophic processes since both half-saturation constants for nitrification are described to be higher than the ones proposed for heterotrophic processes [20]. However, complete oxidation of ammonium should be attained, as nitrite is a reactive species and could react with aliphatic and aromatic amines and other aromatic molecules to give rise to undesirable nitroso- or nitro-derivatives [53]. Apart from the obvious system parameters, also sunlight (380 - 415nm), as well as ultra-

aviolet light can inhibit growth of *Nitrosomonas*. This effect can be significant in water treatment plants [6].

### 1.4.2 Denitrification

Denitrification is the biologically mediated conversion of nitrite and nitrate into inert atmospheric nitrogen. The process is anaerobic, as nitrate is the oxidizing agent as shown simplified in Equation 1.15, whereas A denotes the carbon source in its reduced/oxidated state [22].

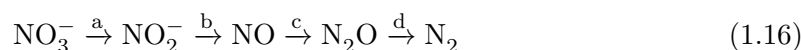


To evaluate the stoichiometry of nitrate to organic compounds for denitrification with a complex carbon source, the oxidation/reduction state of the carbon substrates and the oxygen concentration in the wastewater should be known [40]. The actual denitrification process carried out by heterotrophic bacteria includes several steps as shown below in Equation 1.16.

#### *Denitrifying Bacteria*

The anoxic process is carried out by a diversity of bacteria belonging taxonomically to the various subclasses of the *Proteobacteria*. Denitrification also extends beyond the bacteria to the archaea, where it is found among the halophilic and hyperthermophilic branches of this kingdom and may have evolutionary significance. Nevertheless, over the years, fungi have had an intermittent record of denitrification [57].

The dissimilatory nitrate reduction consists of several enzymatic reactions as shown in Equation 1.16, whereas the indices above the arrows correspond to the catalyzing enzymes, which are given in the text below.



The according enzymes for the sequential denitrification process are (a) Nitrate reductase, (b) Nitrite reductase, (c) NO reductase and (d) N<sub>2</sub>O reductase [41, 40]. It should be noted that nitrite reductase is the key enzyme of denitrification in catalyzing the first committed step that leads to a gaseous intermediate. For the denitrification process to lead to dinitrogen formation, the nitrite reductase reaction is complemented by the activity of two distinct metalloenzymes, which use NO or N<sub>2</sub>O as substrates [57].

All intermediates of the denitrification process are toxic and therefore undesirable and should be avoided. The bacterial process is nearly exclusively a facultative trait, as the expression of the relevant enzymes is triggered in the cell by the environmental parameters of low oxygen tension and availability of an N oxide. As illustrated in Figure 1.10 only when all necessary enzymes are available for the bacteria, complete denitrification will be achieved [57].

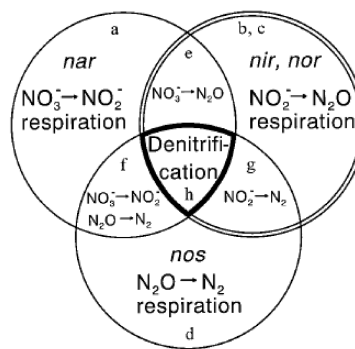


**Figure 1.10:** Modular organization of denitrification. Four modules representing the respiratory systems utilizing nitrate (a), nitrite (b), NO (c), and N<sub>2</sub>O (d) carry out the overall process. Complete denitrification (h) is achieved only when all four modules are activated. Pairwise overlaps (e to g) of the individual respiratory modules occur naturally in denitrifying or other N-oxide-utilizing bacteria (Zumft, 1997 [57]).

The reaction rate constants for the denitrifying bacteria were summarized by Henze et al. [22] and are shown in Table 1.2.

**Table 1.2:** Reaction rate constants for denitrification at 20°C, adopted from Henze et al. 2002 [22].

Parameter	Unit	Denitrification
Maximum specific growth rate	d <sup>-1</sup>	3-6
Half-Saturation constant	g NO <sub>3</sub> -N/m <sup>3</sup>	0.2-0.5
Half-Saturation constant	g O <sub>2</sub> /m <sup>3</sup>	0.1-0.5
Half-Saturation constant	g COD/m <sup>3</sup>	10-20
Maximum yield constant	g COD/g COD	0.4-0.6
Maximum yield constant	g COD/g NO <sub>3</sub> -N	1.6-1.8
Decay constant	d <sup>-1</sup>	0.05-0.10

*Key aspects of the denitrifying process*

Most denitrifiers are aerobic heterotrophic organisms that transfer redox equivalents from the oxidation of a carbon source to an N-oxide under anaerobic conditions, whereas autotrophic denitrifiers utilize nitrite for this purpose [57]. In this process water and CO<sub>2</sub> will be generated by oxidizing the carbon source, using NO<sub>3</sub><sup>-</sup> as the electron acceptor.

As mentioned above, the process of denitrification is a facultative trait, enabling the microorganism to switch from aerobic to anaerobic respiration. The chosen pathway will depend on the available terminal electron acceptor. If oxygen is available, the bacterium will preferably respire aerobic, because the redoxpotential between the last cytochrome in the electron transport is higher for oxygen than for nitrate. Nevertheless, denitrification may also occur in flocs and biofilms, even in aerobic macro-environments [22, 6].

The denitrification process is also subject to pH dependency, determining the endpoint of the sequential reactions. Low pH values favour N<sub>2</sub>O production, whereas higher values favor N<sub>2</sub> gas production, thus complete denitrification [6]. In regard to the temperature sensitivity, the denitrification process resembles that of the aerobic heterotrophic processes. Denitrification can also occur at temperatures between 50-60°C, but experiences are few. The nitrogen removal rate is approximately 50% higher than at 35°C [22]. It has been suggested that the nitrogen concentration has little influence on the denitrification activity, whereas for attached cultures the reaction rate is half-order in respect to nitrogen concentration within the practical range of concentrations found in domestic waste water [6]. However, if the conversion of organic matter is desired, the available N-oxide may become the limiting factor.

A supply of carbon source is vital to drive the oxidation-reduction reaction of denitrifying bacteria. The type of carbon source has a significant impact on the denitrification activity, depending largely on the accessibility for the bacteria. Commonly used external carbon sources include methanol, ethanol, acetic acid, as well as wastewater from breweries and organic matter in wastewater [22]. However, with the exception of the two latter, all chemicals need to be purchased, leading to increased operational costs. Based on the vast variety of possible organic substrates, it is evident that reclaimer waste, rich in organic compounds, may serve just as well as a carbon source for denitrification.

### 1.4.3 Combined Nitrification and Denitrification in Pre-Denitrification configuration

Obviously by sequential combination of nitrification and denitrification, nitrogen removal can be achieved; whereas the overall process is then referred to as 'Biological nitrogen removal'. Depending on the line-up there are several process solutions available, as described previously by Skjæran [47]. In the configuration of pre-denitrification, the wastewater will enter the process in the denitrification reactor and subsequently be transferred to the nitrification reactor, whereas a mixed liquid is recycled from the nitrification reactor to the denitrification reactor. A schema of the set-up is shown in Figure 2.13. The benefit of this configuration is that the heterotrophic denitrifying bacteria can utilize the organic matter as a carbon source as well as an electron donor, whereas the lithoautotrophic nitrifying bacteria are satisfied with  $\text{CO}_2$  as carbon source and have  $\text{O}_2$  as their terminal electron acceptor. By recycling the underflow from the nitrification process to the primary denitrification reactor, the imported nitrite and nitrate will serve as the electron acceptor for denitrification. Thus, an additional carbon source is not required for the denitrification reactor. If the oxidation of organic matter is targeted, additional supplementation of N-oxide might be necessary. One draw-back of the pre-denitrification configuration is that no complete nitrogen removal can be achieved, as only a part of the total flow from the nitrification reactor is recycled and the remaining effluent is discarded.

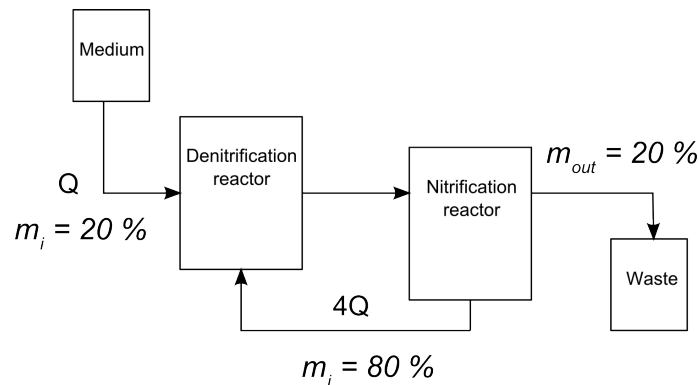


**Figure 1.11:** Set-up and flow scheme of the pre-denitrification system, whereas  $Q$  is the flowrate,  $m_i/m_{out}$  denotes mass in/out respectively.



## 1.5 Moving Bed Biofilm reactors

A biofilm is a self-organized structure of microorganisms growing on a surface, whereas the community of biofilms depends largely on the available substrates. A key feature of a biofilm is the self-developed polymeric matrix, enabling better protection of the individual organism towards environmental changes, such as physical stress, as well as the improved mass transfer in terms of metabolic interactions between the present populations.

Moving bed biofilm reactor (MBBR) systems involve biofilm growing on the inner surfaces of small plastic carriers, suspended within a liquid phase reactor. The carriers are mobilised in suspension either pneumatically or mechanically, and are kept within the reactor by means of a sieve or grill, allowing simple separation of the treated water from the biomass-containing carriers. Excess biomass is sloughed off the biofilm and leaves the reactor with the effluent [18].



**Figure 1.12:** Enlarged Kaldnes K1 carrier with biofilm (left) and two Kaldnes K1 carriers in real size (right) [18].

AnoxKaldnes, now Krüger Kaldnes of Veolia Water Solutions & Technologies (France) developed a number of different carriers, whereas the model Kaldnes K1 was used in this study. Kaldnes K1 carriers, shown in Figure 1.12 are made of polyethylene (PEHD) with a density of  $0.95\text{g/cm}^3$ , and a nominal dimension of 7mm length and a diameter of 9mm. The biomass is growing primarily on the protected surface ( $500\text{cm}^2/\text{cm}^3$ ) on the inside of the carriers, but the total surface area ( $800\text{cm}^2/\text{cm}^3$ ) is significantly larger than the effective biofilm surface area. In order to be able to move the carrier suspension freely, it is recommended that filling fractions should be below 70% [43].

As in every biofilm process, diffusion of compounds in and out of the biofilm plays a key role. Because of the importance of diffusion, the thickness of the effective biofilm (the depth of the biofilm to which the substrates have penetrated) is important. Since this depth of full substrate penetration is normally less than  $100\mu\text{m}$ , the ideal biofilm in the moving bed process is thin and evenly distributed over the surface of the carrier. In order

to obtain this, the turbulence in the reactor is of importance, both in order to transport the substrates to the biofilm and to maintain a low thickness of the biofilm by shearing forces. However, the MBBR Kaldnes K1 carriers were tested previously for removal of organic matter, nitrification, as well as for denitrification. On a biofilm surface area basis the total ammonium nitrogen removal rates in MBBRs have compared very favourably to rates reported in the literature [43].

## 1.6 Previous studies

Ana Borges Colaco [14] investigated the feasibility of applying biological nitrogen removal to convert the ammonia in the process water from a CO<sub>2</sub> capture plant based on amine absorption. In this master thesis, she set-up 1L MBBRs with Kaldnes K1 biofilmcarriers, for combined nitrification and denitrification with MEA and ethanol as a carbon source. Furthermore, she evaluated different analytical test methods to determine ammonium, nitrate, nitrite, total nitrogen and MEA concentrations at-line in a fast and accurate way. Her experiments showed that the LCK 303 Ammonium-Nitrogen assay from Hach-Lange, produced a clear underestimation of the resulting ammonium concentration in the presence of MEA and DEA. The same effect was observed with the LCK 341 Nitrite assay, but not as pronounced. Nevertheless, the same work provides correction-graphs for linear interpolation when the concentration of MEA is known [14]. Both the Hach-Lange assay LCK138 for total nitrogen, as well as LCK 339 for nitrate determination showed unaffected results up to 200mmol/l MEA.

The bench-scale nitrification experiment showed a steep decline in activity when initially exposed to MEA, reaching a 50% decrease at 10mmol/l MEA. During the long term exposure to MEA the nitrifying bacteria adopted, resulting in the ability to aerobically degrade all MEA into ammonium. The bench-scale operated denitrification culture was insensitive up to 316mmol/l MEA when utilizing ethanol as a carbon source. In contrast, they failed to use MEA as a carbon source when ethanol was omitted. When both reactors were combined in a post-denitrification mode, the nitrifying reactor showed no activity in the sense of nitrate or nitrite formation. However, ammonium equivalent to 100% of the fed concentration remained in the outlet, and the ammonium concentration in the reactor increased to about four times the original ammonium input, deriving from the biodegraded MEA [14].

After the post-denitrification configuration, the reactor system was taken over from Skjæran [46] and switched to a pre-denitrification configuration. In this follow up project work of Skjæran the biological nitrogen removal of process water of a CO<sub>2</sub> capture plant

was studied, with emphasis on varification of post-denitrification with ethanol as an additional carbon source, pre-denitrification with MEA as a sole carbon source, as well as the selection of alternative amines. Furthermore, the inhibitory effect of MEA and nitrite werw investigated.

Skjæran's results showed that biological nitrogen removal from waste products of a CO<sub>2</sub> capture plant is possible, as the primary amine MEA may serve as a carbon source. Furthermore, Skjæran found that high concentrations of nitrite inhibit nitrifying bacteria to a certain degree.

Both post- and pre-denitrification configuration resulted in a total nitrogen removal rate between 70 and 80%, whereas for the pre-denitrification system the maximum theoretical value was achieved with a 4-fold recycling flow-rate [46].

Her experiments also showed that the LCK 303 Ammonium-Nitrogen assay from Hach-Lange, gave an underestimation of the resulting ammonium concentration in the presence of AMP. Additionally high concentrations of nitrite produced an overestimation when applying the LCK 339 Nitrate assay. However, since the samples generally have to be diluted in order to fall into the measuring range of the LCK 339 Nitrate assay, this might be a minor problem [46].

Skjæran extended her project work to a master thesis [47], investigating the biodegradability and functionality as a carbon source for biological nitrogen removal of MEA and AMP [47]. Her results showed that MEA may serve as a carbon source in the pre-denitrification system, but not AMP. It appears that AMP is aerobically degraded in the nitrification reactor, but nevertheless, the denitrifying culture was not able to utilize AMP as a carbon source [47]. Skjæran observed a drop in the nitrification activity shortly after AMP addition, accompanied by a simultaneous drop in COD concentration and therefore concluded the biodegradation of AMP could lead to unwanted daughter compounds, which have a toxic effect on the nitrification process. In fact, the acute toxicity test showed that 30mmol/l AMP resulted in a 50% inhibition of the nitrifying activity.

The interference of AMP with the different Hach-Lange assays was also tested by Skjæran, showing relatively unbiased results, except for the LCK 303 Ammonium-Nitrogen assay giving lower results, as mentioned above. Reclaimer waste showed a possible overestimation of the nitrate concentration when applying the LCK 339 Nitrate assay. In general, the analysis of reclaimer waste revealed large amounts of MEA, making high dilutions necessary in order to avoid interferences with the LCK 303 Ammonium-Nitrogen assay [47].

## 1.7 Scope of this work

The objective of this master thesis was to test the feasibility of biological treatment of reclaimer waste from an amine based CO<sub>2</sub> capture plant, as well as from selected, commonly used amines in this process.

The reclaimer waste, consisting mostly of the amine MEA was the main focus of this master thesis, whereas the selected amines AMP, aMDEA, DEA and piperazine were tested for acute toxicity on a nitrifying, as well as on a denitrifying culture. All experiments were run on a lab bench scale and are a continuation of the previously described studies from Colaco [14] and Skjæran [46, 47].

The scope of this master thesis includes following tasks:

- *Reclaimer waste*
  - i) Analysis of the composition by LC-MS and Hach-Lange analyses.
  - ii) Acute toxicity test on a nitrifying culture to estimate the EC<sub>50</sub> and recovery ability.
  - iii) Feasibility of reclaimer waste as a sole carbon source in a pre-denitrification system, with emphasis on consumption of amine and degradation products, as well as COD removal and total nitrogen removal ability.
- *Acute toxicity of selected amines*
  - i) Selected amines are MEA, AMP, aMDEA, DEA and piperazine.
  - ii) Acute toxicity test on a nitrifying culture to estimate the EC<sub>50</sub> and recovery ability.
  - iii) Set up an anaerobic bioreactor with pH and temperature control with biofilm grown on Kaldnes K1 carriers.
  - iv) Acute toxicity test on a denitrifying culture to estimate the EC<sub>50</sub> and recovery ability.
- *Biofilm development*
  - i) Set up a new bioreactor to monitor the biofilm development of nitrifying culture on Kaldnes K1 carriers by measuring the COD.

## Chapter 2

# Materials and Methods

### 2.1 Chemical analysis

Throughout the experiments ammonium, nitrate, nitrite and total nitrogen concentration, as well as the COD were analyzed in an at-line reading mode by Hach-Lange assays. MEA was also determined in an at-line reading mode by the fluorescamine assay. The reclaimer waste was analyzed by LC-MS, as well as by Hach-Lange assays. In the following section these methods will be described including some relevant, previously observed interferences.

#### 2.1.1 Hach-Lange assays

The concentrations of ammonium, nitrate, nitrite and total nitrogen concentration, as well as the COD were determined with assays from Hach-Lange for water quality. All assays used during this work come in kits, whereas all procedures were carried out according to manufacturers instruction. An overview of the used assays is given in Table 2.1 and Table 2.2, including article number, principle and observed interferences with MEA and AMP. All quantifications are based on colorimetric reactions, read by a Dr. Lange Lasa 100 mobile laboratory photometer. The photometer is able to recognize the different assays by the bar code on each cuvette being processed. For some assays (LCK 138 LatoN, LCK 114 and LCK 614 COD) also the Dr. Lange Thermostat LT is required for thermal treatment at a specific temperature and time duration.

**Table 2.1:** Hach-Lange assays used for determining the ammonium, nitrate, nitrite, and total nitrogen. Previously observed interferences are given with the relevant source.

Hach-Lange assay	Analyte	Range [mg/L]	Principle	Interferences
LCK303 Ammonium-Nitrogen	$\text{NH}_4\text{-N}$	2-47	Ammonium ions react at pH 12.6 with hypochlorite ions and salicylate ions in the presence of sodium nitroprusside as a catalyst to form indophenol blue.	Underestimation with MEA and AMP [14, 47].
LCK339 nitrate	$\text{NO}_3\text{-N}$	0.23-13.5	nitrate ions in solutions containing sulphuric and phosphoric acids react with 2.6-dimethylphenol to form 4-nitro-2.6-dimethylphenol.	Unaffected up to 200mmol/L MEA [14], Overestimation with high concentrations of nitrite [47].
LCK341 nitrite	$\text{NO}_2\text{-N}$	0.015-0.6	nitrites react with primary aromatic amines in acidic solution to form diazonium salts. These combine with aromatic compounds that contain an amino group or a hydroxyl group to form intensively coloured azo dyes.	Underestimation with MEA [14].
LCK138 LatoN	Total Nitrogen	1-16	Inorganically and organically bonded nitrogen is oxidized to nitrate by digestion with peroxodisulphate. The nitrate ions react with 2.6-dimethylphenol in a solution of sulphuric and phosphoric acid to form nitrophenol.	

**Table 2.2:** Hach-Lange assays used for determining the chemical oxygen demand.

Hach-Lange assay	Analyte	Range [mg/L]	Principle
LCK014 COD	Chemical Oxygen Demand	1000- 10000	Oxidizable substances react with sulphuric acid-potassium dichromate solution in the presence of silver sulphate as a catalyst. Chloride is masked by mercury sulphate. The green coloration of $\text{Cr}^{3+}$ is evaluated.
LCK114 COD	Chemical Oxygen Demand	150- 1000	Oxidizable substances react with sulphuric acid-potassium dichromate solution in the presence of silver sulphate as a catalyst. Chloride is masked by mercury sulphate. The green coloration of $\text{Cr}^{3+}$ is evaluated.
LCK614 COD	Chemical Oxygen Demand	50- 300	Oxidizable substances react with sulphuric acid-potassium dichromate solution in the presence of silver sulphate as a catalyst. Chloride is masked by mercury sulphate. The reduction in the yellow coloration of $\text{Cr}^{6+}$ is evaluated.

Due to an assumed competitive reaction of the amines with the assay's reactants, a clear underestimation of the ammonium concentration in samples containing MEA or DEA was found previously by Colaco [14]. Therefore the same work provides a graph for quantitative correction, based on linear interpolation of recorded ammonium levels when the MEA concentration is known, as shown in Figure 2.1. This correction was applied for all samples with concentrations higher than 10mmol/L MEA.

In the studies of Colaco, 2009 [14], also the nitrite assay from Hach-Lange showed biased results when MEA was present, therefore the measurements should be corrected according to the correction graph shown below in Figure 2.2. This quantitative correction was applied for all samples containing concentrations higher than 10mmol/L MEA.

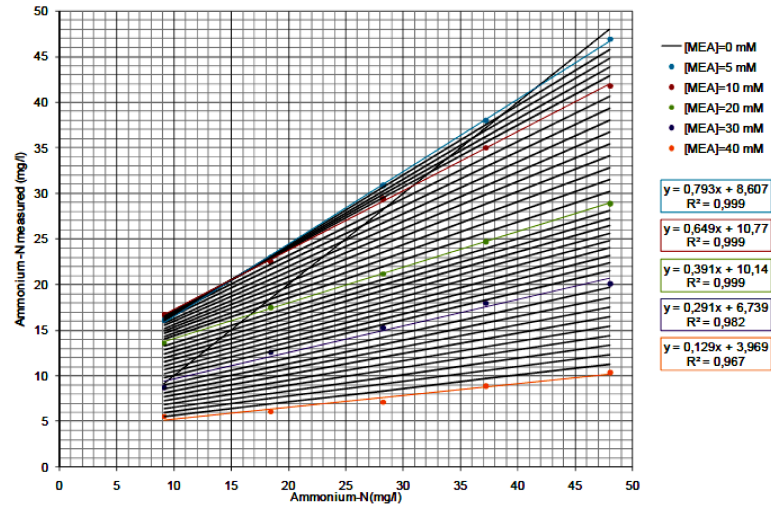


**Figure 2.1:** Ammonium-N recordings according to the LCK 303 Ammonium-Nitrogen assay as a function of ammonium-N concentration, while MEA concentration was kept constant at 0, 5, 10, 20, 30 and 40mM [14]. Secondary lines, in grey, provide guidance for linear interpolation.

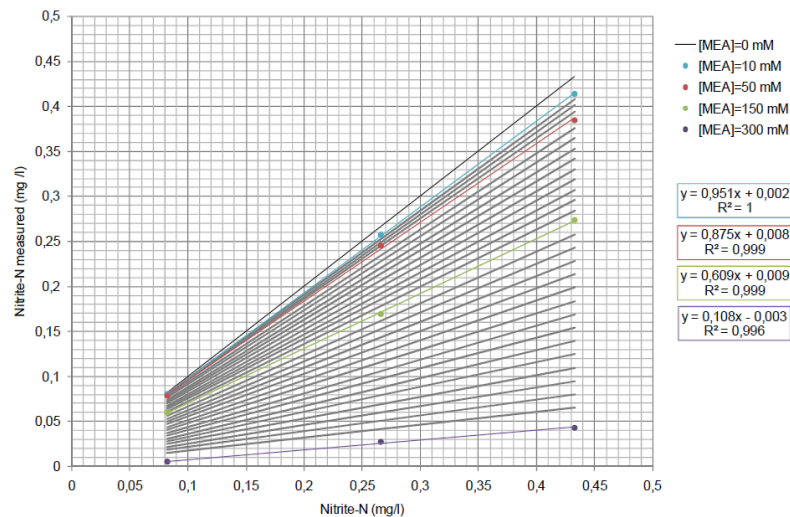


**Figure 2.2:** Nitrite-N recordings according to the LCK 341 Nitrite-Nitrogen assay as a function of nitrite-N concentration, while MEA concentration was kept constant at 0, 10, 50, 150 and 300mM [14]. Secondary lines, in grey, provide guidance for linear interpolation.



### 2.1.2 Fluorescamine assay

Fluorescamine allows the detection of primary amines in the picomole range, whereas the reaction occurs almost instantaneously at room temperature in aqueous solutions. The products are stable highly fluorescent compounds with an excitation wavelength of 392nm and an emission at 480nm. The fluorescamine assay carried out in this work was based on the adapted procedure from Colaco, 2009 [14] and is briefly described as follows.

- i) A 10mg/mL fluorescamine solution in acetone was prepared and kept in the dark for 24 hours (Fluorescamine from Sigma-Aldrich, acetone from BDH Prolabo).
- ii) 100mmol/L boric acid buffer with a pH of 7.0-9.5 was prepared in Milli-Q water (Boric acid analytical grade from Roth, NaOH from BDH Prolabo).
- iii) For each measurement series a calibration curve of fluorescamine, being 0, 0.2, 0.4, 0.6, 0.8 and 1.0mg/mL was prepared to determine the concentration in the samples by interpolation.
- iv) Samples were diluted in Milli-Q water according to the measuring range.
- v) 2.9mL boric acid buffer was added to 100 $\mu$ L sample, respectively standards, and rapidly 200 $\mu$ L of the fluorescamine solution was added.
- vi) The solution was inverted 4-5 times and incubated for 20 minutes in the dark at room temperature.
- vii) The fluorescence signal was measured in UV-grade polymethylmethacrylate disposable cuvettes from VWR, using a Perkin Elmer LS50B fluorimeter. The excitation wavelength was set to 392nm and the emission was measured at 480nm, with 5-10nm slit width.

### 2.1.3 LC-MS

LC-MS (liquid chromatography - mass spectrometry) is a combination of analytical processes to determine the mass-charge ratio of a compound, enabling its identification as well as quantification.

The principle of liquid chromatography (LC) is based on the specific distribution of a compound between a stationary (e.g. column) and mobile (liquide) phase. The separation depends on chemical and physical properties of each phase, such as length and diameter of the column, pressure, temperature and also the particle size of the analyte. The different extents to which molecules are adsorbed to the stationary phase leads to the separation effect. By the process of elution, the specific retention time of various

compounds is determined. Following the separation by LC, the compounds are lead to a mass spectrometer (MS). As a first step, the compounds need to be ionized and subsequently, the mass is analyzed and quantified by a detector [29].

All LC-MS analyses were accomplished at SINTEF Material and Chemistry, Biotechnology division by Kai Vernstad, using a 6460 Triple Quadrupole Mass Spectrometer coupled with 1290 Infinity LC Chromatograph from Agilent Technologies.

## 2.2 Reclaimer waste analysis

The reclaimer waste was obtained from the ACC mobile test unit stationed at Longanet, a coal-fired power plant, collected during a campaign with MEA in 2009.

The reclaimer waste was analyzed by LC-MS to quantify the MEA content and for a qualitative and quantitative scan of degradation products. The reclaimer waste was diluted 1:1000 with Milli-Q water, whereas 1mL was forwarded to SINTEF for the LC-MS positive and negative scan analyses.

The reclaimer waste was also analyzed by Hach-Lange assays, which are described in section 2.1.1. In order to fit into the measuring range, the reclaimer waste was diluted with Milli-Q water as given in Table 2.3.

**Table 2.3:** Dilutions of the reclaimer waste for various Hach-Lange assays and the Fluorescamine assay.

Assay	Dilutions		
LCK303 Ammonium-Nitrogen	1:1000	1:1500	1:2000
LCK339 nitrate	1:200	1:500	1:1000
LCK341 nitrite	1:50	1:100	
LCK614 COD	1:2000		
LCK114 COD	1:1000		
LCK014 COD	1:10000		
LCK138 LatoN	1:10000		
Fluorescamine assay	1:20000	1:50000	

## 2.3 Biofilm development

To track the development of nitrifying biofilm on Kaldnes K1 carriers over time, the gained COD was taken as a measure. COD is the chemical oxygen demand and represents the total organic content which can be oxidized by sulphuric acid-potassium dichromate solution in the presence of silver sulphate as a catalyst.

### 2.3.1 Inoculum

The reactor was inoculated with sludge from a sludge return of an existing nitrification bioreactor and immobilized on 350mL Kaldnes K1 carriers. The inoculum was partly fresh sewage from Ladehammeren domestic wastewater treatment plant in Trondheim, as well as enriched nitrifying sludge frozen from a previous lab course (TBT4130 Environmental Biotechnology at NTNU). In order to make the carriers less hydrophobic, they were incubated for one week in the sludge trap with aeration.

### 2.3.2 Medium

The medium for the nitrification reactor was based on the reactivation medium of Vogel-sang et al. [54] and is shown in Table 2.6 and Table 2.7. All compounds were analytical grade from Merck.

**Table 2.4:** Media composition for the nitrification reactor.

Compound	Concentration
$(\text{NH}_4)_2\text{SO}_4$	0.236g/L [50mg/L $\text{NH}_4\text{-N}$ ]
$(\text{NH}_4)_2\text{SO}_4$	0.472g/L [100mg/L $\text{NH}_4\text{-N}$ ]
$\text{K}_2\text{HPO}_4$	0.4mg/L
$\text{NaHCO}_3$	1.0mg/L
Trace metal solution	10mL/L

All components were dissolved in tap water and the pH was adjusted to 7.5 with 6mol/L HCl solution. Media batches of 10L were prepared at a time.

### 2.3.3 Reactor

The reactor for the nitrification culture was set up as a standard 1L glass reactor with aeration, equipped as follows:

**Table 2.5:** Composition of the trace metal stock solution (100-fold).

Compound	Concentration [mg/L]
MgSO <sub>4</sub> · 7 H <sub>2</sub> O	25
CaCl <sub>2</sub> · 2 H <sub>2</sub> O	15
FeCl <sub>2</sub> · 4 H <sub>2</sub> O	2.0
MnCl <sub>2</sub> · 2 H <sub>2</sub> O	5.5
ZnCl <sub>2</sub>	0.68
CoCl <sub>2</sub> · 6 H <sub>2</sub> O	1.2
NiCl <sub>2</sub> · 6 H <sub>2</sub> O	1.2
EDTA	2.8

- Outer glass jacket for temperature control
- Water bath set to 25°C (Cole-Parmer polystat)
- pH-electrode and controller displaying pH and temperature (CONSORT CONTROLLER R301)
- Air sparger
- Pump for medium supply (Masterflex model 7518-00, Cole-Parmer Instrument Company)
- Pumps for adding acid and base (Masterflex model 7016-20, Cole-Parmer Instrument Company)
- Magnetic stirrer at 300rpm with a 5cm magnetic stirrer bar (Heidolph MR3001)
- 350mL biofilm carriers

The experimental set-up of the bioreactor is shown in Figure 2.5.

The range of pH was set between 7.3 and 7.8 and controlled by automatic addition of 0.5mol/L HCl or NaOH solution. As the optimum for nitrification in biofilm lies at approximately 7.5, the wide pH range was chosen in order to avoid high salinity through increased additions of acid and base. The air was cleaned and humidified in distilled water before being dispersed in the reactor, as shown in Figure 2.6.

During the stabilization phase of the nitrification reactor, the reactor was operated in batch mode and fed with 50mg/L NH<sub>4</sub>-N. Once the activity was stable it was switched to a continuous flow mode, taken as day 1, with a flowrate of 100mL/h and the ammonium

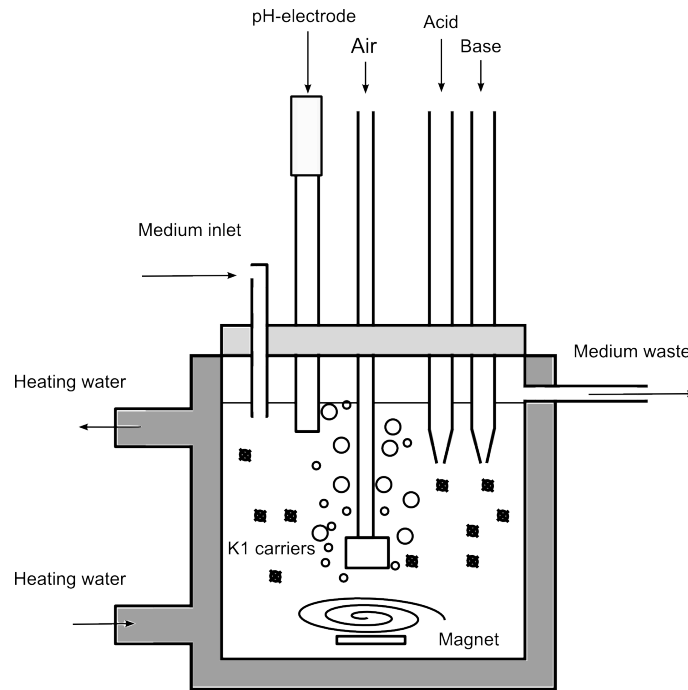


**Figure 2.3:** Experimental set-up of the nitrification reactor.

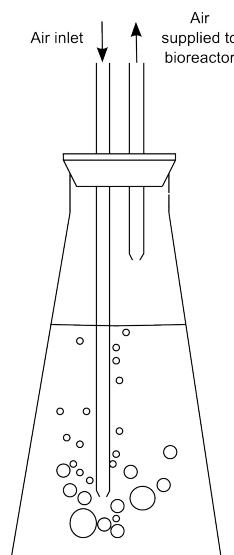


**Figure 2.4:** Set-up of the aeration for the nitrification reactor.

concentration was increased from 50mg/L  $\text{NH}_4\text{-N}$  to 100mg/L  $\text{NH}_4\text{-N}$ . To verify the substrate dependency of growth, the flowrate was then increased to 200mL/h, resulting in the double amount of incoming  $\text{NH}_4\text{-N}$ . The outlet of the reactor was at approximately 700mL, allowing used medium to be removed at the same rate as new medium came in. To prevent unwanted algal growth in the system, the reactor was covered with black plastic bags during the entire experiment.

### 2.3.4 Monitoring

The biofilm development on the Kaldnes K1 carriers was monitored between day 1 and day 77, whereas 5 replicates were analyzed at a time for their COD with Hach-Lange assay LCK014. Each carrier was rinsed with distilled water and cut with a scalpel into small pieces, big enough to fit in the opening of the test cuvette. Distilled water was added according to manufacturers instruction. To monitor the nitrification activity of the biofilm, samples of 10mL were taken from the reactor at least three times a week. The samples were collected with a syringe from BD Plastipak and filtered with 0.45 $\mu\text{m}$  filters from Sarstedt to remove suspended biomass. Subsequently, the filtrates were analyzed with Hach-Lange assays for ammonium, nitrate and nitrite concentration, and when necessary diluted with distilled water to fit in the detection range of each assays.

## 2.4 Nitrification

### 2.4.1 Inoculum

The nitrification reactor was inoculated during the work of Skjæran [47] and immobilized on 400mL carriers. The inoculum was partly fresh sewage from Ladehammeren domestic wastewater treatment plant in Trondheim, as well as enriched nitrifying sludge frozen from a previous lab course (TBT4130 Environmental Biotechnology at NTNU).

### 2.4.2 Medium

The medium for the nitrification reactor was based on the reactivation medium of Vogel-sang et al. [54] and is shown in Table 2.6 and Table 2.7. All compounds were analytical grade from Merck.

All components were dissolved in tap water and the pH was adjusted to 7.5 with 6mol/L HCl solution. Media batches of 10L were prepared at a time.

**Table 2.6:** Media composition for the nitrification reactor.

Compound	Concentration
$(\text{NH}_4)_2\text{SO}_4$	0.236g/L [50mg/L $\text{NH}_4\text{-N}$ ]
$(\text{NH}_4)_2\text{SO}_4$	0.472g/L [100mg/L $\text{NH}_4\text{-N}$ ]
$\text{K}_2\text{HPO}_4$	0.4mg/L
$\text{NaHCO}_3$	1.0mg/L
Trace metal solution	10mL/L

**Table 2.7:** Composition of the trace metal stock solution (100-fold).

Compound	Concentration [mg/L]
$\text{MgSO}_4 \cdot 7 \text{H}_2\text{O}$	25
$\text{CaCl}_2 \cdot 2 \text{H}_2\text{O}$	15
$\text{FeCl}_2 \cdot 4 \text{H}_2\text{O}$	2.0
$\text{MnCl}_2 \cdot 2 \text{H}_2\text{O}$	5.5
$\text{ZnCl}_2$	0.68
$\text{CoCl}_2 \cdot 6 \text{H}_2\text{O}$	1.2
$\text{NiCl}_2 \cdot 6 \text{H}_2\text{O}$	1.2
EDTA	2.8

### 2.4.3 Reactor

The reactor for the nitrification culture was set up as a standard 1L glass reactor with aeration, equipped as follows:

- Outer glass jacket for temperature control
- Water bath set to 25°C (Cole-Parmer polystat)
- pH-electrode and controller displaying pH and temperature (CONSORT CONTROLLER R301)
- Air sparger
- Pump for medium supply (Masterflex model 7518-00, Cole-Parmer Instrument Company)
- Pumps for adding acid and base (Masterflex model 7016-20, Cole-Parmer Instrument Company)
- Magnetic stirrer at 300rpm with a 5cm magnetic stirrer bar (Heidolph MR3001)
- 400mL biofilm carriers

The experimental set-up of the bioreactor is shown in Figure 2.5.

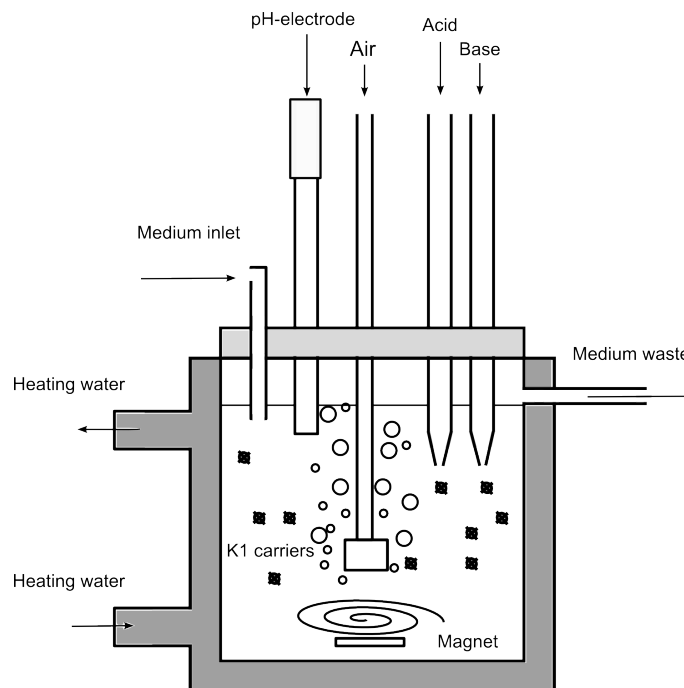


**Figure 2.5:** Experimental set-up of the nitrification reactor.

The range of pH was set between 7.3 and 7.8 and controlled by automatic addition of 0.5mol/L HCl or NaOH solution. As the optimum for nitrification in biofilm lies at approximately 7.5, the wide pH range was chosen in order to avoid high salinity through increased additions of acid and base. The air was cleaned and humidified in distilled water before being dispersed in the reactor, as shown in Figure 2.6.

Throughout the experiment the reactor was operated in a continuous flow mode with a flowrate of 100mL/h and an ammonium concentration of 100mg/L  $\text{NH}_4\text{-N}$ . The outlet of the reactor was at approximately 700mL, allowing used medium to be removed at the same rate as new medium came in. To prevent unwanted algal growth in the system, the reactor was covered with black plastic bags during the entire experiment.

#### 2.4.4 Monitoring

Samples of 10mL were taken from the nitrification reactor at least three times a week to monitor the nitrification activity. The samples were collected with a syringe from BD



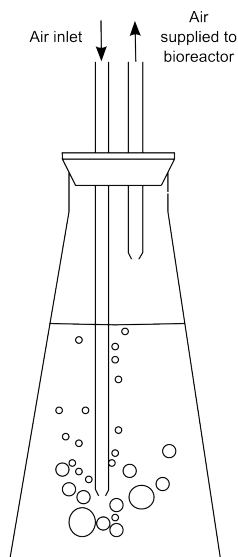


**Figure 2.6:** Set-up of the aeration for the nitrification reactor.

Plastipak and filtered with 0.45 $\mu$ m filters from Sarstedt to remove suspended biomass. Subsequently, the filtrates were analyzed with Hach-Lange assays for ammonium, nitrate and nitrite concentration, and when necessary diluted with distilled water to fit in the detection range of each assay.

### 2.4.5 Acute Toxicity Test

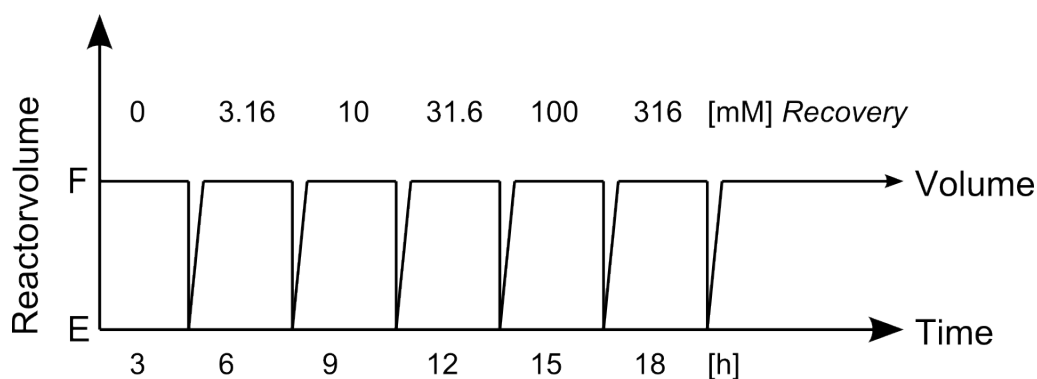
Two acute toxicity tests were carried out on the nitrifying culture to estimate firstly the  $EC_{50}$  of reclaimer waste and MEA, and secondly the  $EC_{50}$  of 4 commonly used amines in CCS, which are AMP, DEA, aMDEA and piperazine. A brief description of the investigated compounds is given in Table 2.8. The standardized assay was previously also done by Colaco for MEA [14] and by Skjæran for AMP [47] on a nitrifying culture.

MEA and reclaimer waste were first tested for acute toxicity on the nitrifying culture, which at the time was never exposed to shock loads of amines before. For this assay 200mL of carriers were transferred from the nitrifying reactor into 2 empty batch reactors, with the same set-up as shown in Figure 2.5, containing 100mL carriers each. Both reactors were then filled with 500mL medium as described in section 2.4.2 with an ammonium concentration of 50mg/L  $NH_4$ -N.

Samples of 5mL were taken every 30 minutes, over a total time range of 3 hours. The samples were collected with a syringe from BD Plastipak and filtered with 0.45 $\mu$ m

filters from Sarstedt to remove suspended biomass. The filtrates were then analyzed with Hach-Lange assays for their  $\text{NO}_3\text{-N}$  concentration, and when necessary diluted with distilled water to fit in the detection range of the assay.

After 3 hours the reactors were drained and refilled with 500mL media containing either MEA or reclaimer waste. Following this procedure, the biofilm carriers were subsequently exposed to a series of logarithmic increasing concentrations of MEA and reclaimer waste ranging from 0; 3.16; 10; 31.6; 100 to 316mmol/L. The respective solutions were prepared in 500mL medium as described in section 2.4.2 with an ammonium concentration of 50mg/L  $\text{NH}_4\text{-N}$ . Because of the alkalinity in higher concentrations, the pH was again adjusted to 7.5 with 6mol/L HCl solution. The flow diagram of the experiment is depicted in Figure 2.7.

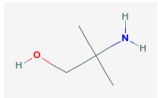
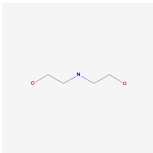
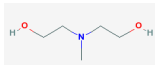
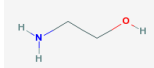
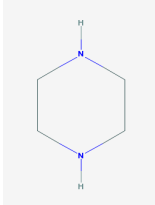


**Figure 2.7:** Flow schema of the acute toxicity assay, whereas E means Empty and F denotes Full.

After monitoring the highest concentration, the biofilm was washed with tap water and left in medium (as given in section 2.4.2) with an ammonium concentration of 50mg/L  $\text{NH}_4\text{-N}$  for recovery and an activity monitoring over 3h was done again after 30 hours. After recovery the biofilm was returned to the main nitrification reactor.

The four amines AMP, DEA, aMDEA and piperazine (as described in Table 2.8 below) were tested approximately four months later using the same procedure. The four batch reactors had the same set-up as shown in Figure 2.5 and contained 100mL carriers each. After monitoring the highest concentration, the biofilm was washed with tap water and left in medium (as given in section 2.4.2) with an ammonium concentration of 50mg/L  $\text{NH}_4\text{-N}$  for recovery and an activity monitoring over 3h was done again after either 30 hours, 39 hours, 14 days or 44 days, as stated in the results. After recovery the biofilm was frozen.

**Table 2.8:** Chemicals tested for acute toxicity on the nitrifying culture.

	AMP	DEA	aMDEA	MEA	Piperazine
Structure					
MW [g/mol]	89.14	105.14	119.16	61.08	86.14
MF	C <sub>4</sub> H <sub>11</sub> NO	C <sub>4</sub> H <sub>11</sub> NO <sub>2</sub>	C <sub>5</sub> H <sub>13</sub> NO <sub>2</sub>	C <sub>2</sub> H <sub>7</sub> NO	C <sub>4</sub> H <sub>10</sub> N <sub>2</sub>
Density [g/mL]	0.934	1.097	1.038	1.012	1.1
CAS-Number	124-68-5	111-42-2	105-59-9	141-43-5	110-85-0
Distributor	Sigma-Aldrich	Fluka	Sigma-Aldrich	Sigma-Aldrich	Merck

The results of the NO<sub>3</sub>-N formation were taken to calculate the respective effect on the nitrifying culture. EC<sub>50</sub> is a common parameter to compare the concentration dependent effect of a substance, whereas this value is the effect concentration at which the activity reaches a level of 50%. By plotting the produced amount of NO<sub>3</sub>-N as a function of time, the slope expresses the nitrification activity in [mg/h]. The respective activity, as well as the recovery, were then normalized with the initial activity, expressed in percent, and plotted versus concentration in log-scale. To interpolate the EC<sub>50</sub> value, a descriptive regression model was applied, being a logistic model [28, 33, 44, 31]. The equation for the interpolation of the logistic model is given below in Equation 2.1.

$$y = A2 + (A1 - A2)/(1 + (x/x_0)^p) \quad (2.1)$$

## 2.5 Denitrification

### 2.5.1 Inoculum

The denitrification reactor was inoculated with biofilm carriers provided by Igor Ivanovic from the Department of Hydraulic and Environmental Engineering at NTNU. According

to him, the carriers were a mix of different history and ages, some older than 10 years, but all were used for municipal wastewater treatment in aerobic and anoxic tanks.

### 2.5.2 Medium

The medium for the denitrification reactor was based, as in previous work of Colaco [14], on Christensson et al. [13] and is show in Table 2.9 and Table 2.10. All compounds were analytical grade from Merck, except for the yeast extract and Ethanol. These were technical grade and purchased from Oxoid and Kemetyl, respectively.

**Table 2.9:** Media composition for the denitrification reactor.

Compound	Concentration
$K_2HPO_4$	0.533g/L
$NH_4Cl$	0.253g/L
$KNO_3$	4.0g/L
Yest extract	0.05g/L
Ethanol	1.0g/L
Trace metal solution	10mL/L

**Table 2.10:** Composition of the trace metal stock solution (100-fold).

Compound	Concentration [mg/L]
$MgSO_4 \cdot 7H_2O$	25
$CaCl_2 \cdot 2H_2O$	15
$FeCl_2 \cdot 4H_2O$	2.0
$MnCl_2 \cdot 2H_2O$	5.5
$ZnCl_2$	0.68
$CoCl_2 \cdot 6H_2O$	1.2
$NiCl_2 \cdot 6H_2O$	1.2
EDTA	2.8

All components were dissolved in deaerated tap water and the pH was adjusted to 7.5 with 6mol/L HCl solution. The deaeration of the water was done by connecting the water flask to a water suction pump, as the pressure reduction inside the flask makes the dissolved oxygen boil out. The deaeration set-up is shown in Figure 2.8. In order to facilitate complete removal of dissolved oxygen, the water was additionally being stirred over a time period of approximately 2 hours for a volume of 4L  $H_2O$ , as described previously by Colaco [14].

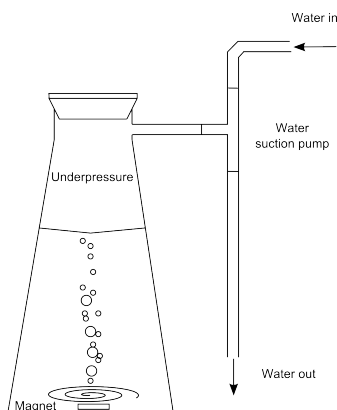


**Figure 2.8:** Set-up of the deaeration for the denitrification water.

### 2.5.3 Reactor

The denitrification reactor was set-up as a standard anoxic 2L glass reactor, equipped as follows:

- Outer glass jacket for temperature control
- Water bath set to 25°C (Cole-Parmer polystat)
- pH-electrode and controller displaying pH and temperature (CONSORT CONTROLLER R301)
- Pumps for adding acid and base (Masterflex model 7016-20, Cole-Parmer Instrument Company)
- Magnetic stirrer at 150rpm with a 5cm magnetic stirrer bar (Heidolph MR3001)

The experimental set-up of the bioreactor is shown in Figure 2.9.

The bioreactor was filled up to 1500mL with medium, whereas the carriers took up about 400mL. The range of pH was set between 6.8 and 7.3 and controlled by automatic addition of 0.5mol/L HCl or NaOH solution. As the optimum for denitrification in biofilm lies at approximately 7, the wide pH range was chosen in order to avoid high salinity through increased additions of acid and base.

Throughout the experiment the reactor was operated in batch mode with a nitrate concentration of 553mg/L  $\text{NO}_3\text{-N}$ . To prevent unwanted algal growth in the system, the reactor was covered with black plastic bags during the entire experiment.

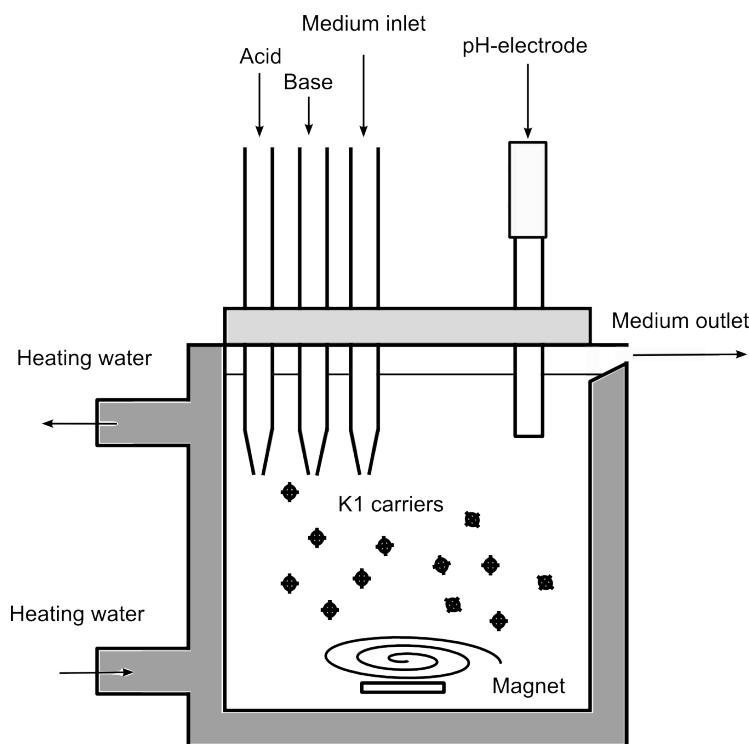


**Figure 2.9:** Experimental set-up of the denitrification reactor.

#### 2.5.4 Monitoring

Samples of 10mL were taken from the denitrification reactor at least three times a week to monitor the denitrification activity. The samples were collected with a syringe from BD Plastipak and filtered with 0.45 $\mu$ m filters from Sarstedt to remove suspended biomass. Subsequently, the filtrates were analyzed with Hach-Lange assays for ammonium, nitrate and nitrite concentration, and when necessary diluted with distilled water to fit in the detection range of each assay.

#### 2.5.5 Acute Toxicity Test

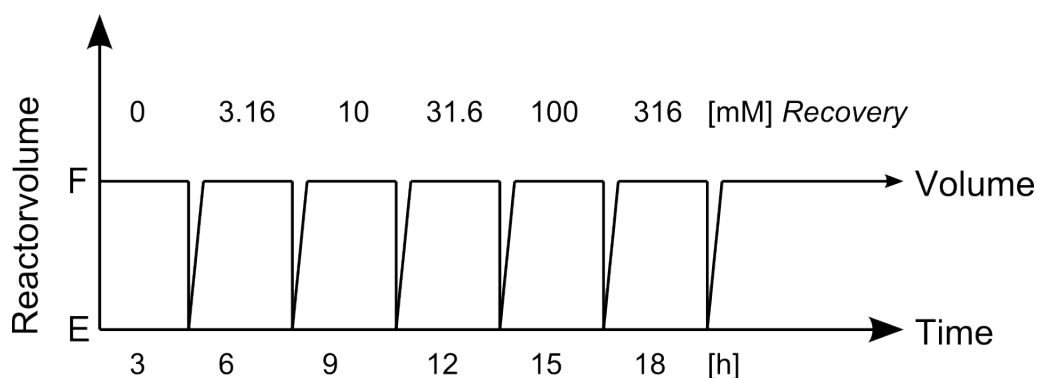
An acute toxicity test was carried out on the denitrifying culture to determine the  $EC_{50}$  of 4 commonly used amines in CCS (see 1.2.2), which are AMP, DEA, aMDEA and piperazine. A brief description of the investigated compounds is given in Table 2.11.

AMP, DEA, aMDEA and piperazine were tested for acute toxicity on the denitrifying culture, which at the time was never exposed to shock loads of amines before. For this assay 400mL of carriers were transferred from the denitrifying reactor into 4 empty 1L batch reactors with the same set-up as shown in Figure 2.9, containing 100mL carriers

each.

All four reactors were then filled with 500mL medium as described in section 2.5.2 with a nitrate concentration of 553mg/L  $\text{NO}_3\text{-N}$ . Samples of 5mL were taken every 30 minutes, over a total time range of 3 hours. The samples were collected with a syringe from BD Plastipak and filtered with 0.45 $\mu\text{m}$  filters from Sarstedt to remove suspended biomass. The filtrates were then analyzed with Hach-Lange assays for their  $\text{NO}_3\text{-N}$  concentration, and when necessary diluted with distilledwater to fit in the detection range of the assay.

After 3 hours the reactors were drained and refilled with 500mL media containing either AMP, DEA, aMDEA or piperazine. Following this procedure, the biofilm carriers were subsequently exposed to a series of logarithmic increasing concentrations of the amines ranging from 0; 3.16; 10; 31.6; 100 to 316mmol/L. The respective solutions were prepared in 500mL medium as described in section 2.5.2 with a nitrate concentration of 553mg/L  $\text{NO}_3\text{-N}$ . Because of the alkalinity in higher concentrations, the pH was again adjusted to 7.5 with 6mol/L HCl solution. The flow diagram of the experiment is depicted in Figure 2.10.

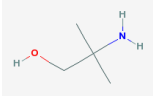
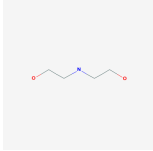
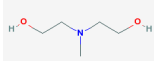
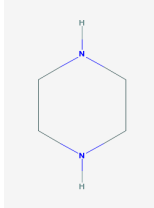


**Figure 2.10:** Flow schema of the acute toxicity assay, whereas E means Empty and F denotes Full.

After monitoring the highest concentration, the biofilm was washed with tap water and left in medium (as given in 2.5.2) with a nitrate concentration of 553mg/L  $\text{NO}_3\text{-N}$  for recovery and an activity monitoring over 3h was done again after 39 hours. After recovery the biofilm was frozen.

The expected results of the  $\text{NO}_3\text{-N}$  consumption would be taken to calculate the respective effect on the denitrifying culture.  $\text{EC}_{50}$  is a common parameter to compare the concentration dependent effect of a substance, whereas this value is the effect concentration at which the activity reaches a level of 50%.

**Table 2.11:** Chemicals tested for acute toxicity on the denitrifying culture.

	AMP	DEA	aMDEA	Piperazine
Structure				
MW [g/mol]	89.14	105.14	119.16	86.14
MF	C <sub>4</sub> H <sub>11</sub> NO	C <sub>4</sub> H <sub>11</sub> NO <sub>2</sub>	C <sub>5</sub> H <sub>13</sub> NO <sub>2</sub>	C <sub>4</sub> H <sub>10</sub> N <sub>2</sub>
Density [g/mL]	0.934	1.097	1.038	1.1
CAS-Number	124-68-5	111-42-2	105-59-9	110-85-0
Distributor	Sigma-Aldrich	Fluka	Sigma-Aldrich	Merck

## 2.6 Pre-Denitrification System

### 2.6.1 Inoculum

The pre-denitrification system consisted of both a (pre-) denitrification and a nitrification reactor.

The nitrification reactor was inoculated in spring 2009 by students taking a biotechnology lab course (TBT4130 Environmental Biotechnology at NTNU), with partly fresh sewage from Ladehammeren domestic wastewater treatment plant in Trondheim and partly enriched nitrifying sludge frozen from a previous lab course.

The denitrification reactor was inoculated in spring 2009 by Colaco [14], whereas the inoculum of fresh sewage was also obtained from Ladehammeren domestic wastewater treatment plant in Trondheim.

Both nitrification and denitrification cultures were utilized for the entire work of Colaco in 2009 [14] as well as for the work of Skjæran in 2009 and 2010 [46, 47].



### 2.6.2 Medium

The medium for the pre-denitrification reactor system was based on the reactivation medium of Vogelsang et al. [54] and is shown in Table 2.12 and Table 2.13. All compounds were analytical grade from Merck.

**Table 2.12:** Media composition for the pre-denitrification reactor.

Compound	Concentration
Reclaimer waste	1.0mL/L
$(\text{NH}_4)_2\text{SO}_4$	0.236g/L
$\text{KNO}_3$	2.43mg/L [34mg/L $\text{NO}_3\text{-N}$ ]
	3.57mg/L [50mg/L $\text{NO}_3\text{-N}$ ]
	5.35mg/L [75mg/L $\text{NO}_3\text{-N}$ ]
$\text{K}_2\text{HPO}_4$	0.4mg/L
$\text{NaHCO}_3$	1.0mg/L
Trace metal solution	10mL/L

**Table 2.13:** Composition of the trace metal stock solution (100-fold).

Compound	Concentration [mg/L]
$\text{MgSO}_4 \cdot 7\text{H}_2\text{O}$	25
$\text{CaCl}_2 \cdot 2\text{H}_2\text{O}$	15
$\text{FeCl}_2 \cdot 4\text{H}_2\text{O}$	2.0
$\text{MnCl}_2 \cdot 2\text{H}_2\text{O}$	5.5
$\text{ZnCl}_2$	0.68
$\text{CoCl}_2 \cdot 6\text{H}_2\text{O}$	1.2
$\text{NiCl}_2 \cdot 6\text{H}_2\text{O}$	1.2
EDTA	2.8

All components were dissolved in tap water and the pH was adjusted to 7.5 with 6mol/L HCl solution. Media batches of 10L were prepared at a time and stored in a fridge (MATSUI modell MUR1107WWE) at 4°C.

### 2.6.3 Reactors

The pre-denitrification system consisted of both a denitrification and a nitrification reactor. The set-up of the reactor system is shown in 2.11 and is described separately as follows.

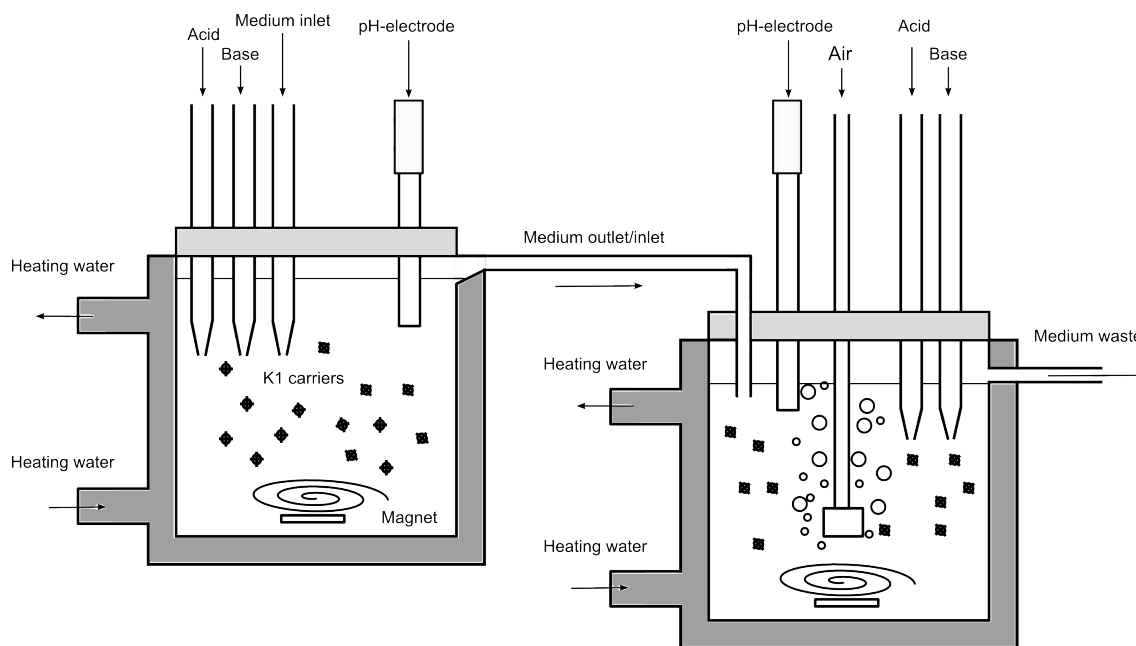


**Figure 2.11:** Experimental set-up of the pre-denitrification system. The denitrification reactor is shown on the left connected to the nitrification reactor on the right side.

#### *Nitrification reactor*

The reactor for the nitrification culture was set up as a standard 1L glass reactor with aeration, equipped as follows:

- Outer glass jacket for temperature control
- Water bath set to 25°C (Cole-Parmer polystat)
- pH-electrode and controller displaying pH and temperature (CONSORT CONTROLLER R301)
- Air sparger
- Oxygen electrode (Mettler Toledo) connected to a display (Ingold 531 O<sub>2</sub> Amplifier)
- Pump for medium supply (Masterflex model 7518-00, Cole-Parmer Instrument Company)

- Pumps for adding acid and base (Masterflex model 7016-20, Cole-Parmer Instrument Company)
- Magnetic stirrer at 300rpm with a 5cm magnetic stirrer bar (Heidolph MR3001)
- 250mL biofilm carriers

The experimental set-up of the nitrification reactor is shown on the right side of Figure 2.11. The range of pH was set between 7.3 and 7.8 and controlled by automatic addition of 0.5mol/L HCl or NaOH solution. As the optimum for nitrification in biofilm lies at approximately 7.5, the wide pH range was chosen in order to avoid high salinity through increased additions of acid and base. The air was cleaned and humidified in distilled water before being dispersed in the reactor, as shown in Figure 2.12.

Throughout the experiment the reactor was operated in a continuous flow mode with a flowrate of 400mL/h, fed by the outlet stream of the denitrification reactor. The outlet of the reactor was at approximately 700mL, allowing used medium to be removed at the same rate as new medium came in. To prevent unwanted algal growth in the system, the reactor was covered with black plastic bags during the entire experiment.

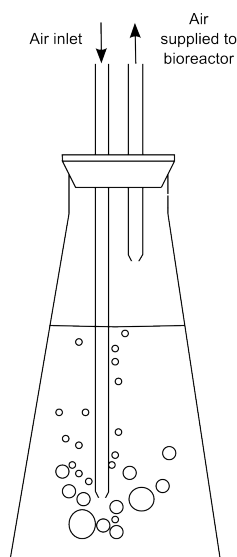


**Figure 2.12:** Set-up of the aeration for the nitrification reactor.

*Denitrification reactor*

The denitrification reactor was set-up as a standard anoxic 1L glass reactor, equipped as follows:

- Outer glass jacket for temperature control
- Water bath set to 25°C (Cole-Parmer polystat)
- pH-electrode and controller displaying pH and temperature (CONSORT CONTROLLER R301)
- Pump for medium supply (Masterflex model 7518-00, Cole-Parmer Instrument Company)
- Pumps for adding acid and base (Masterflex model 7016-20, Cole-Parmer Instrument Company)
- Magnetic stirrer at 150rpm with a 5cm magnetic stirrer bar (Heidolph MR3001)
- 150mL biofilm carriers

The experimental set-up of the denitrification reactor is shown on the left side of Figure 2.11.

The range of pH was set between 6.8 and 7.3 and controlled by automatic addition of 0.5mol/L HCl or NaOH solution. As the optimum for denitrification in biofilm lies at approximately 7, the wide pH range was chosen in order to avoid high salinity through increased additions of acid and base.

To prevent unwanted algal growth in the system, the reactor was covered with black plastic bags during the entire experiment.

Throughout the experiment the reactor was operated in a continuous flow mode with a flowrate of 100mL/h of medium. The medium composition, as described in 2.12, varied in respect to the ammonium concentration (being either 50 or 0mg/L) and in the nitrate concentration (0, 34, 50, 75mg/L). To prevent microbial growth and further degradation of the reclaimer waste, the medium was stored in a fridge (MATSUI modell MUR1107WWE) at 4°C. The outlet of the denitrification reactor was at approximately 700mL, allowing excess medium to flow into the nitrification reactor.

The content of the nitrification reactor was further recycled to the denitrification reactor with a 4-fold rate of the incoming media stream, thus being 400mL/h. This flow scheme is visualized in Figure 2.13.

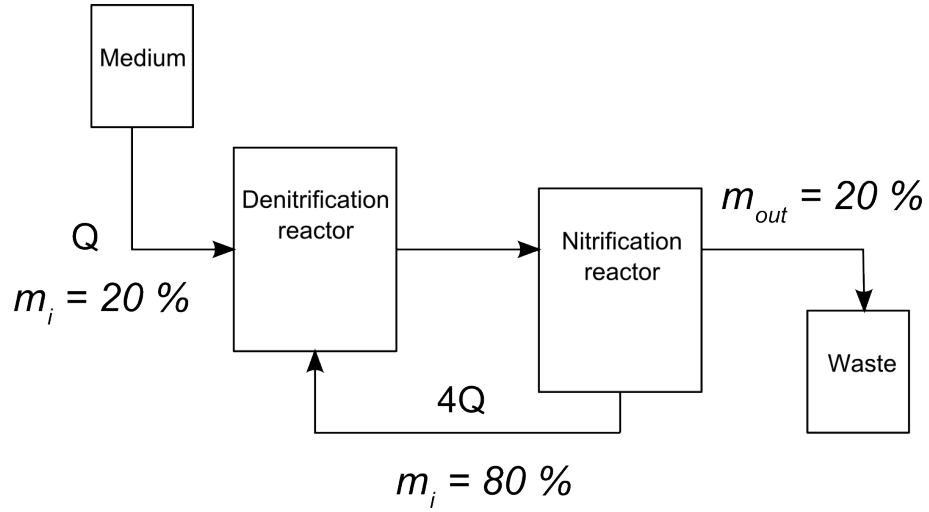


**Figure 2.13:** Flow scheme of the pre-denitrification system, whereas  $Q$  is the flowrate,  $m_i/m_{out}$  denotes mass in/out respectively.

According to this set-up, the mass balances of the reactors can be calculated as shown for the denitrification reactor in Equation 2.2, and nitrification reactor in 2.3 respectively.

$$m_{in} = 20\% m_{media} + 80\% m_{Nitrification} \quad (2.2)$$

$$m_{in} = m_{out} \text{ (Denitrification)} \quad (2.3)$$

#### 2.6.4 Monitoring

Samples of 10mL were taken from the denitrification reactor, the nitrification reactor and the medium at least every second day to monitor the activity of the pre-denitrification system. The samples were collected with a syringe from BD Plastipak and filtered with 0.45 $\mu$ m filters from Sarstedt to remove suspended biomass. Subsequently, the filtrates were analyzed with Hach-Lange assays for ammonium, nitrate and nitrite concentration, and when necessary diluted with distilled water to fit in the detection range of each assay. Additionally, the samples were also analyzed for primary amines, COD and total nitrogen concentration using the fluorescamine Assay and the Hach-Lange assays respectively. The time, pH and dissolved oxygen (%DO) were noted whenever samples were taken. The flowrate and consumption of acid and base were also checked from time to time.

### 2.6.5 Reclaimer waste as a sole carbon source

In order to test the ability to utilize the reclaimer waste as a sole carbon source, the pre-denitrification system was operated as follows: The concentration of MEA, the main constituent of reclaimer waste, was assumed to be approximately 11mol/L, therefore it was diluted 1:1000 with medium as described in section 2.6.2. Throughout the experiment the denitrification reactor was fed with medium containing approximately 11mmol/L reclaimer waste with a flowrate of 100mL/h. Figure 2.14 shows the operational timeline of the pre-denitrification system with the changes in regard to ammonia and nitrate addition.

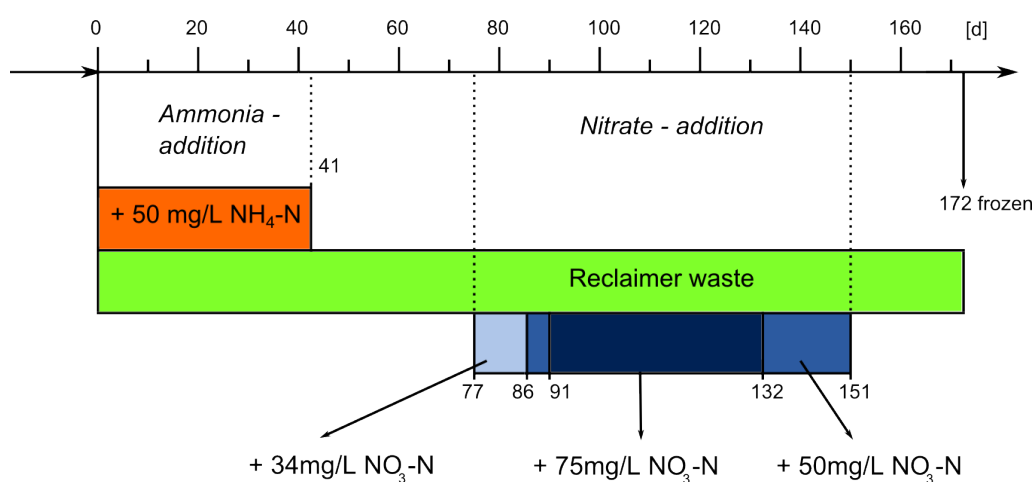


**Figure 2.14:** Operational timeline of the pre-denitrification system in days.

#### *LC-MS analysis*

Samples were analyzed by LC-MS at two different timepoints, being day 17 and day 97. Although the fluorescamine assay seems to be relatively reliable, it is unspecific and detects any primary amine. In order to determine the specific concentration of MEA, the LC-MS provides highly accurate and reliable results. For quantification of MEA, samples were taken at day 17 and day 97 from the media, the nitrification reactor and the denitrification reactor. A qualitative LC-MS positive and negative scan of the reclaimer waste, as well as a quantification of some known degradation products was done with samples taken at day 97 from the media, the nitrification and denitrification reactor. All samples were collected with a syringe from BD Plastipak and filtered with 0.45µm filters from Sarstedt to remove suspended biomass, whereas 1mL each was forwarded to SINTEF for the LC-MS analysis.

### 2.6.6 Acute Toxicity Test

An acute toxicity test was carried out to determine the  $EC_{50}$  of reclaimer waste on the nitrifying culture. The standardized assay was previously also done by Colaco for MEA [14] and by Skjæran for AMP [47] on the same nitrifying culture.

For this assay 100mL of carriers were transferred from the nitrifying reactor into an empty batch reactor with the same set-up as shown in Figure 2.11. The reactor was then filled with 500mL medium as described in section 2.6.2, without reclaimer waste and an ammonium concentration of 50mg/L  $NH_4-N$ .

Samples of 5mL were taken every 30 minutes, over a total time range of 3 hours. The samples were collected with a syringe from BD Plastipak and filtered with 0.45 $\mu$ m filters from Sarstedt to remove suspended biomass. The filtrates were then analyzed with Hach-Lange assays for their  $NO_3-N$  concentration, and when necessary diluted with distilled water to fit in the detection range of the assay.

After 3 hours the reactor was drained and refilled with 500mL media containing reclaimer waste. Following this procedure, the biofilm carriers were subsequently exposed to a series of logarithmic increasing concentrations of reclaimer waste ranging from 0; 3.16; 10; 31.6; 100 to 316mmol/L. The respective solutions were prepared in 500mL medium as described in section 2.6.2, with an ammonium concentration of 50mg/L  $NH_4-N$ . Because of the alkalinity in higher concentrations, the pH was again adjusted to 7.5 with 6mol/L HCl solution. The flow diagram of the experiment is depicted in Figure 2.15.

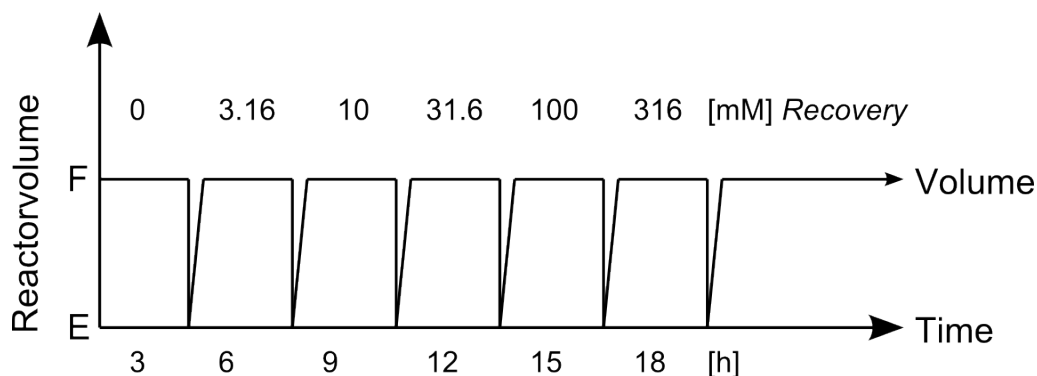


**Figure 2.15:** Flow schema of the acute toxicity assay, whereas E means Empty and F denotes Full.

After monitoring the highest concentration, the biofilm was washed with tap water and left in medium (as given in 2.6.2) with an ammonium concentration of 50mg/L  $\text{NH}_4\text{-N}$  for recovery and an activity monitoring over 3h was done again after 30 hours, respectively 14 days. After recovery the biofilm was returned to the main nitrification reactor.

The results of the  $\text{NO}_3\text{-N}$  formation were taken to calculate the respective effect on the nitrifying culture.  $\text{EC}_{50}$  is a common parameter to compare the concentration dependent effect of a substance, whereas this value is the effect concentration at which the activity reaches a level of 50%. By plotting the produced amount of  $\text{NO}_3\text{-N}$  as a function of time, the slope expresses the nitrification activity in [mg/h]. The respective activity, as well as the recovery, were then normalized with the initial activity, expressed in percent, and plotted versus concentration in log-scale. To interpolate the  $\text{EC}_{50}$  value a descriptive regression model was applied, being a three-parameter logarithm model [28, 33, 44, 31]. The equation for the interpolation of the three-parameter logarithm model is given below in Equation 2.4.

$$y = a - b * \ln(x + c) \quad (2.4)$$

## 2.7 Waste handling

Throughout the experiments, the generated waste containing either amines or reclaimer waste, was collected and disposed of at the Department of Chemical Engineering, NTNU, and further processed according to the regulations.



## Chapter 3

# Results and Discussion

### 3.1 Reclaimer waste analysis

#### 3.1.1 LC-MS analysis

Samples of the reclaimer waste were analyzed by LC-MS. The suggested identified compounds were quantified as shown in Table 3.1. Besides the listed compounds, also 2-oxazolidone (CAS number 497-25-6) was identified, but due to interference and bad chromatography it could not be quantified. Some problems for MEA also occurred, as the mass/charge ratio equals MEA, but the retention time differs. Both full chromatograms of the positive and negative scan are shown in Appendix B.

**Table 3.1:** Quantification of suggested compounds of the reclaimer waste analyzed by LC-MS.

Compound	Quantity	Unit	IUPAC Nomenclature	CAS Number
MEA	9.6	mol/L	2-aminoethanol	141-43-5
HEEDA	38.7	mmol/L	N-(2-hydroxyethyl)ethylenediamine	111-41-1
HEGly	42.3	mg/mL	N-(2-hydroxyethyl)glycine	5835-28-9
HEF	28.1	mg/mL	2-hydroxyethylformamide	693-06-1
HEPO	12.04	mg/mL	4-(2-hydroxyethyl) piperazine-2-one	23936-04-1
HEI	10.5	mg/mL	1-(2-Hydroxyethyl)imidazole	1615-14-1
HEA	8.18	mg/mL	(2-hydroxyethyl)-acetamide	142-26-7
BHEOX	0.06	mg/mL	N,N-Bis(2-hydroxyethyl)oxamide	1871-89-2

### 3.1.2 Hach-Lange analysis

The results of the reclaimer waste analysis based on Hach-Lange assays and the Fluorescamine assay are listed in Table 3.2.

**Table 3.2:** Analysis of the reclaimer waste based on Hach-Lange and fluorescamine assay. The average values are given with the respective standard deviation.

Compound	Quantity	Unit
COD	1575±40	g/L
NH <sub>4</sub> <sup>+</sup> -N	7.2 ±2	g/L
NO <sub>3</sub> -N	1.7 ±0.13	g/L
NO <sub>2</sub> -N	0.014 ±0.01	g/L
MEA-N	140.5 ±27	g/L
Total Nitrogen	235.3 ±10	g/L

The unidentified nitrogen content, being 86g/L, could be accounted for unidentified degradation products of MEA. The nitrogen content of the identified degradation products (by LC-MS) amounts to approximately 15g/L, still leaving roughly 70g/L unidentified. Although 2-oxazolidone could not be quantified, this compound does not account for such a large quantity of nitrogen, as it usually reacts to form other products (Eide-Haugmo, I. 2011, person. comm.). The chromatogram of the LC-MS scan shows many other peaks, suggesting the presence of further products. Strazisar et al. [50], identified a big amount of 3-hydroxyethylamine-N-hydroxy-ethyl propanamide, as well as 2-hydroxyethylamino-N-hydroxyethyl acetamide, but neither of them were identified in this study. Particularly the latter is a major degradation product, as also confirmed by Lepaumier et al. 2011 [26] when comparing the MEA degradation in pilot-scale with lab-scale experiments.

## 3.2 Biofilm development

Based on the measured COD value per Kaldnes K1 carrier, the geometric mean of 5 replicates was calculated for each time point and the geometric mean of empty carriers, being 748mg/L ±75, was subtracted. The results of the gained COD are shown as a function of time in Figure 3.1. The error bars represent the SEM (standard error of the mean), calculated upon the standard deviation of each time point.

During the entire time course no significant change in the amount of gained COD could be recorded. Even with the 4-fold available amount of initial substrate, the organic load on the carriers did not increase considerably. When doubling the flowrate it appears that the shear stress sloughed off excess biomass, preventing further growth. Furthermore, the start point of the experiment should be reconsidered in future experiments, as the organic

load was already 5-times higher than that of empty Kaldnes K1 carriers. The nitrifying activity of the biofilm during the experiment is given in Appendix A.

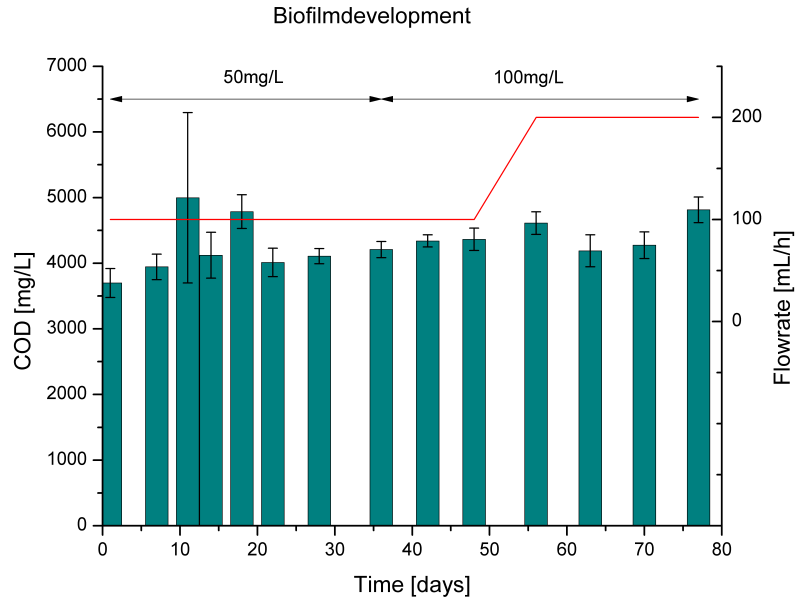


**Figure 3.1:** The geometric mean of gained COD during the development of nitrifying biofilm on Kaldnes K1 carriers as a function of time. The error bars indicate the SEM; the flowrate is represented by the solid red line and corresponds to the right ordinate. Varying concentrations of ammonia are indicated by the horizontal arrows.

### 3.3 Inhibition of nitrification

#### 3.3.1 Biofilm history

The acute toxicity of reclaimer waste and other amines was tested in three independent experiments. Table 3.3 gives an overview of the chronological order and which amines were tested on which biofilm. As described in section 2.4, the biofilm was returned to the bioreactor after Experiment 2, therefore the biofilm in Experiment 3 was previously exposed to amines. In the following section the results will be organized according to this experimental outline.

**Table 3.3:** Acute Toxicity experiments on nitrifying culture

	Date	Tested compound	Biofilm origin	Previous exposure
Experiment 1	09.06.2010	Reclaimer waste	Pre-denitrification (Section 2.6)	AMP, MEA
Experiment 2	25.06.2010	Reclaimer waste, MEA	Nitrification (Section 2.4)	none
Experiment 3	14.10.2010	AMP, DEA, aMDEA, Piperazine	Nitrification (Section 2.4)	Reclaimer waste, MEA

### 3.3.2 Acute Toxicity Test

The results of Experiment 1 are given in Figure 3.2 as the nitrification activity during the acute toxicity test of reclaimer waste on the nitrifying culture and the corresponding recovery as a function of time. The shift in the amount of nitrate at the starting point of measurements in the higher concentration range may be explained by an interference of components in the reclaimer waste with the quantification assay. The linear activity during the first hours of the experiment should be pointed out, as a stable nitrification activity is vital in order to proceed with the experiment. Due to the high inhibition at a concentration of 100mmol/L, the experiment had to be aborted and the last concentration of 316mmol/L was not tested. The recovery in respect to the initial activity was 44% after 30 hours, respectively 60% after 14 days.

In Experiment 2 of the reclaimer waste, all concentrations could be tested as shown in Figure 3.3. The recovery in respect to the initial activity was 108% after 30 hours.

The experimental results of the acute toxicity of MEA in Experiment 2 are shown in Figure 3.4, whereas the recovery in respect to the initial activity was 109% after 30 hours.

For estimating the  $EC_{50}$ , the calculated slope of each concentration is set relative to the slope of the initial activity without the test substance. Based on the calculated percental activity, a logistic model was applied to interpolate the concentration at 50% activity. This applies for all tested substances, except for Experiment 1. In this case a three-parameter

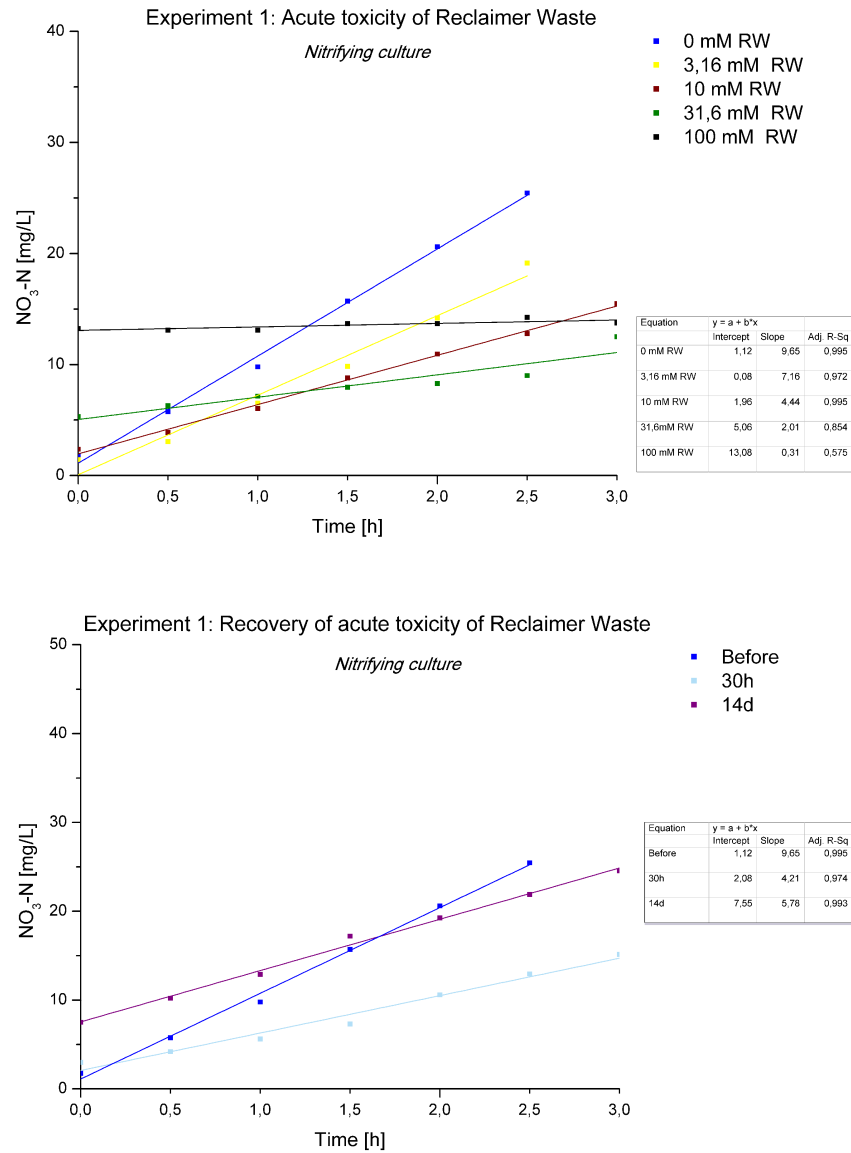


**Figure 3.2:** Experiment 1: The nitrification activity during the acute toxicity of reclaimer waste on the nitrifying culture (upper panel), and the activity after 30 hours, respectively 14 days of recovery of the acute toxicity (lower panel).

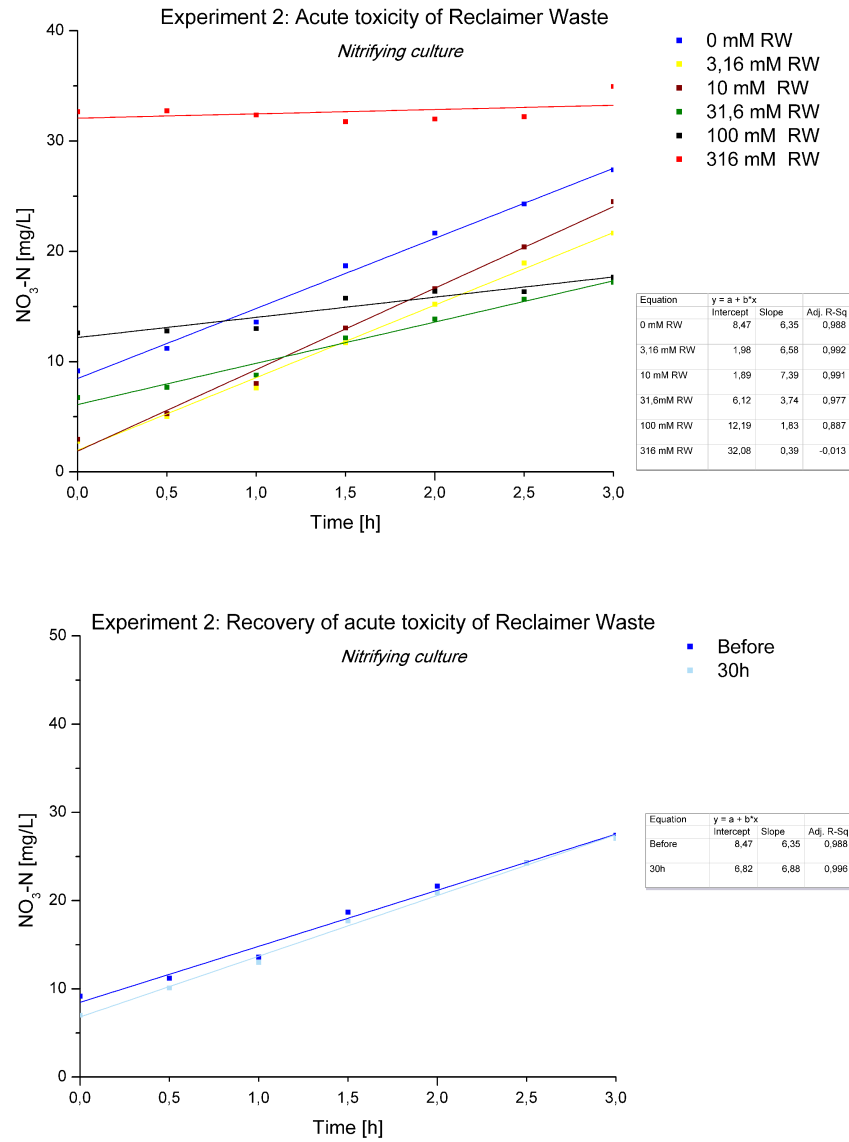


**Figure 3.3:** Experiment 2: The nitrification activity during the acute toxicity of reclaimer waste on the nitrifying culture (upper panel), and the activity after 30 hours recovery of the acute toxicity (lower panel).

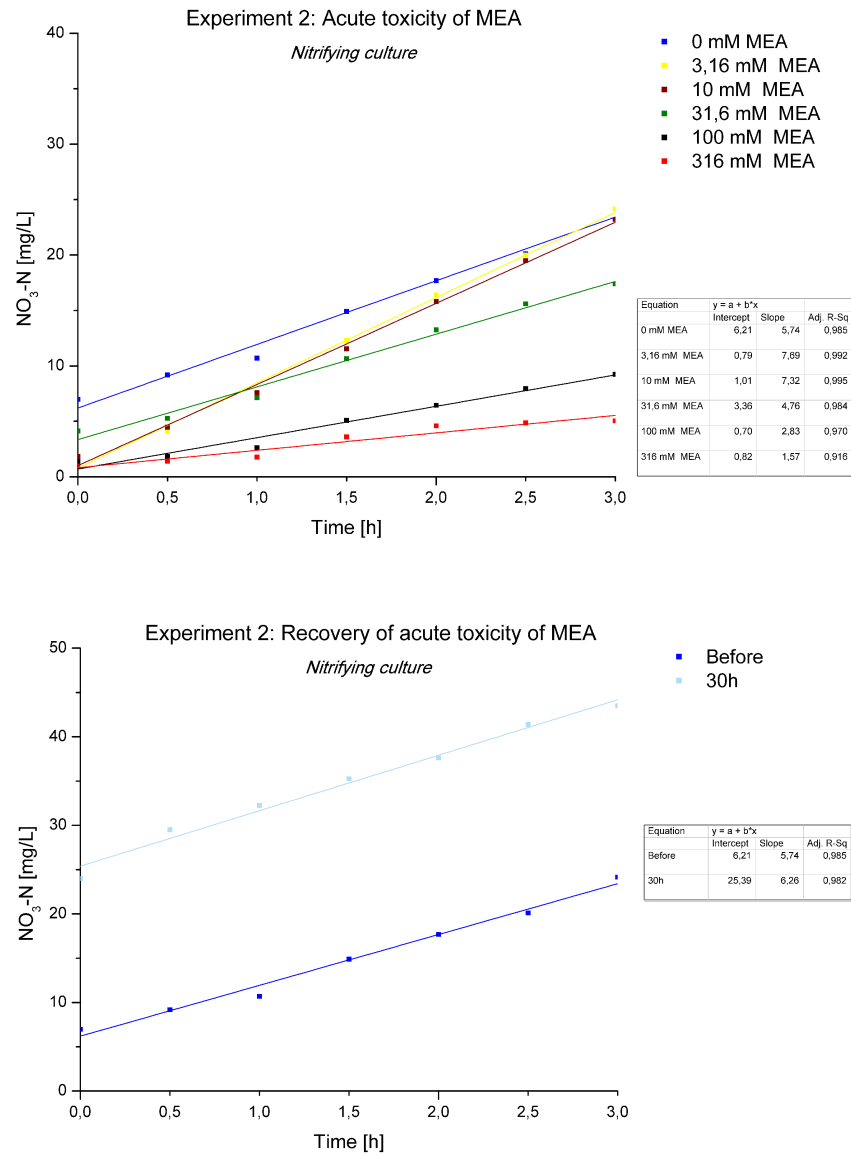


**Figure 3.4:** Experiment 2: The nitrification activity during the acute toxicity of MEA on the nitrifying culture (upper panel), and the activity after 30 hours recovery of the acute toxicity (lower panel).

logarithm model had to be applied, due to lack of datapoints. The  $EC_{50}$  of reclaimer waste in Experiment 1 is 8mmol/L and 40mmol/L in Experiment 2. For MEA the  $EC_{50}$  was estimated to be 86mmol/L. Figure 3.5 shows the relative activity as a function of the logarithmic dose, with the fitted curves and the estimated  $EC_{50}$  for reclaimer waste and MEA. The values for  $EC_{50}$  and recovery kinetics are summarized in Table 3.4, whereas the respective parameters for each model are given in Appendix C.

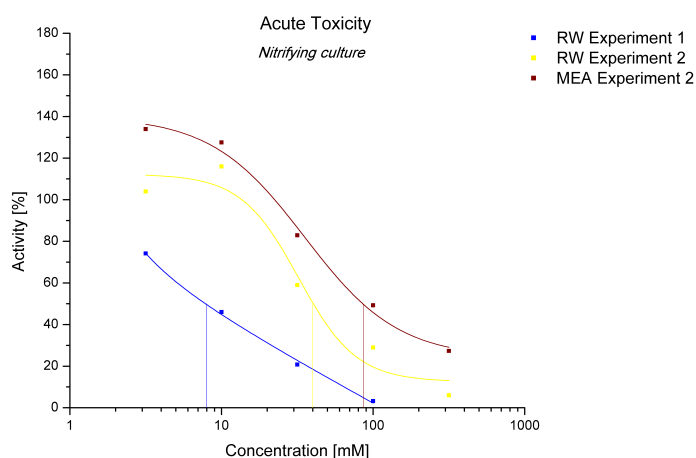


**Figure 3.5:** Acute toxicity of reclaimer waste, as well as MEA on the nitrifying culture. Experiment 1: The estimated  $EC_{50}$  of reclaimer waste is 8mmol/L, based on a three-parameter logarithm model; Experiment 2: Reclaimer waste and MEA, whereas the estimated  $EC_{50}$  of 40, respectively 86mmol/L is based on a logistic model. All tests had a monitoring time range of 3 hours for each concentration.

The following section describes the effect of piperazine, AMP, DEA, and aMDEA on the nitrifying culture in Experiment 3, accomplished as described in section 2.4.5. For all responses towards the tested amines a logistic model, calculated with Origin 8.0 [28], showed the best fit with a corrected R-square ranging from 0.986 to 1.000. The respective parameters for each model are given in Appendix C.

The nitrification activity of biofilm exposed to piperazine is shown in Figure 3.6. The recovery after 39h was 17%, 14 days showed 16%, and after 44 days 5% of the initial activity was measured.

The results of the acute toxicity of AMP are given in Figure 3.7, whereas after 39 hours recovery, 41% of the nitrification activity was given.



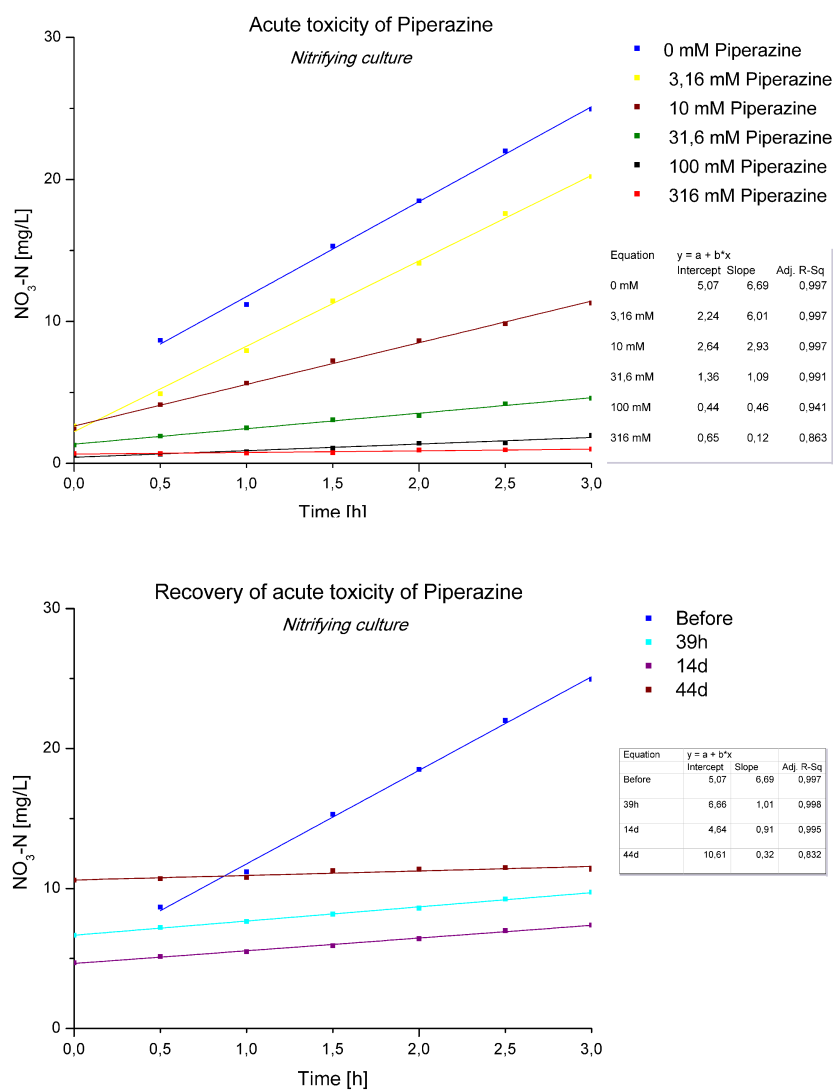


**Figure 3.6:** Experiment 3: The nitrification activity during the acute toxicity of piperazine on the nitrifying culture (upper panel), and the activity after 39 hours, 14 days and 44 days recovery of the acute toxicity (lower panel).

The results of the acute toxicity of DEA are given in Figure 3.8, whereas after 39 hours recovery, 27% of the initial nitrification activity was measured.

The results of the acute toxicity of aMDEA are shown in Figure 3.9, whereas the recovery after 39h was 84%, 14 days showed 47%, and after 44 days 4% of the initial activity was recorded.

The relative activity as a function of the logarithmic dose, with the fitted curves and the estimated  $EC_{50}$  of the selected amines is shown in Figure 3.10. The values for  $EC_{50}$  and the recovery kinetics are summarized in Table 3.4.

**Table 3.4:** Summary of the acute toxicity on the nitrifying culture.

	Amine	$EC_{50}$		Recovery[%]			
		[mmol/L]	[g/L]	30h	39h	14d	44d
Experiment 1	RW	8	-	44%	-	60%	-
Experiment 2	RW	40	-	108%	-	-	-
	MEA	86	5	109%	-	-	-
Experiment 3	Piperazine	10	0.9	-	17%	16%	5%
	AMP	30	3	-	41%	-	-
	DEA	18	2	-	27%	-	-
	aMDEA	39	5	-	84%	47%	4%

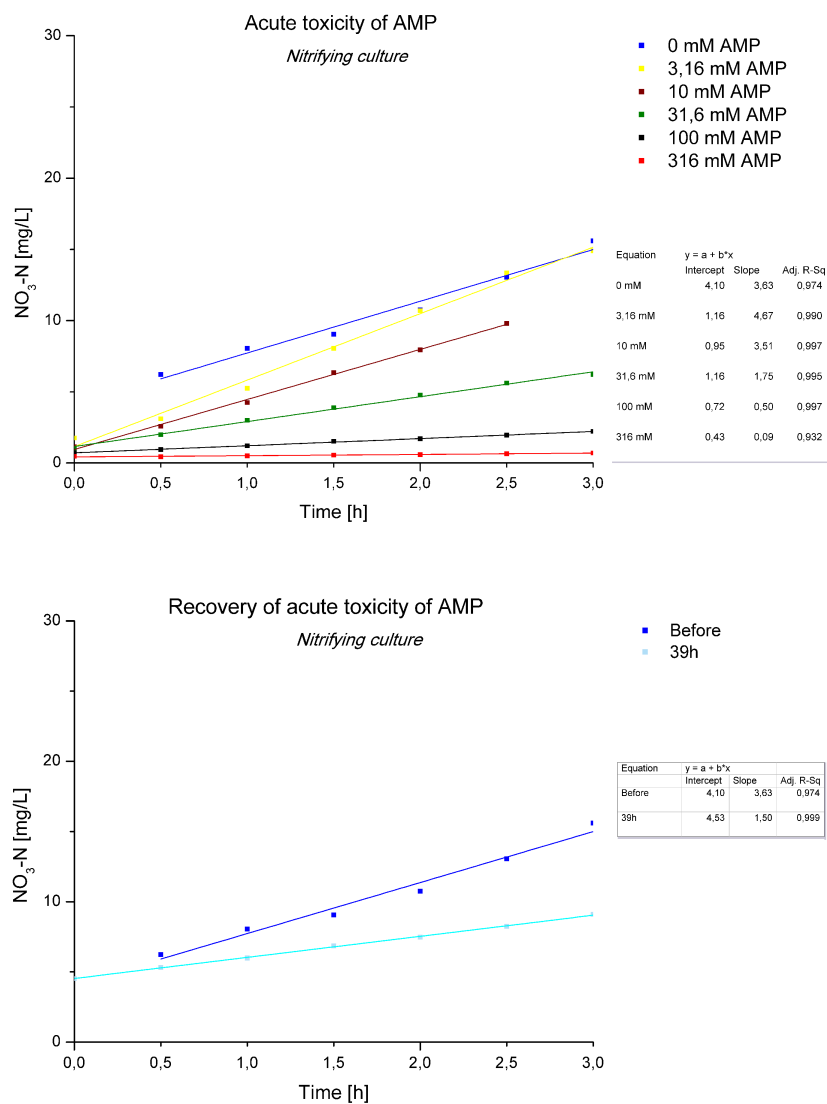


**Figure 3.7:** Experiment 3: The nitrification activity during the acute toxicity of AMP on the nitrifying culture (upper panel), and the activity after 39 hours recovery of the acute toxicity (lower panel).

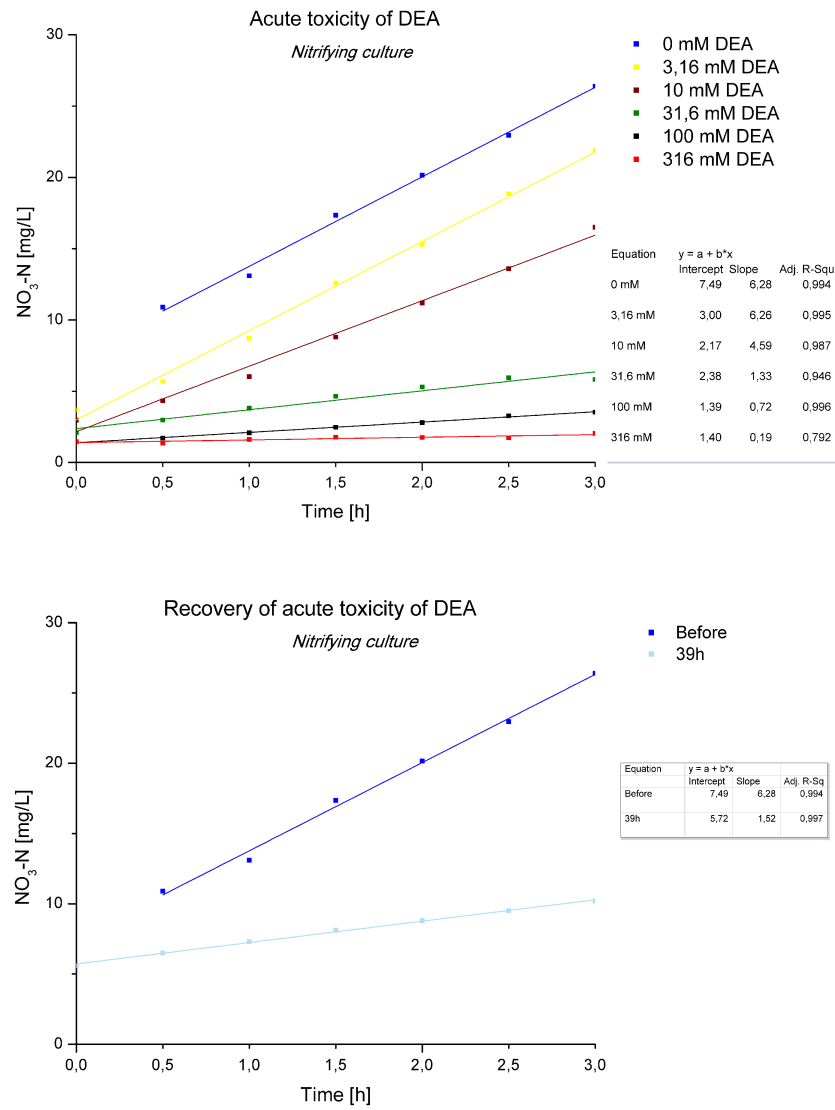


**Figure 3.8:** Experiment 3: The nitrification activity during the acute toxicity of DEA on the nitrifying culture (upper panel), and the activity after 39 hours recovery of the acute toxicity (lower panel).

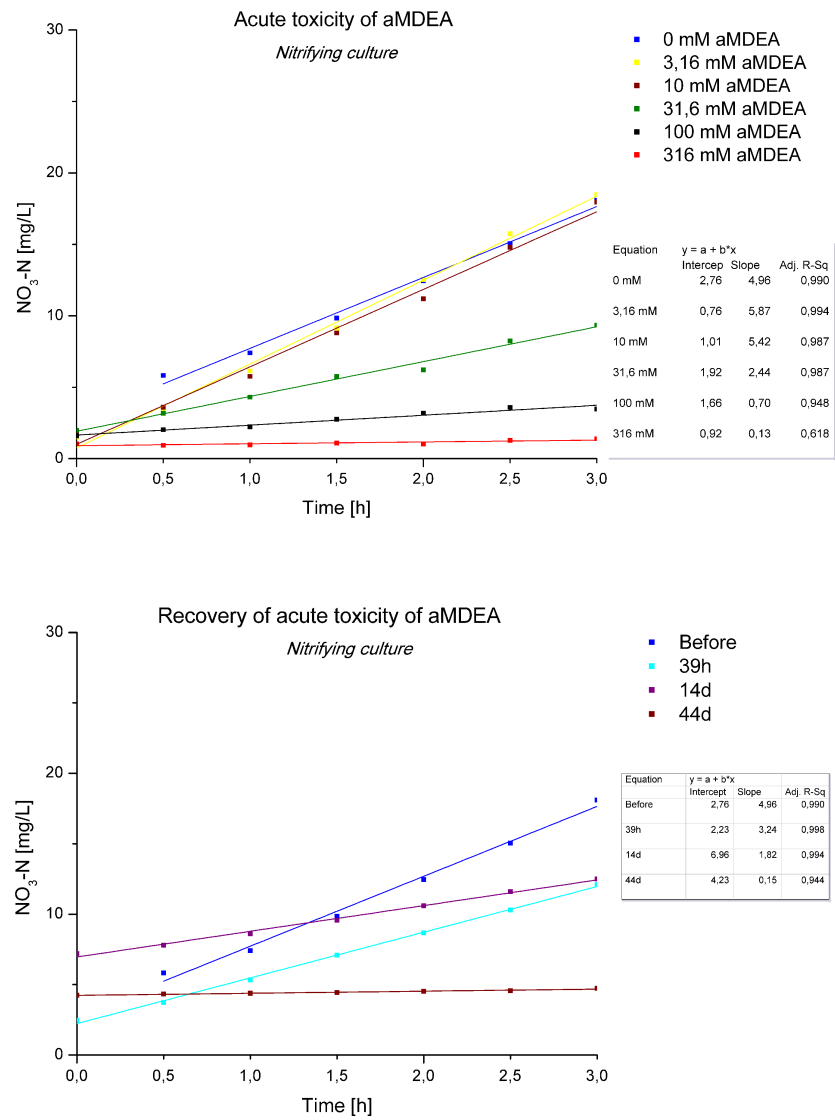


**Figure 3.9:** Experiment 3: The nitrification activity during the acute toxicity of aMDEA on the nitrifying culture (upper panel), and the activity after 39 hours, 14 days and 44 days recovery of the acute toxicity (lower panel).

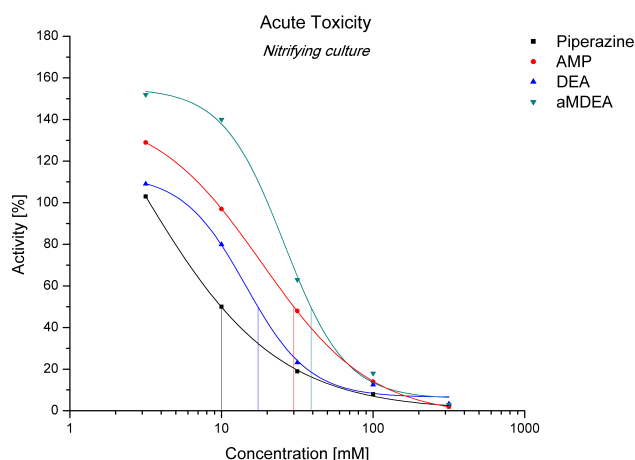


**Figure 3.10:** Experiment 3: Comparison of the acute toxicity test of piperazine, AMP, DEA, as well as aMDEA on the nitrifying culture. The calculations of  $EC_{50}$  are based on a logistic model as described in section 2.4.5, with a monitoring time range of 3 hours for each concentration.

### 3.3.3 Discussion

The stimulated nitrification activity in low doses of AMP, DEA, aMDEA, as well as MEA and reclaimer waste, could possibly be explained by the phenomenon of hormetic dose response as postulated by Calabrese [12]. In this work, it is suggested that the dose response of most, if not all, peptides conform to the hormetic model - Stimulating effect in low doses, followed by inhibition. A similar stimulating effect of toxins on nitrifying bacteria was already observed a long time ago by Wang et. al 1984 [55]. An interesting aspect of this study on the toxic effect of metal ions is, that it was also found that nickel ion, which is less toxic (or inhibiting) to *Nitrobacter sp.* than cadmium ion, is less stimulating as well. Their two hypotheses to explain the stimulation effect was firstly, during the initial exposure to toxicity, *Nitrobacter sp.* under stress are undergoing hyperactivity to cope with the metal toxicity. With the hyperactivity of *Nitrobacter sp.*, it is possible to lead to the greater consumption of nitrite because nitrite is the sole energy source. Secondly, the metal treatment results in a greater permeability of bacterial cell membranes, so that nutrient uptake increases [55]. Their hypotheses of hyperactivity and greater permeability might also apply for the nitrification culture exposed to various amines in this experiment. The correlation they found between stimulating and inhibiting effects could not be observed in these experiments. In contrast, the stimulating effect was negatively correlated; in other words piperazine, which showed the highest toxicity of an  $EC_{50}$  below 1000mg/L, had the lowest stimulating effect. aMDEA, AMP, DEA and MEA

showed much higher  $EC_{50}$  values, all in a range greater than 1000mg/L, and showing stimulating effects in descending order respectively.

Nevertheless, the determination of the  $EC_{50}$  value is a source of error in several aspects. Firstly, the pH of the respective solutions had to be adjusted prior to application, possibly leading to changes in the chemical properties of the test substances such as solubility or volatilization. This could also have an effect on the actual concentration in the bioreactor. Furthermore, the  $EC_{50}$  is calculated by means of a descriptive regression model and appears to be chosen arbitrarily, since no model prevails for describing experimental data with accuracy. Some calculations in recent literature are based on the linear fraction of the test results, which would exclude data points of the result and shift the value towards a higher or lower concentration, depending on the assumed area of linearity. After testing different descriptions, the most unbiased calculation of the  $EC_{50}$  value seems to be achieved by applying a curve-fitting model, including all datapoints, such as the logistic or three-parameter logarithmic model.

However, when calculating the  $EC_{50}$  of AMP on data from Skjæran [47] with the same logistic model as applied in the presented data, the value is well in agreement with 30mmol/L, shown in Figure 3.11. The parameters for this model, with a corrected R-square of 0.997, were  $A1 = 70.14$ ,  $A2 = -1.35$ ,  $x_0 = 57.37$ , with  $p = 1.49$ .

The accordance of the  $EC_{50}$  of 30mmol/L for AMP on two independent experiments on nitrifying culture suggests a constant respond behaviour towards the acute toxicity of AMP. Nevertheless, the experiments should be repeated to verify the reproducibility on other biofilm carriers too. In terms of recovery, the result is not consistent with Skjæran [47], as she had a recovery of 100% after 30 hours, being only 41% in this experiment.

For acute toxicity towards reclaimer waste, two different batches of nitrification biofilm were tested. Experiment 1 showed an  $EC_{50}$  of 8mmol/L in contrast to Experiment 2, showing a higher  $EC_{50}$  of 40mmol/L. It would have been expected that the previously exposed to AMP and MEA biofilm of Experiment 1 would be less sensitive towards the reclaimer waste, as the culture had experienced toxic exposure, thus being able to adapt over a longer time period. Despite this assumption, they were highly sensitive, therefore the experiment was aborted after a concentration of 100mmol/L reclaimer waste, since the activity was already as low as 3%.

Experiment 2 was run on biofilm carriers never exposed to toxic loads of amines before, showing a much higher tolerance level. Also in regard to the recovery rate after 30 hours, a huge difference was observed, being 108% for unexposed (Experiment 1) and 44% for

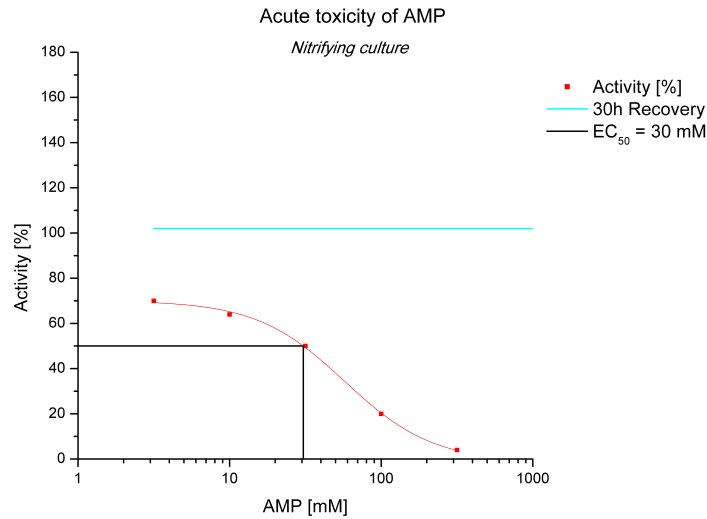


**Figure 3.11:** Effect concentration of AMP on the nitrifying culture, calculated with data from Skjæran [47]. The regression analysis is based on the logistic model, as used for the calculations of the  $EC_{50}$  value of AMP presented in this work. The monitoring time range was 3 hours for each concentration.

the exposed biofilm (Experiment 2). It is difficult to assess whether the varying results of reclaimer waste are due to the biofilmage, respectively the thickness limiting diffusion over the surface, or due to changes in the biofilm community, as more resistant cultures could be more pronounced in one of the biofilms, therefore showing a higher tolerance level.

In any case, the experiments should be repeated for statistical reasons, as well as to state a clear answer in respect to the biofilm composition. Thus, molecular biological methods such as FISH (Fluorescence in situ hybridization) and DGGE (Denaturing gradient gel electrophoresis) should be utilized to characterize the microbial community at the time of each test. Furthermore, a quantification of the biofilm on the carriers, e.g. by determination of the average COD per carrier used in the experiment, would allow to estimate the impact of diffusional limitation over the surface. Thus, making a correlation between biofilm age, respectively thickness and the respond possible.

In the previous inhibition studies of MEA by Colaco [14], an  $EC_{50}$  of 10mmol/L MEA was estimated for the nitrification culture previously unexposed to amines. Her value was calculated within the linear region of her dataset, which could be the reason for the lower result compared to the  $EC_{50}$  of 86mmol/L MEA in the here presented experiment, which was also run on nitrifying culture previously neither exposed amines.



When recalculating her data with the same logistic model, an  $EC_{50}$  of 19mmol/L was interpolated, still showing a large discrepancy. The second acute toxicity test she did on the same biofilmcarriers, accomplished after approximately 40 days recovery, showed an  $EC_{50}$  of 100mmol/L, based on the same linear calculation method [14]. However, the latter recalculated result of 118mmol/L is in the same order of magnitude as the  $EC_{50}$  of 86mmol/L MEA.

A reason for the varying  $EC_{50}$  of MEA could again be found in the biofilm age, respectively thickness, since at the first acute toxicity test, the biofilm carriers of Colaco were approximately 80 days, respectively 120 days at the time of the second acute toxicity test. In addition, a shift in microbial community was suggested during the recovery time, as the appearance of the carriers had changed to a darker colour. Moreover, Colaco suggested microbial death instead of inhibition, leading to a culture better adapted to an environment with MEA [14]. The biofilm used for the acute toxicity test of MEA in this study was at least 120 days old, making the thickness comparable with the second test of Colaco [14].

Since nitrifying bacteria have a relatively low growth rate and are mostly situated in the inner core of aerobic biofilm [36], it would be possible that the outer layer of heterotrophic bacteria acts as a protective shield, dying off first. If the inhibitional/toxic effect of selected amines depends largely on the diffusional barrier dependent on the microbial community, this could be shown in future works by characterizing and quantifying the biofilm before and after the acute toxicity test.

For piperazine, DEA and aMDEA no comparable data exists yet, therefore the experiments should be repeated to verify the reproducibility on other biofilm carriers too. Piperazine can react with nitrosating agents, such as nitrogen oxides, nitrites, or nitrous acid, to form nitrosamine derivatives [1], perhaps explaining the comparably high acute toxicity, as well the deteriorating recovery after the acute toxicity test, as residues could have been left in the reactor. The latter also seems to apply for the worsening recovery of biofilm carriers exposed to aMDEA.

For all amines the obtained  $EC_{50}$  values are at least one order of magnitude greater than the  $LC_{50}$  values for algae/bacteria as presented in the report of NIVA [10], as well as from Eide-Haugmo et al. [17]. Their values are generally based on freeze dried luminescent bacteria (*Photobacterium phosphoreum*), respectively (*Skeletonema Costatum*) as the test organisms. Therefore, the lower responds in the here presented data could also be as a result of different properties of bacteria/algae, especially the robustness within the community of a biofilm.

## 3.4 Inhibition of denitrification

### 3.4.1 Acute Toxicity Test

The acute toxicity test on the denitrifying culture was accomplished as described in section 2.5.5.

The results of the acute toxicity, respectively recovery of piperazine are shown in Figure 3.12. The lower initial level at a concentration of 316mmol/L piperazine might be due to an interference with the quantification assay, resulting in an understimation of the actual nitrate concentration.

The results of the acute toxicity test, as well as the recovery of AMP on the denitrifying culture are shown in Figure 3.13. Also in this case, the highest concentration of AMP, being 316mmol/L showed a lower concentration of nitrate compared to the rest of the dataset. This might also be explained by an interference with the nitrate quantification assay.

The results of the acute toxicity, respectively recovery of DEA are shown in Figure 3.14. The lower initial level at a concentration of 316mmol/L DEA might be due to an interference with the quantification assay, resulting in an understimation of the actual nitrate concentration.

The results of the acute toxicity, respectively recovery of aMDEA are shown in Figure 3.15.

Since none of the tested amines showed a significant inhibition on the denitrification culture, no effect concentration could be calculated. A comparison of the percentual activity for each corresponding concentration is given in the Figure 3.16, as well as in Table 3.5 below.

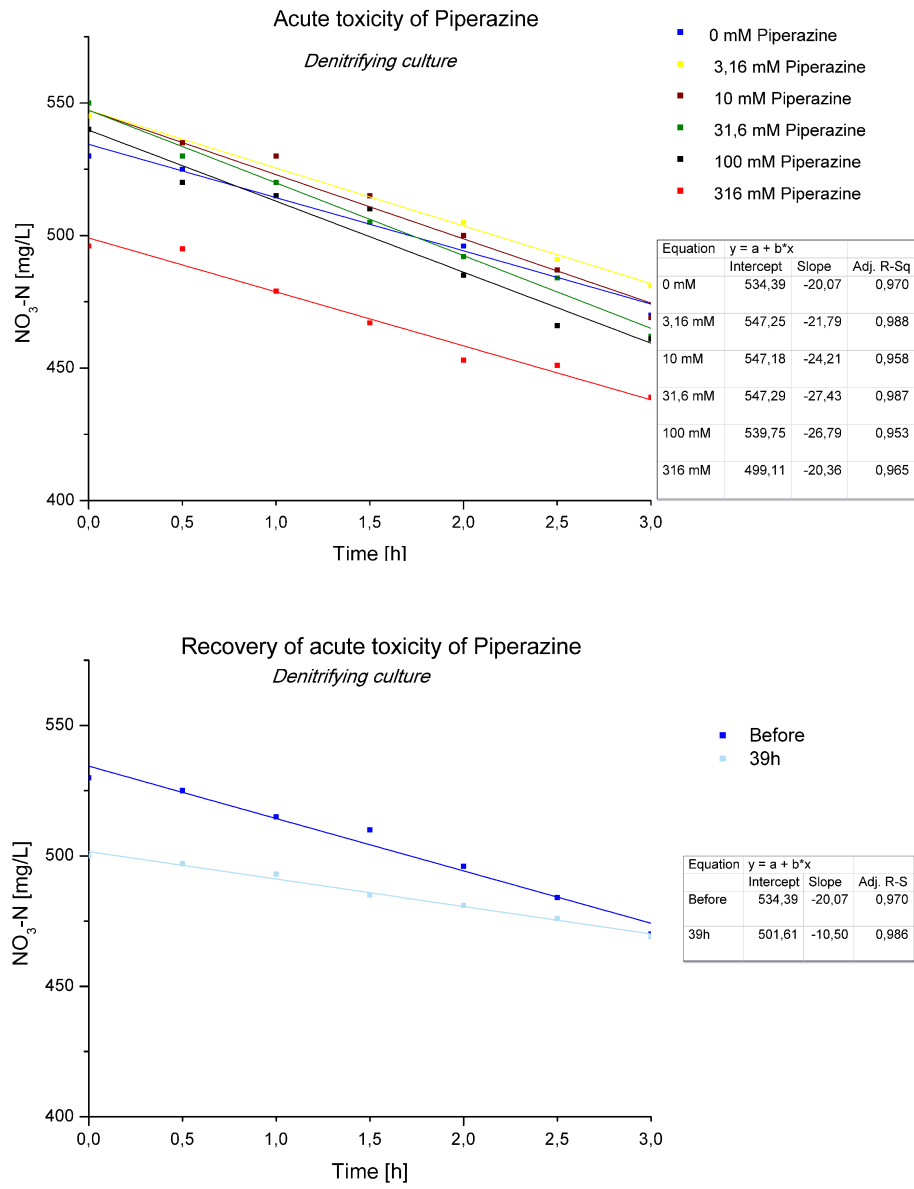


**Figure 3.12:** The denitrification activity during the acute toxicity of piperazine on the denitrifying culture (upper panel), and the activity after 39 hours recovery of the acute toxicity (lower panel).

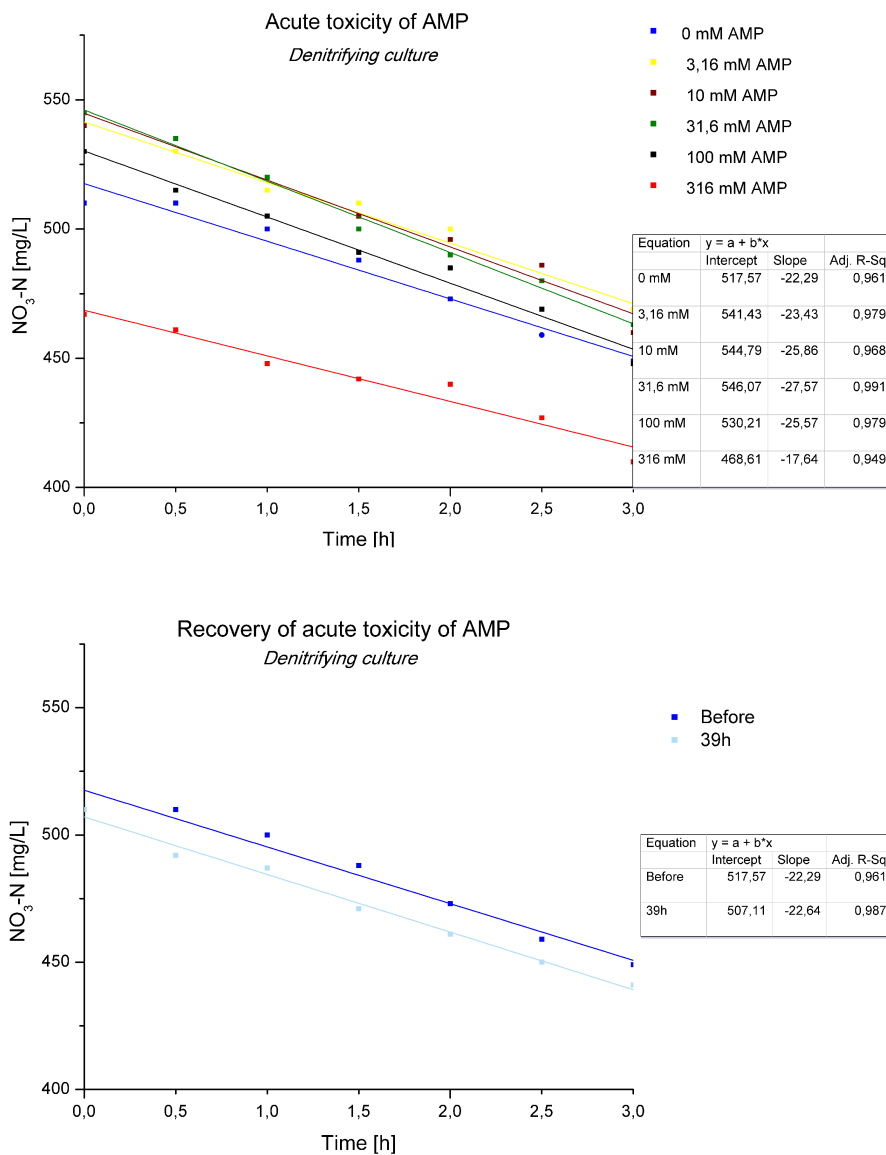


**Figure 3.13:** The denitrification activity during the acute toxicity of AMP on the denitrifying culture (upper panel), and the activity after 39 hours recovery of the acute toxicity (lower panel).

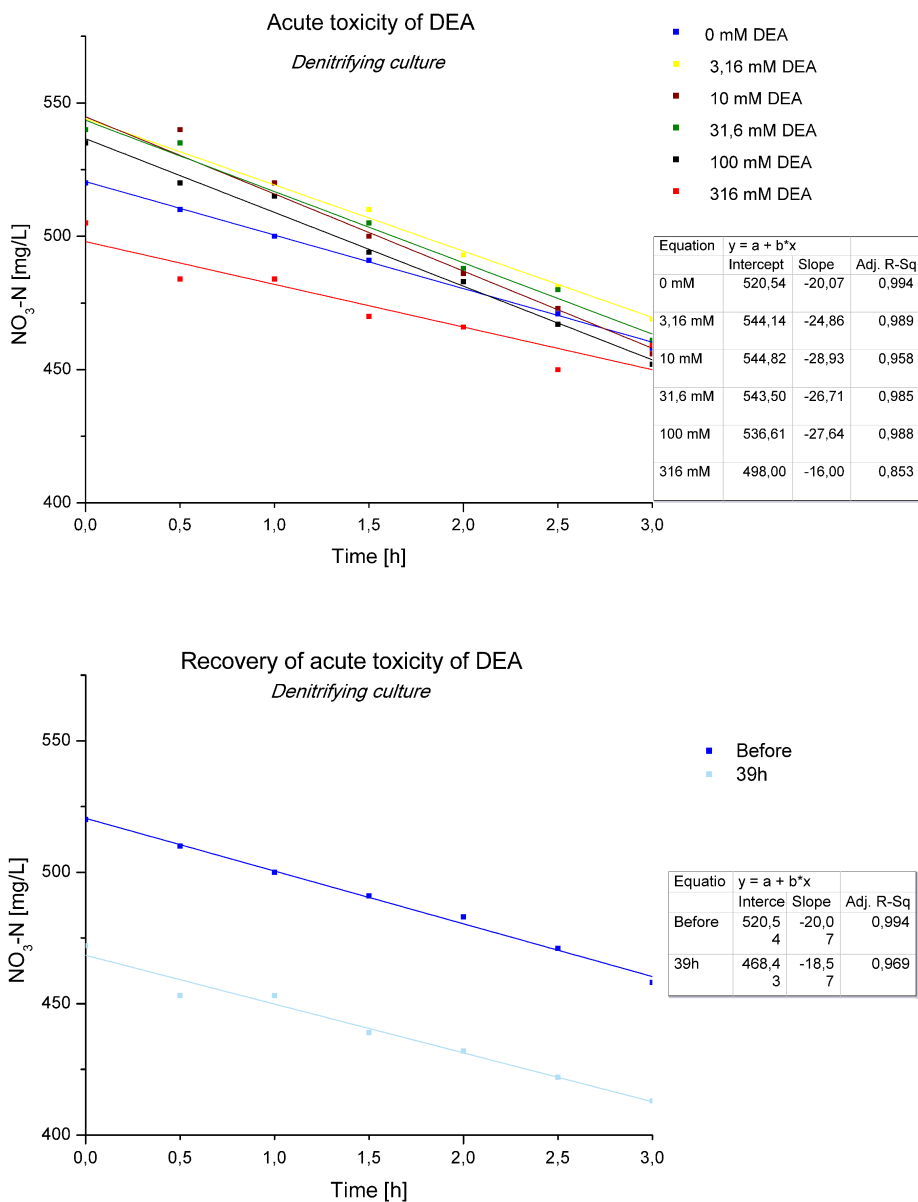


**Figure 3.14:** The denitrification activity during the acute toxicity of DEA on the denitrifying culture (upper panel), and the activity after 39 hours recovery of the acute toxicity (lower panel).

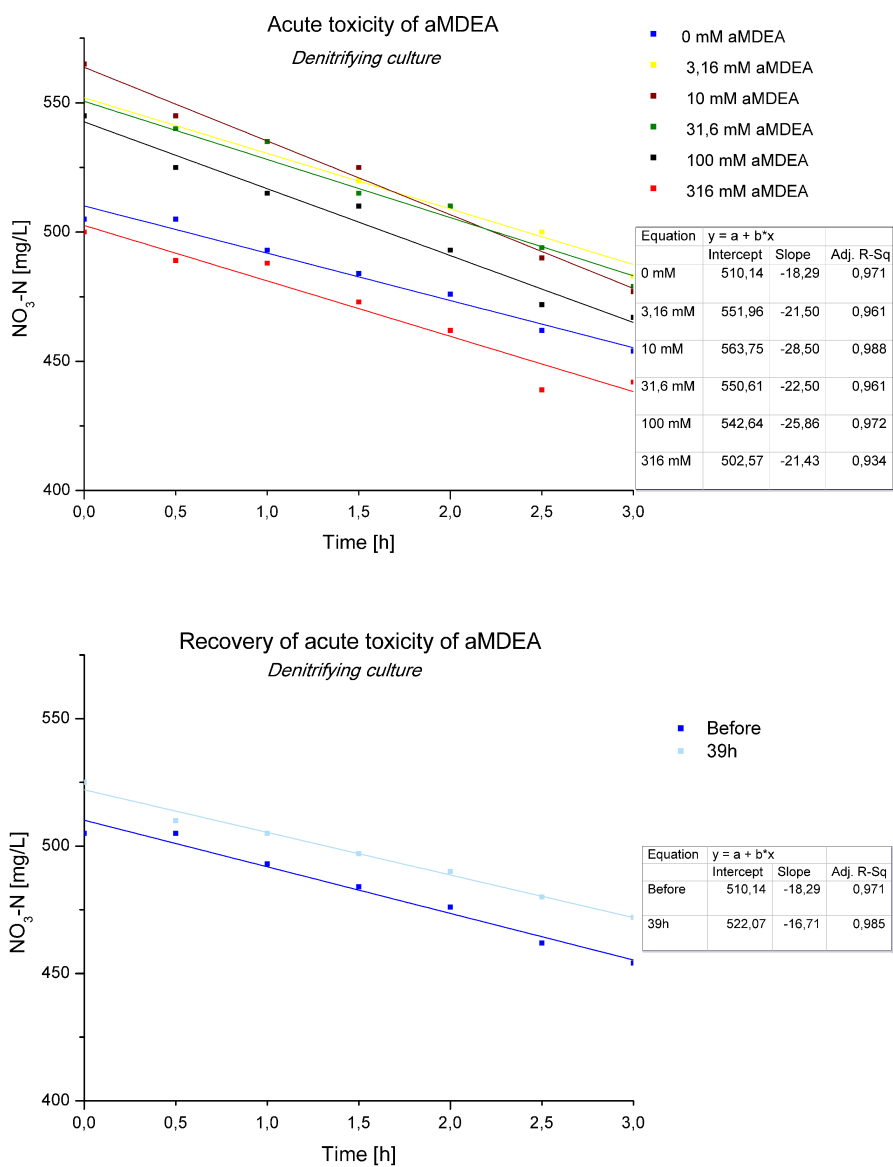


**Figure 3.15:** The denitrification activity during the acute toxicity of aMDEA on the denitrifying culture (upper panel), and the activity after 39 hours recovery of the acute toxicity (lower panel)

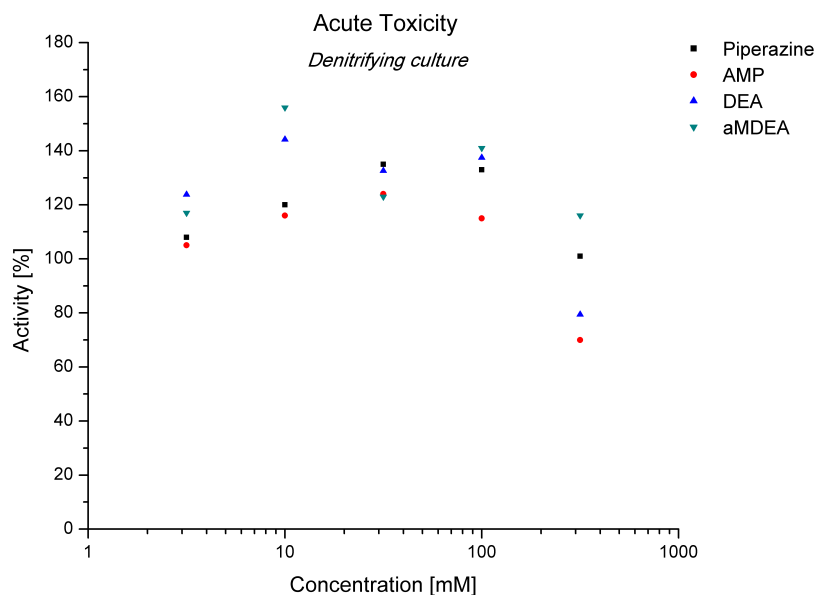


**Figure 3.16:** Comparison of the acute toxicity test of the 4 selected amines run on the denitrifying culture.

**Table 3.5:** Denitrification activity in [%] during the acute toxicity and recovery of selected amines on the denitrifying culture.

[mmol/L]	Piperazine	AMP	DEA	aMDEA
0	100	100	100	100
3.16	108	105	124	117
10	120	116	144	156
31.6	135	124	133	123
100	133	115	137	141
316	101	70	80	116
Recovery	52	101	92	92

### 3.4.2 Discussion

The denitrification activity did not show any major inhibition in the presence of any of the selected amines. Contrary to expectations, the activity was even stimulated in moderate concentrations, especially pronounced in the presence of aMDEA, reaching 156% of the initial activity. Even when considering the phenomenon of hormetic dose response as postulated by Calabrese [12] - Stimulating effect in low doses, followed by inhibition - the results show no biphasic behaviour, but an overall stimulating effect. AMP and DEA triggered an inhibitory effect of 30%, respectively 20% at the highest concentration of 316mmol/L. This respond could be addressed to high salinity of the respective solutions, since increased amounts of HCl were necessary to reach the desired pH of 7.5 in both cases.

Generally, the results suggest a high robustness of the denitrifying culture towards the tested amines. Whether this is due to the composition of the biofilm, as heterotrophs could lead to a more diverse culture within the biofilm, or the amount of biofilm on the carriers, cannot be assessed with the available data.

In any case the experiments should be repeated for statistical reasons, as well as to state a clear answer in respect to the biofilm composition. Thus, molecular biological methods such as FISH (Fluorescence In Situ Hybridization) and DGGE (Denaturing Gradient Gel Electrophoresis) should be utilized to characterize the microbial community at the time of each test. Furthermore, a quantification of the biofilm on the carriers, e.g. by determination of the average COD per carrier used in the experiment would allow to estimate the impact of diffusional limitation over the surface. Thus, making a correlation between biofilm age, respectively thickness and the respond possible.

## 3.5 Total pre-Denitrification System

### 3.5.1 Reclaimer waste as a sole carbon source

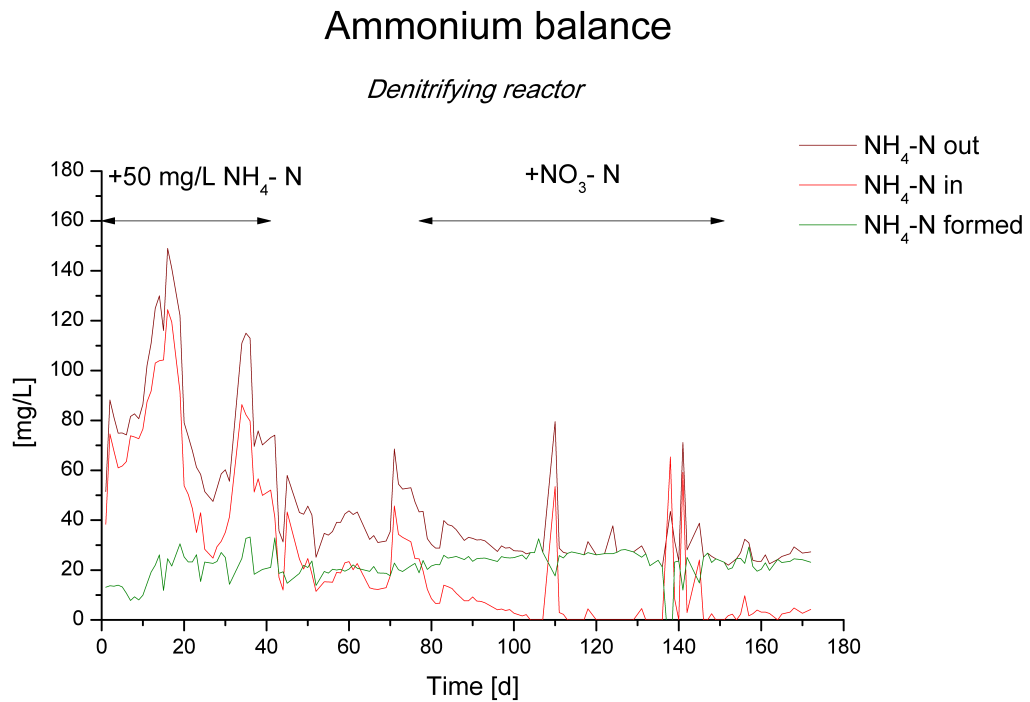
In order to test the ability of the pre-denitrification system to utilize the reclaimer waste as a sole carbon source, the pre-denitrification system was operated as described in section 2.6.5. During the entire experiment, reclaimer waste was added in a continuous mode as the sole carbon source to the pre-denitrification system. The desired concentration of approximately 11mmol/L was based on preliminary experiments of Colaco [14], where the EC<sub>50</sub> of MEA, the main constituent of reclaimer waste, was estimated to be 10mmol/L for the biofilm carriers. Changes in the media composition were in the amount of added ammonium and nitrate.



*Denitrification reactor*

The mass flow into the denitrification reactor was calculated according to Figure 2.13, respectively Equation 2.2. The total mass in, being 20% measured mass in media and 80% measured mass in the nitrification reactor, is based on the rawdata given in Appendix D.1.

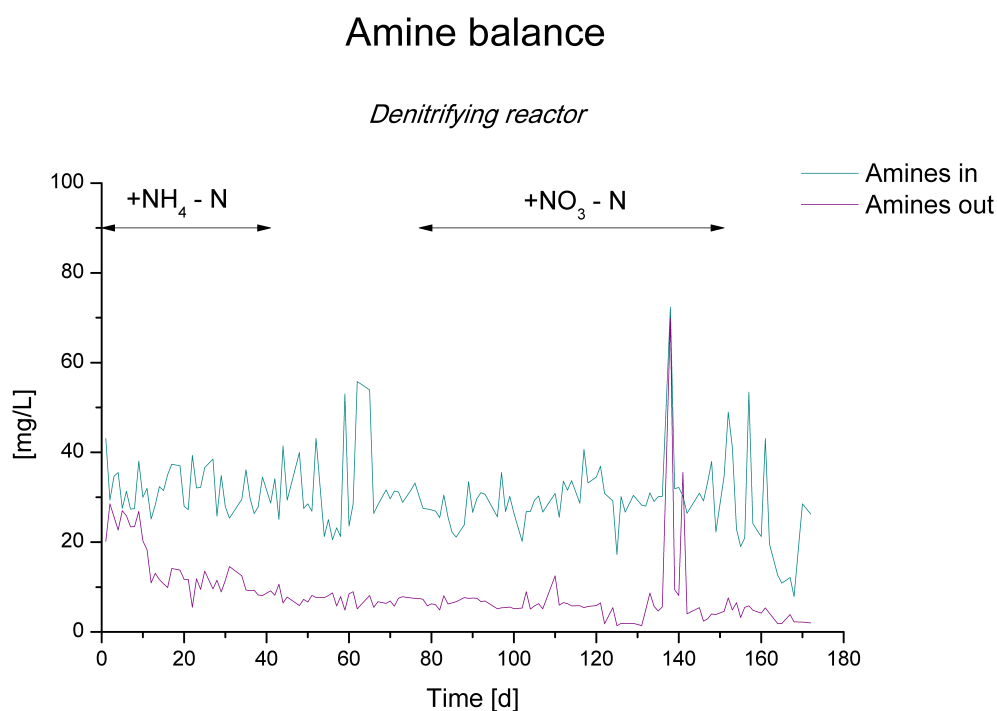
Figure 3.17 shows the calculated incoming mass of ammonium during the experiment and the measured values of the outgoing amount of ammonium in the denitrification reactor. The increase in the outgoing concentration of ammonium, is due to the degradation of MEA in the denitrifying reactor. Based on the derived mass balance, the amount of formed  $\text{NH}_4\text{-N}$  appears to be relatively constant throughout the experiment, as also shown in Figure 3.17.



**Figure 3.17:** Ammonium concentrations going in and out of the denitrifying reactor with reclaimer waste as sole carbon source. 50mg/L ammonium were added between day 0 and day 41, as indicated by the horizontal arrow; after then no more ammonium was added. The amount of formed  $\text{NH}_4\text{-N}$  is calculated upon the mass balance.

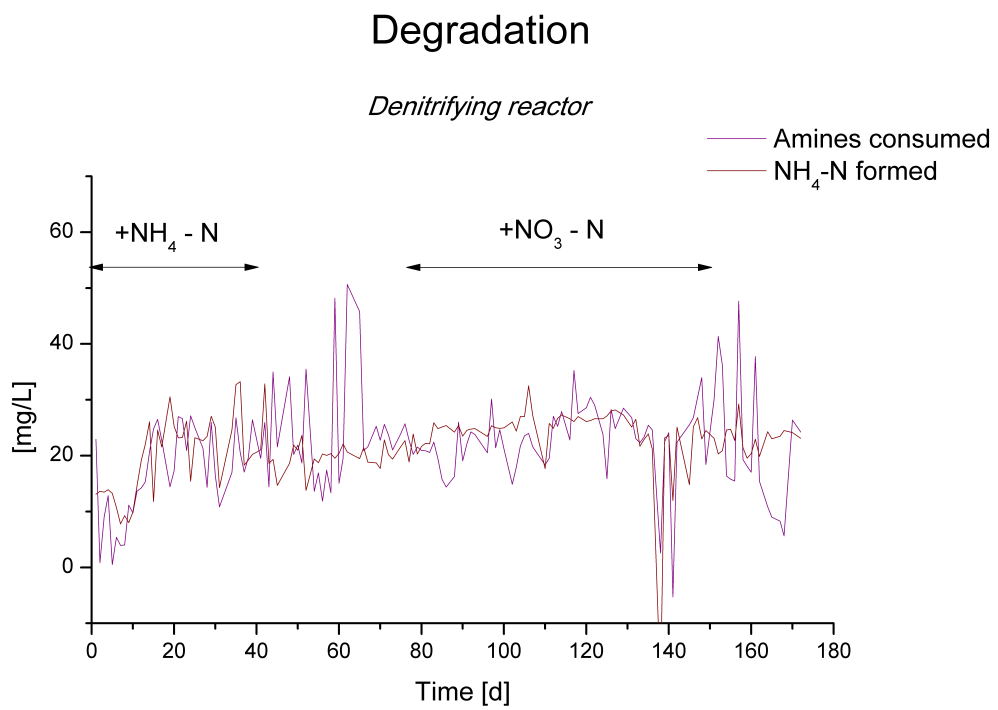
Figure 3.18 shows the calculated incoming mass of primary amines, being MEA,

during the experiment and the measured values for the outgoing amount of amines in the denitrification reactor. The large peak around day 140 can be addressed to a transient high load of primary amines. The addition of nitrate to the media lead to severe clogging of the tube system for the media supply and on day 139 the precipitate, hence containing accumulated amines, entered the denitrification reactor. After approximately 10 days adaption the denitrifying culture continuously improved degrading MEA throughout the time period.



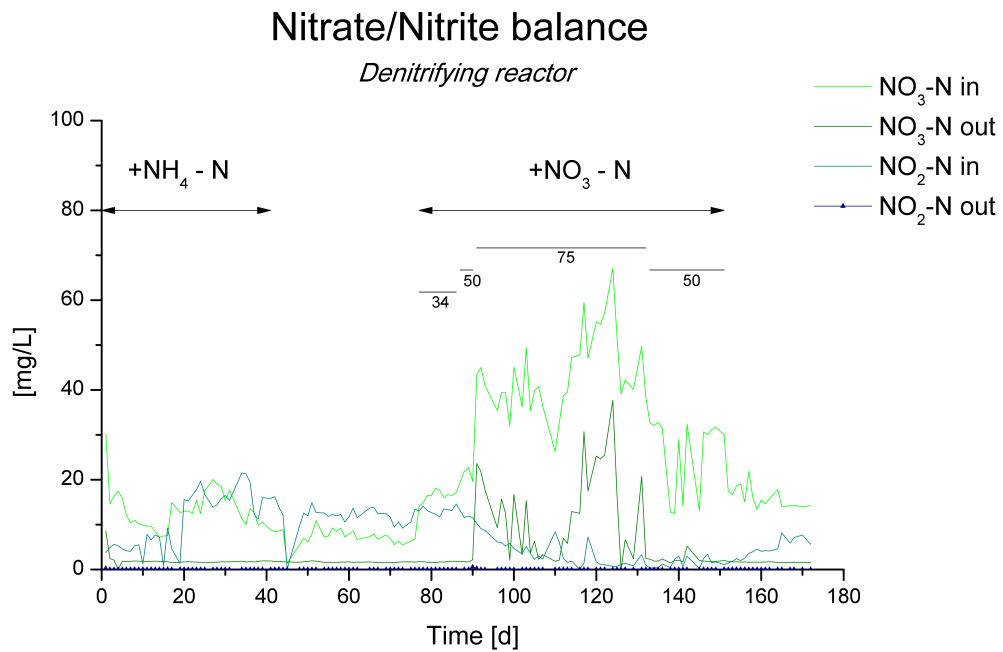
**Figure 3.18:** Primary amine concentrations going in and out of the denitrifying reactor with reclaimer waste as sole carbon source. 50mg/L ammonium were added between day 0 and day 41, and varying amounts of nitrate between day 77 and day 151, as indicated by the horizontal arrows.

The correlation between the amount of degraded amines and the amount of formed  $\text{NH}_4\text{-N}$  is shown in Figure 3.19. On day 20 the degradation reached a plateau, indicating that from this time point on all incoming MEA could be degraded to ammonium. Throughout the experiment the amount of formed  $\text{NH}_4\text{-N}$  was relatively constant, regardless of adding  $\text{NH}_4\text{-N}$  or  $\text{NO}_3\text{-N}$ .



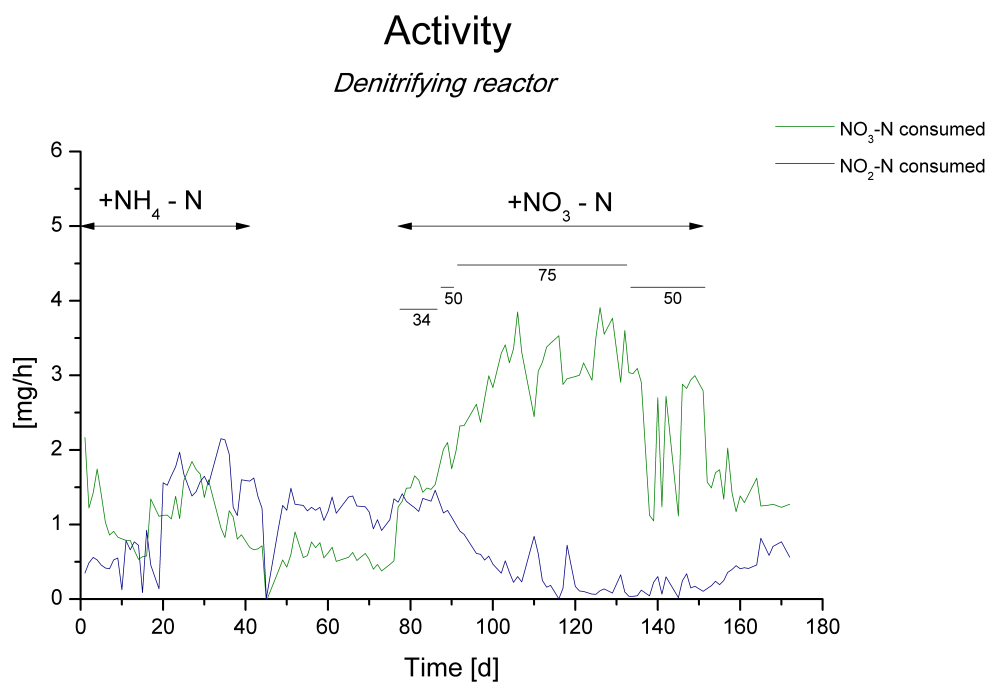
**Figure 3.19:** Amine degradation and formed NH<sub>4</sub>-N in the denitrifying reactor with reclaimer waste as sole carbon source. Ammonium was added between day 0 and day 41, and varying amounts of nitrate between day 77 and day 151, as indicated by the horizontal arrows.

The mass balances of nitrate and nitrite in the denitrification reactor are shown in Figure 3.20, whereas the incoming masses are calculated and the outgoing amounts are measured values. It can be seen that nitrite was reduced almost completely during all the time, with varying incoming amounts when nitrate was added to the system. Nitrate was also consumed almost completely until day 90, when 75mg/L  $\text{NO}_3\text{-N}$  was added. By adding 34, respectively 50mg/L of  $\text{NO}_3\text{-N}$ , no excess  $\text{NO}_3\text{-N}$  was recorded.



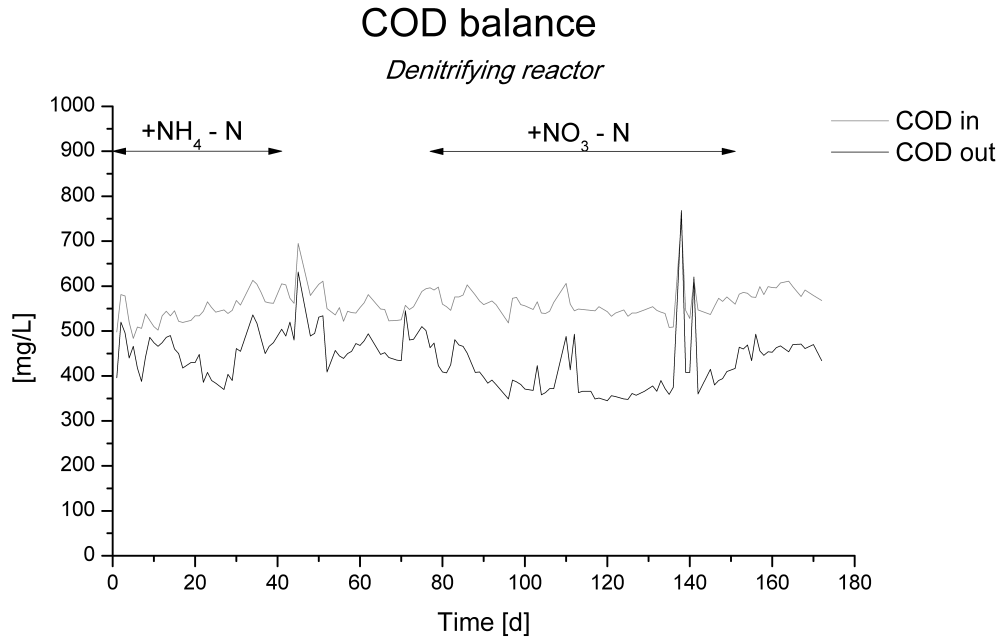
**Figure 3.20:** Nitrate and nitrite concentrations going in and out of the denitrifying reactor with reclaimer waste as sole carbons source. Ammonium was added between day 0 and day 41, and varying amounts of nitrate between day 77 and day 151, as indicated by the horizontal arrows. The numbers under the inserted bars correspond to the added amount of  $\text{NO}_3\text{-N}$ , being 34, 50 and 75mg/L respectively.

Based on these mass balances, the denitrification activity was calculated as nitrate, respectively nitrite consumption per hour and is shown as a function of time in Figure 3.21. A clear increase of nitrate consumption can be seen from day 77 onwards, when excess amount of  $\text{NO}_3\text{-N}$  was available. When omitting the nitrate addition at day 151, the nitrite consumption increased again.



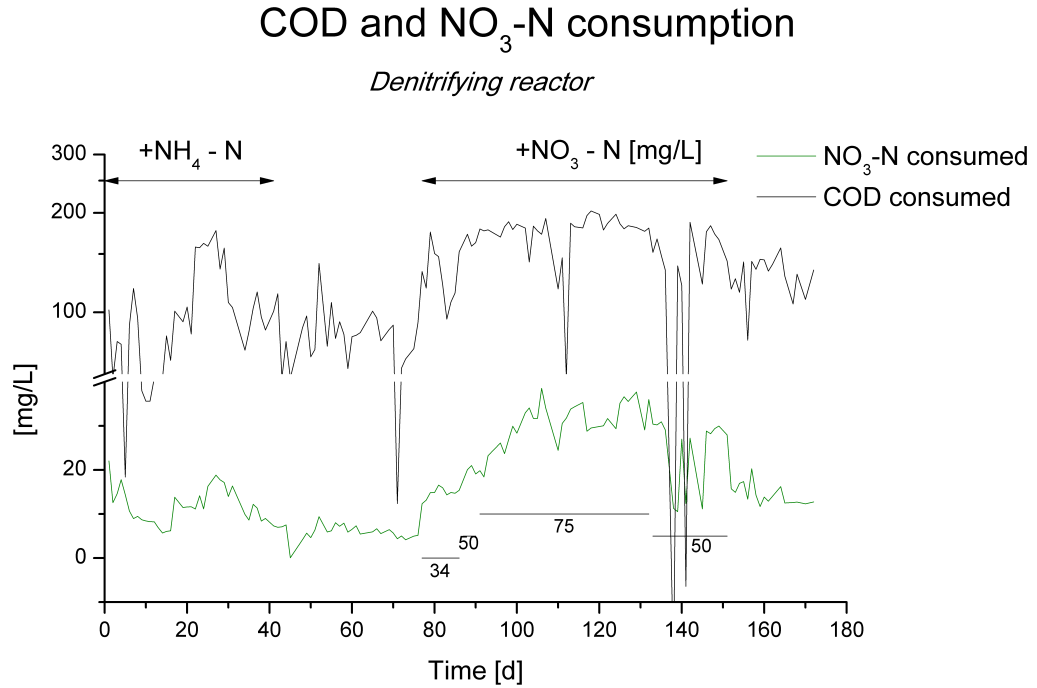
**Figure 3.21:** Nitrate and nitrite consumption per hour of the denitrifying reactor with reclaimer waste as sole carbon source. Ammonium was added between day 0 and day 41, and varying amounts of nitrate between day 77 and day 151, as indicated by the horizontal arrows. The numbers under the inserted bars correspond to the added amount of NO<sub>3</sub>-N, being 34, 50 and 75mg/L respectively.

Figure 3.22 shows the calculated incoming amount of COD into the denitrification reactor and the measured values for the outgoing amount during the experiment.



**Figure 3.22:** Amount of COD going in and out of the denitrifying reactor with reclaimer waste as sole carbon source. Ammonium was added between day 0 and day 41, and varying amounts of nitrate between day 77 and day 151, as indicated by the horizontal arrows.

With the excess amount of electron acceptor, the oxidation of organic matter was increased, as shown in Figure 3.23. The highest level of COD consumption was achieved by adding 75mg/L, with an average COD consumption of 175mg/L during this timeframe, compared to 84mg/L between day 42 to day 76. A summary of the calculated activity of the denitrification reactor in regard to the consumption of COD, amine, nitrate, nitrite and the formation of ammonium is given in Table 3.6.



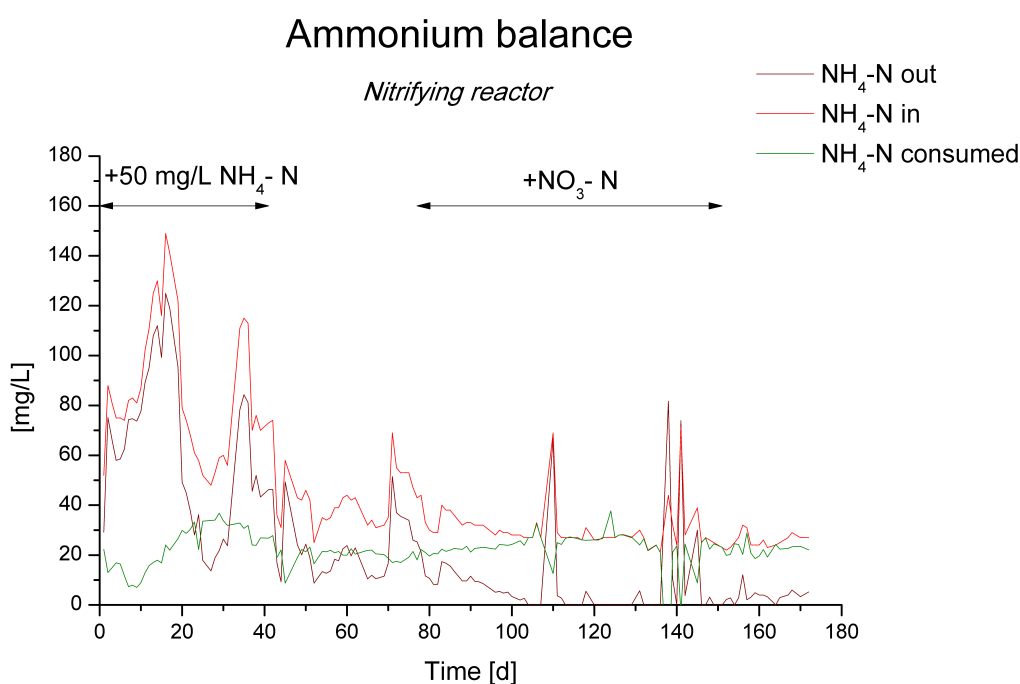
**Figure 3.23:** Amount of COD consumed in the denitrifying reactor with reclaimer waste as sole carbon source. Ammonium was added between day 0 and day 41, and varying amounts of nitrate between day 77 and day 151, as indicated by the horizontal arrows. The numbers under the inserted bars correspond to the added amount of NO<sub>3</sub>-N, being 34, 50 and 75mg/L respectively. Note the break in the ordinate.

**Table 3.6:** Average consumption, respectively formation of NH<sub>4</sub>-N in the denitrification reactor with reclaimer waste as sole carbon source for the pre-denitrification system. The values are given in [mg/L] with the respective standard deviation.

Time	Regime	NH <sub>4</sub> -N	MEA-N	NO <sub>3</sub> -N	NO <sub>2</sub> -N	COD
d0-41	+50mg/L NH <sub>4</sub> -N	19.5±7	17.0±8	11.3±4	10.7±6	95.6±40
d42-76		20.3±3	24.7±10	5.6±2	11.8±3	83.8±20
d77-86	+35mg/L NO <sub>3</sub> -N	23.0±2	19.9±3	14.7±1	13.1±1	131.5±20
d88-90	+50mg/L NO <sub>3</sub> -N	24.4±1	20.4±5	20.1±1	11.5±0.5	164.3±7
d91-132	+75mg/L NO <sub>3</sub> -N	26.0±2	24.2±5	30.6±5	3.7±3	174.5±30
d133-151	+50mg/L NO <sub>3</sub> -N	19.3±10	21.8±10	24.3±8	1.5±1	131.8±60
d152-172		22.9±2	21.5±10	14.4±2	4.3±2	128.7±20

*Nitrifying reactor*

Figure 3.24 shows the measured incoming and outgoing amount of ammonium, as well as the consumption in the nitrifying reactor. The consumption of ammonium shows an increase until day 30, followed by a decrease, even during the addition of 50mg/L  $\text{NH}_4\text{-N}$ , until day 41. Thereafter the ammonium consumption was relatively constant at approximately 30mg/L throughout the rest of the experiment, reaching complete utilization at day 105. During this time the media was supplemented with 75mg/L  $\text{NO}_3\text{-N}$ .



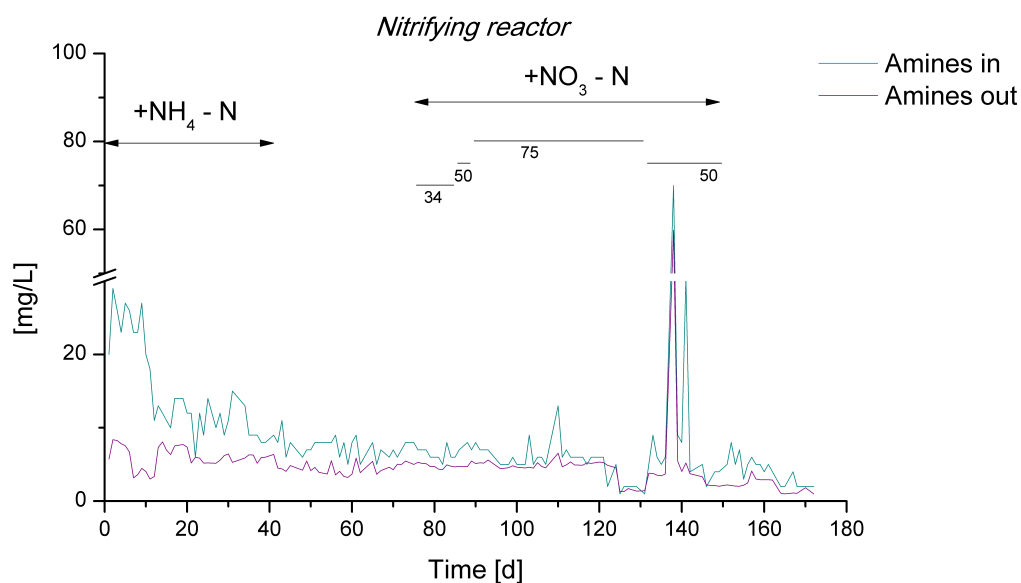
**Figure 3.24:** Ammonium concentrations going in and out of the nitrifying reactor with reclaimer waste as sole carbon source. 50mg/L ammonium were added between day 0 and day 41, as indicated by the horizontal arrow; thereafter no more ammonium was added. The amount of consumed  $\text{NH}_4\text{-N}$  is calculated upon the mass balance.

Figure 3.25 shows the measured incoming and outgoing mass of primary amines, being MEA, in the nitrifying reactor during the experiment. The large peak around day 140 indicates a very high load of amines or degradation products at the time. The addition of nitrate to the media led to severe clogging of the tube system for the media supply and on day 139 the precipitate, hence containing accumulated amines, entered the denitrifying reactor and subsequently the nitrifying reactor. The consumption of MEA was highest



between day 1 and day 12, because the denitrifying culture was not adapted to the new substrate and therefore a higher concentration of amine entered the nitrifying reactor.

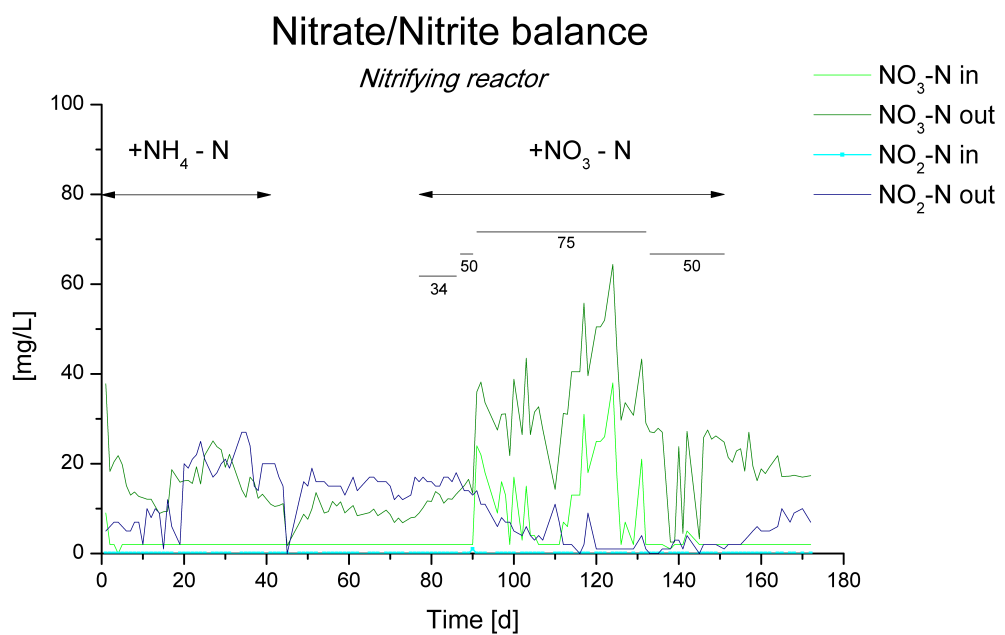
### Amine balance



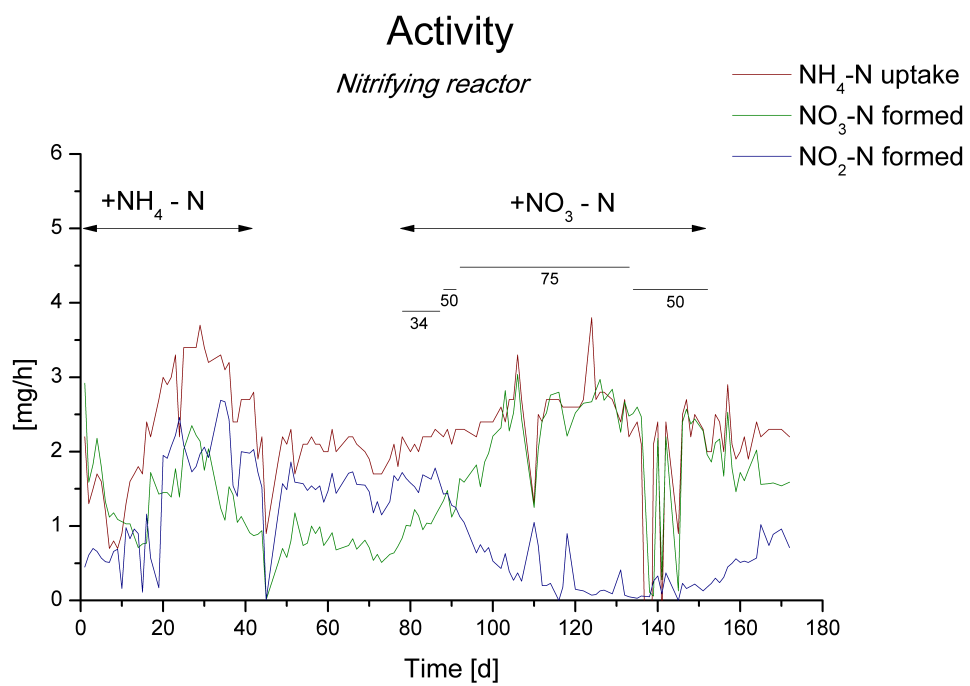
**Figure 3.25:** Primary amine concentrations going in and out of the nitrifying reactor with reclaimer waste as sole carbon source. 50mg/L ammonium were added between day 0 and day 41, and varying amounts of nitrate between day 77 and day 151, as indicated by the horizontal arrows.

Figure 3.26 shows the measured incoming and outgoing masses of nitrate and nitrite during the experiment in the nitrifying reactor. After addition of 34mg/L  $\text{NO}_3\text{-N}$ , the formation of nitrate was promoted and nitrite accumulation decreased at the same time, leading to complete nitrification at day 87, when 50mg/L  $\text{NO}_3\text{-N}$  were added.

The nitrification activity was calculated as nitrate, respectively nitrite formation per hour and is presented in Figure 3.27. A clear shift from nitrite to nitrate formation can be seen from day 90 onwards, when excess amount of  $\text{NO}_3\text{-N}$  was available. The increased nitrification activity during this time could be addressed to a decrease in heterotrophic bacteria, because the available COD decreased simultaneously, thus providing improved oxygen supply to the nitrifying culture. When omitting the nitrate addition at day 151, the nitrite accumulation increased again.

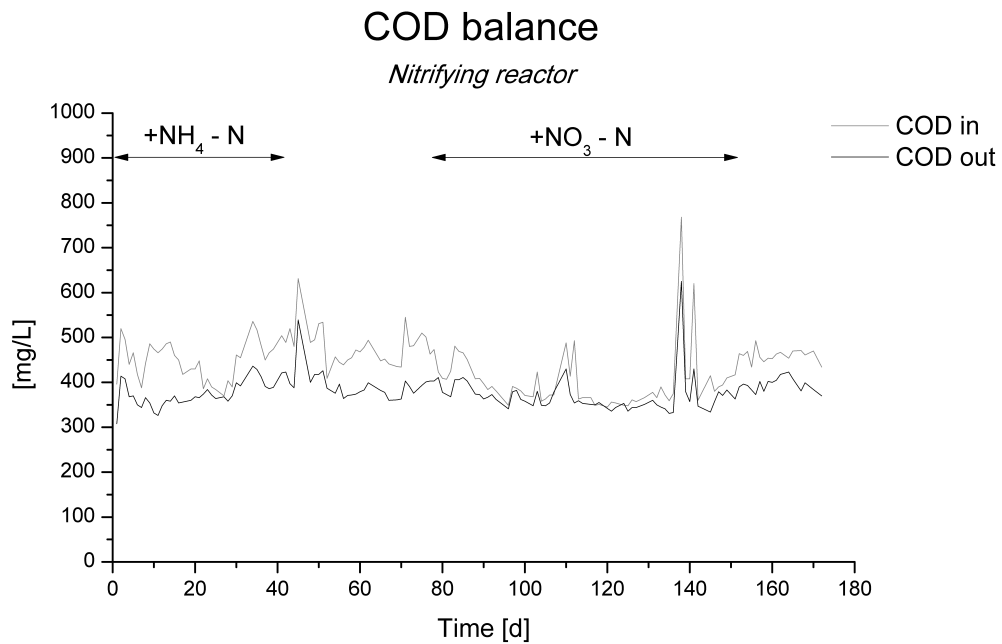


**Figure 3.26:** Nitrate and nitrite concentrations going in and out of the nitrifying reactor with reclaimer waste as sole carbon source. Ammonium was added between day 0 and day 41, and varying amounts of nitrate between day 77 and day 151, as indicated by the horizontal arrows. The numbers under the inserted bars correspond to the added amount of  $\text{NO}_3\text{-N}$ , being 34, 50 and 75mg/L respectively.



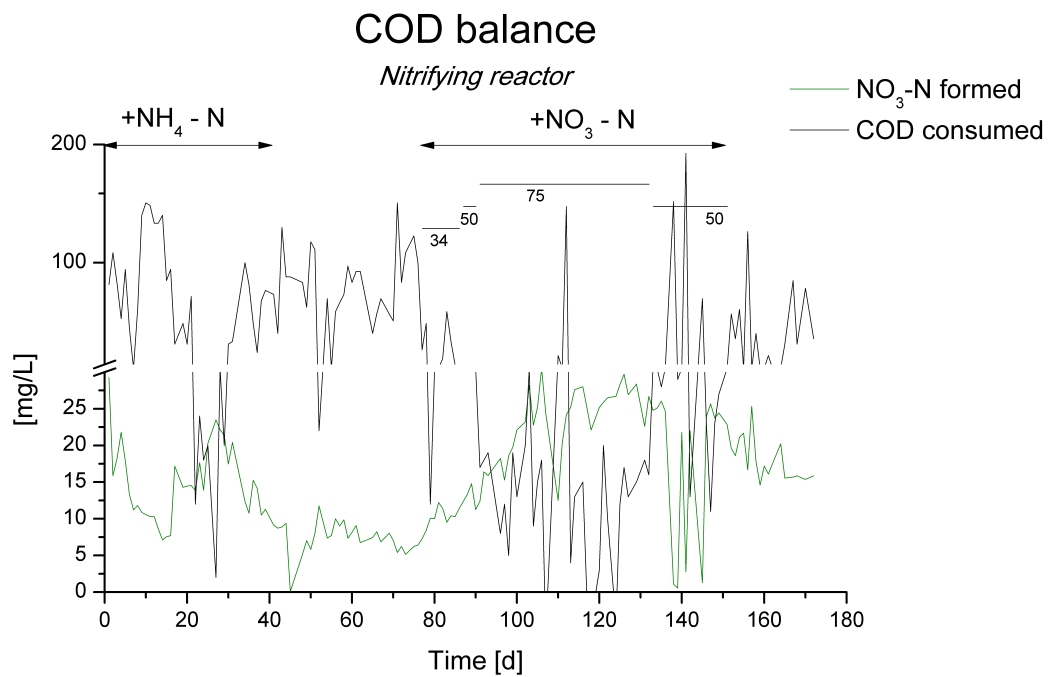
**Figure 3.27:** Nitrate and nitrite production per hour of the nitrifying reactor with reclaimer waste as sole carbon source. Ammonium was added between day 0 and day 41, and varying amounts of nitrate between day 77 and day 151, as indicated by the horizontal arrows. The numbers under the inserted bars correspond to the added amount of  $\text{NO}_3\text{-N}$ , being 34, 50 and 75mg/L respectively.

Figure 3.28 shows the measured incoming and outgoing amount of COD during the experiment in the nitrifying reactor of the pre-denitrification system. The amount of incoming COD was less when nitrate was added to the media between day 77 and day 151, as more COD was consumed in the denitrifying reactor during this time.



**Figure 3.28:** Amount of COD going in and out of the nitrifying reactor with reclaimer waste as sole carbon source. Ammonium was added between day 0 and day 41, and varying amounts of nitrate between day 77 and day 151, as indicated by the horizontal arrows.

Figure 3.29 compares the consumption of COD with formation of nitrate, whereas the enhanced nitrate formation can be noticed between day 77 and day 152.



**Figure 3.29:** Amount of consumed COD in the nitrifying reactor with reclaimer waste as sole carbon source. Ammonium was added between day 0 and day 41, and varying amounts of nitrate between day 77 and day 151, as indicated by the horizontal arrows. The numbers under the inserted bars correspond to the added amount of NO<sub>3</sub>-N, being 34, 50 and 75mg/L respectively. Note the break in the ordinate.

*LC-MS analysis*

The concentration of MEA was analyzed in two sets of samples, being day 17 and day 97. Table 3.7 shows the results obtained by LC-MS, as well as the results from the Fluorescamine assay. Although the results are consistent, the Fluorescamine assay seems to have a worse resolution in low ranges.

**Table 3.7:** Quantification of MEA in samples from media (M), nitrification (N) and denitrification (D) reactor measured by LC-MS and Fluorescamine assay, respectively.

Day	Sample	LC-MS MEA [mmol/L]	Fluorescamine assay MEA [mmol/L]
17	M	10.1	11.0
	N	0.23	0.54
	D	1.5	1.01
97	M	8.4	11.4
	N	0.45	0.32
	D	0.53	0.38

Samples from day 97 were analyzed qualitatively by LC-MS, as described in section 2.6. The results of the reclaimer waste composition are shown in Figure 3.30, whereas intensity is plotted against mass/charge ratio. It should be noted that the intensity does not represent an absolute quantification. Nevertheless, a change in complexity can be seen, as some peaks occurring in the media were not found in the denitrification, respectively nitrifying reactor. The marked peaks indicate the main degradation products, which subsequently were also quantified by LC-MS, illustrated in Figure 3.31.

Both substituted amides, HEF (2-hydroxyethylformamide) and HEA (2-hydroxyethyl)-acetamide, as well as the amino acid HEGly (N-(2-hydroxyethyl)glycine), could be readily degraded by the denitrifying reactor, whereas the nitrifying reactor utilized the leftovers of HEF and HEA almost completely and HEGly to a lesser extent. HEPO (4-(2-hydroxyethyl) piperazine-2-one) and BHEOX (N,N-Bis(2-hydroxyethyl)oxamide) could not be further degraded in the nitrifying reactor, as the level from the denitrifying reactor remained.

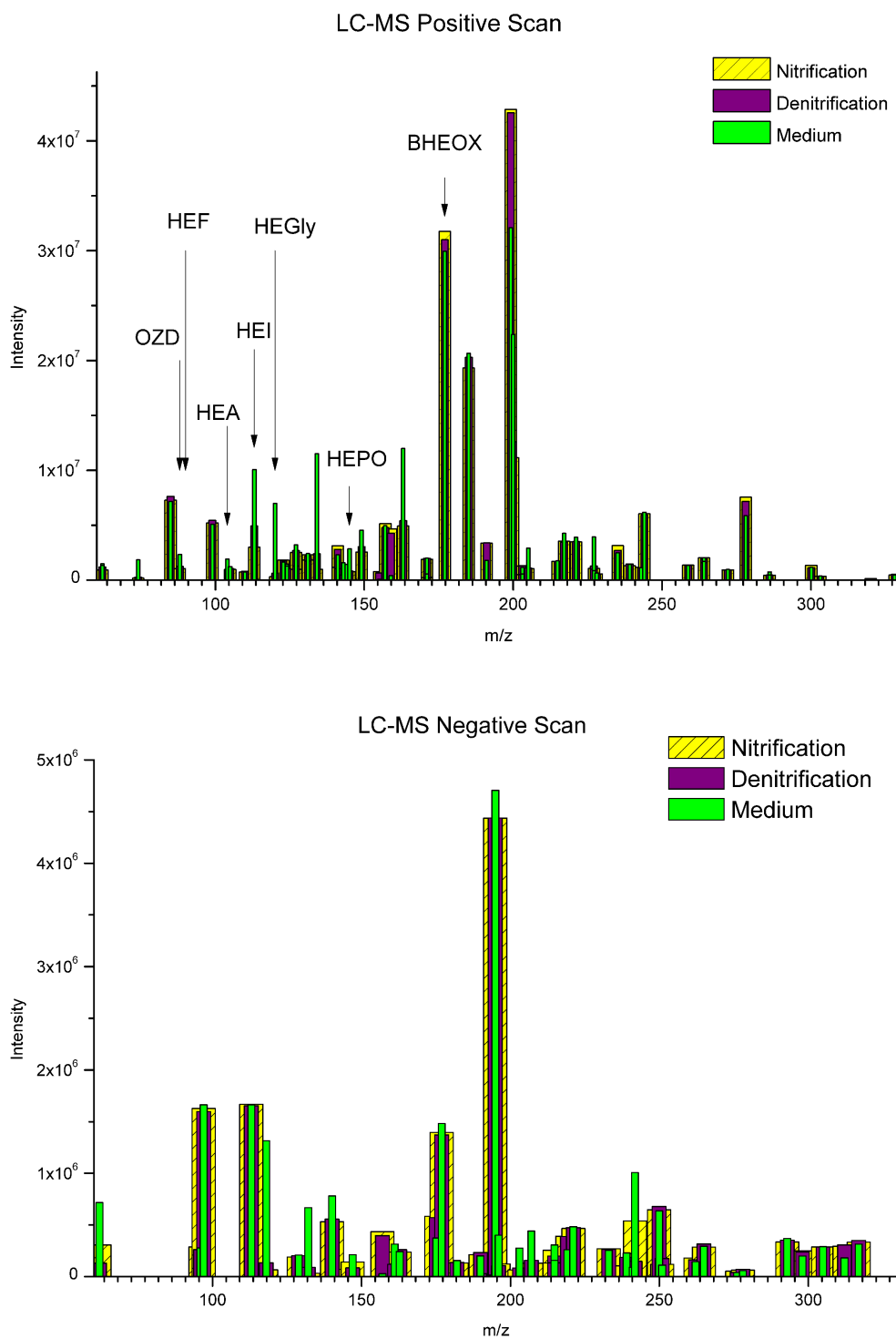


**Figure 3.30:** LC-MS positive and negative scan (upper and lower panel, respectively) of samples taken on day 97 from the medium, nitrification and denitrifying reactor of the pre-denitrification system.

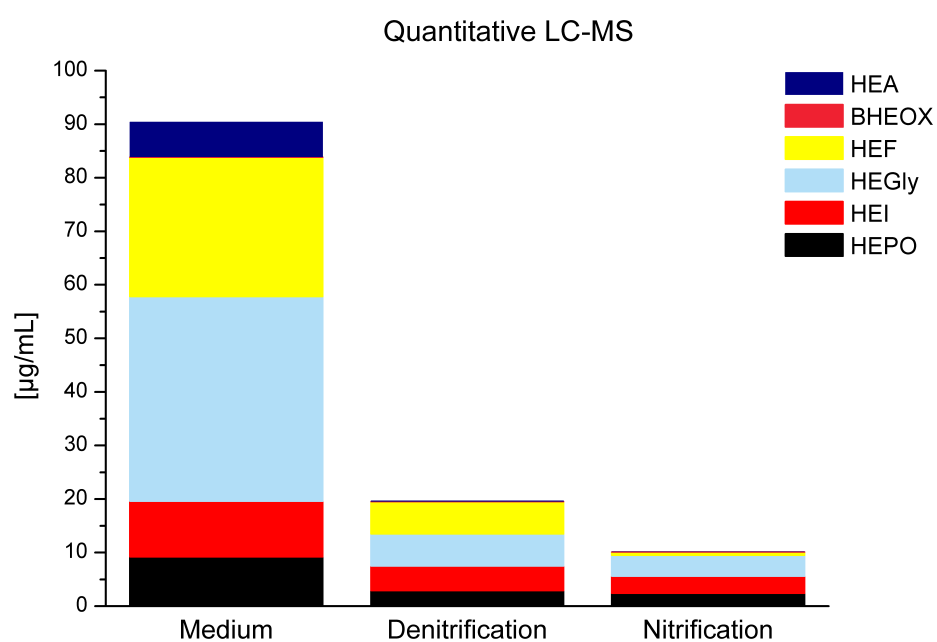


**Figure 3.31:** LC-MS quantification of selected degradation products of MEA. Samples were taken on day 97 from the medium, nitrification and denitrifying reactor of the pre-denitrification system.



*Efficiency*

The total nitrogen removal efficiency is calculated with the total amount of nitrogen from ammonium, nitrate, nitrite and MEA entering the reactor system, and the amount of these compounds exiting the nitrifying reactor. The results for each regime are shown in Table 3.8. The nitrogen removal efficiency of 104% between day 152 and day 172 might be a result of inaccuracies in quantifying MEA in samples from the media, because the samples were stored for a longer time period of 4 weeks and showed much lower results than average. The underestimation of total nitrogen entering the system leads to this high efficiency, as the amount of exiting nitrogen exceeds the initial value.

**Table 3.8:** Average total nitrogen removal efficiency of the pre-denitrification system.

Time	Regime	Nitrogen Removal Efficiency [%]
d1-41	+50mg/L NH <sub>4</sub> -N	54
d42-76		69
d77-86	+35mg/L NO <sub>3</sub> -N	69
d88-90	+50mg/L NO <sub>3</sub> -N	74
d91-132	+75mg/L NO <sub>3</sub> -N	76
d133-151	+50mg/L NO <sub>3</sub> -N	68
d152-172		104

The efficiency of nitrogen removal from MEA is calculated to be between 96 and 97% throughout the experiment. The COD removal achieved 68 to 73%, whereas the highest COD removal efficiency was obtained during the addition of 75mg/L NO<sub>3</sub>-N nitrate. All calculations are given in Appendix D.2.

The total COD of reclaimer waste consisted of approximately 58% MEA (see Appendix D.3), indicating that all COD from MEA could be utilized by the pre-denitrification system. This is consistent with a recent study from Kim et al. [24], showing that MEA has sufficient electrons for the complete removal of its nitrogen compounds by nitrification and denitrification. They state that the electrons for denitrification originate either from MEA itself or from its anoxic degradation products being acetate, ethanol and acetaldehyde [24].

### 3.5.2 Summation

The activity of the denitrifying reactor through the experiment proved that reclaimer waste is a competitive carbon source for denitrification. When adding the reclaimer waste, the denitrifying culture needed 2 weeks for adaptation. In the first 2 weeks the nitrate consumption, respectively reduction, decreased. When the culture had adapted to the

new available carbon source, they reduced more nitrite than nitrate, for the simple reason that more nitrite was available to them. At this timepoint, the degradation of MEA also reached its maximum constant activity. With the addition of nitrate, the denitrifying culture switched to nitrate respiration, leading to total denitrification. The consumed stoichiometric amount of  $0.9\text{molNO}_3/\text{molMEA}$  is consistent with recent findings of Kim et al. [24]. The surplus nitrate generally had a positive impact on the denitrifying culture. With the extra amount of available electron acceptor, the bacteria were able to oxidize more organic carbon in the reclaimer waste, resulting in promoted growth of the heterotrophic community and therefore an increased activity. On the other hand, during the addition of  $75\text{mg/L NO}_3\text{-N}$  some accumulation of nitrate occurred in the denitrifying reactor for approximately 2 weeks. Perhaps the oxidation of degradation products in the reclaimer waste, led to more or less toxic daughter products, requiring adaptation of the microbial community. Nevertheless, the denitrifying bacteria showed even higher activity afterwards. This also implies that the denitrification activity in the pre-denitrification configuration was previously limited by the amount of nitrate produced by the nitrifying culture.

The increase in the ammonium concentration is due to the degradation of MEA to ammonium and acetaldehyde in the denitrifying reactor. Based on the derived mass balance, the amount of formed  $\text{NH}_4\text{-N}$  appears to be relatively constant during the entire duration of the experiment. This is also plausible, as one mole degraded MEA produces one mole ammonium [34].

The nitrifying reactor needed approximately 3 weeks adaptation until steady ammonium consumption could be noted. This startup phase was accompanied by increased heterotrophic growth in the nitrifying reactor, feeding off the rich reclaimer waste and thus, the high consumption rate of MEA can be led back to this bacterial community and not to the nitrifying bacteria. This circumstance was countered by the addition of nitrate to the denitrifying reactor. The readily available COD was mainly consumed by the denitrifying bacteria, thereby limiting heterotrophic growth in the nitrifying reactor. This fact may lead to improved oxygen supply of the nitrifying culture, resulting in the increased nitrification activity. Another possible explanation could be the increased amount of dissolved  $\text{CO}_2$  supplied to the nitrifying reactor, which was generated by the boosted oxidation of organic carbon in the denitrifying reactor, as a recent study suggests that some autotrophic bacteria, including NOB, are carbon-limited [23]. However, in the nitrifying reactor a COD level below  $350\text{mg/L}$  could not be achieved, indicating that below this threshold the organic matter was not available for degradation.

The LC-MS analyses showed a shift in complexity of the composition of reclaimer waste at various stages of the pre-denitrification system. Some known degradation products, yet not all, could be quantified and thus revealed their fate within the system. The majority of HEF, HEA and HEGly could be readily degraded in the denitrifying reactor,

whereas only HEF and HEA could be further degraded almost completely in the nitrifying reactor, and HEGly to a lesser extent. For the other quantified degradation products, the level of degradation in the denitrifying reactor remained also in the nitrifying reactor. Nevertheless, the nitrogen removal efficiency of MEA achieved 97%, of total nitrogen 76% and the removal efficiency of organic matter 73%.

### 3.6 Summary and Outlook

The nitrifying biofilm development on Kaldnes K1 carriers could not be successfully tracked by monitoring the gained COD per carrier. This is due to the preincubation of the carriers in a sludge return, leading to a already high initial value of organic matter at the beginning of the experiment. Therefore, the gained COD should be measured as soon as the carriers are incubated in the sludge return, even if no biofilm is visible. This would provide information about the attachment kinetics on Kaldnes K1 carriers, as well as development behaviour of nitrifying biofilm under substrate-limited conditions.

The acute toxicity test of reclaimer waste, as well as selected amines, being AMP, aMDEA, DEA, MEA and piperazine on nitrifying biofilm showed differing results. The  $EC_{50}$  and especially the recovery kinetics of the nitrification activity varied considerably. A declined activity after recovery was found with piperazine, as well as aMDEA. It appears that the acute toxicity of reclaimer waste depends on the history of the tested biofilm community, as previously unexposed biofilm was less sensitive than exposed. This should be verified by additional testings. In general the tested amines exhibited a stimulation in lower concentrations, most pronounced when testing aMDEA. However, the  $EC_{50}$  of the tested amines towards the nitrifying biofilm ranged between 1 and 5g/L. This is a relatively high value compared to the respective  $EC_{50}$  inhibiting algal growth in the range of mg/L [17].

To verify the respond of nitrifying biofilm towards toxic loads of amines, the biofilm composition should be considered in future. With different amounts of heterotrophic bacteria on the outside of the biofilm, the nitrifying activity may depend on diffusional limitation over this community. Thus, molecular biological methods such as FISH (Fluorescence in situ hybridization) and DGGE (Denaturing gradient gel electrophoresis) should be utilized to characterize the microbial community at the time of each test. Furthermore a quantification of the biofilm on the carriers, e.g. by determination of the average COD per carrier used in the experiment would allow to estimate the impact of diffusional limitation over the surface. Thus, making a correlation between biofilm age,

respectively thickness and the respond possible.

The acute toxicity on the more robust denitrifying biofilm did not show any major inhibition in the presence of any of the selected amines. Contrary to expectations, the activity was even stimulated in moderate concentrations, especially pronounced in the presence of aMDEA compared to the initial activity. Also in this case, the recovery from piperazine gave a declined activity. Nevertheless, also in this case molecular biological methods to characterize the microbial community, as well as the biofilm thickness at the time of each test, should be considered.

The biological degradation of reclaimer waste in the pre-denitrification system was successful, with MEA and its degradation products serving as a sole carbon source for denitrification. After 2 weeks adaption the denitrifying reactor was able to degrade all MEA to ammonium. With the addition of nitrate, the denitrifying culture switched from nitrite to nitrate respiration, leading to total denitrification. The consumed stoichiometric amount of  $0.9\text{molNO}_3/\text{molMEA}$  is consistent with recent findings of Kim et al. [24].

The nitrifying reactor needed approximately 3 weeks for adaption before steady ammonium consumption could be noted. Besides the degradation of MEA, also other COD could successfully be removed from the reclaimer waste. The LC-MS analysis of the reclaimer waste revealed approximately  $10\text{mol/L}$  of MEA, accounting for 58% of the COD. Furthermore, the LC-MS analyses showed a shift in complexity of the composition of reclaimer waste at various stages of the pre-denitrification system. Selected degradation products were quantified, whereas the majority was readily degraded in the denitrifying reactor, whilst others were further degraded in the nitrifying reactor. Overall, the nitrogen removal efficiency of MEA achieved 97%, of total nitrogen 76% and the removal efficiency of organic matter 73%.

The chemical analyses with Hach-Lange assays should be further tested with reclaimer waste, as unidentified compounds could lead to cross-interferences with these assays. Previous works of Colaco [14] and Skjæran [47, 46] only investigated the effects of pure MEA and AMP on the discussed assays. Especially the LCK 303 Ammonium-Nitrogen seemed to be biased with reclaimer waste in low detection ranges. This also applies for the Fluorescamine assay, where it should furthermore be tested if the accuracy is also given with previously  $\text{CO}_2$ -loaded MEA, especially in low detection ranges. Generally, the analysis of reclaimer waste should be pushed, as current literature is still incomplete.

Regarding the biodegradability of reclaimer waste in a pre-denitrification system, ex-

tended HRT (Hydraulic Retention Time) could lead to improved COD removal, as some degradation products might need more time for biological degradation. Although, if the removal of COD is not the main attention, but rather the removal of MEA is desired, a different approach should be considered. In the startup phase of the nitrifying reactor it came to nitrite accumulation, possibly due to increased presence of heterotrophs competing with nitrifying bacteria for oxygen. At the same time the MEA degradation was working well, although less COD was removed. Considering the process of partial nitrification to nitrite and nitrite denitrification, this circumstance may offer a novel process for MEA removal by denitrification via the nitrite pathway. Partial nitrification requires less oxygen, thus less energy and results in higher denitrification rates, as well as reduced CO<sub>2</sub> emissions [38].

## Chapter 4

# Conclusions

The objective of this work was to study the feasibility of biological treatment of reclaimer waste from an amine based CO<sub>2</sub> capture plant, as well as from selected, commonly used amines in this process.

The toxicity of reclaimer waste, AMP, aMDEA, DEA, MEA and Piperazine was tested both on nitrifying and denitrifying biofilms, revealing varying sensitivity of the nitrifying culture and an almost unaffected respond from the denitrifying culture. This result can be addressed to the differing composition of the bacterial communities, whereas the heterotrophic community of denitrifying bacteria is generally more robust towards environmental changes.

Nevertheless, this circumstance can be exploited in a positive manner by treating reclaimer waste in a pre-denitrification system. The biological degradation of reclaimer waste in the pre-denitrification system was successful, with MEA and its degradation products serving as a sole carbon source for denitrification. After 2 weeks adaption, the denitrifying reactor was able to degrade all MEA to ammonium. With the external addition of 75mg/L nitrate, the denitrifying culture achieved total denitrification. As expected, the nitrifying reactor needed approximately 1 week longer for adaption before steady ammonium consumption could be noted. Besides the degradation of MEA, also other COD could successfully be removed from the reclaimer waste.

The LC-MS analysis of the reclaimer waste revealed approximately 10mol/L of MEA, accounting for 58% of the COD. Furthermore, the LC-MS analyses showed a shift in complexity of the composition of reclaimer waste at various stages of the pre-denitrification system. Selected degradation products were quantified, whereas the

majority was readily degraded in the denitrifying reactor, others were further degraded in the nitrifying reactor. Overall, the nitrogen removal efficiency of MEA achieved 97%, of total nitrogen 76% and the removal efficiency of organic matter 73%.

Generally, it appears favourable to apply biological treatment on the reclaimer waste, since no external carbon source is required, thus minimizing the operational costs. The requirement of additional nitrate may lead to extra costs, but if the process is adapted to MEA removal instead of COD removal, this might not be necessary. For the removal of MEA the concept of partial nitrification would circumvent the addition of nitrate, and also generally lead to lower energy costs, as less oxygen is needed for nitrification to nitrite and subsequent nitrite denitrification.

# Bibliography

- [1] Diamines and higher amines, aliphatic. In *Kirk-Othmer Encyclopedia of Chemical Technology*. 70
- [2] CO<sub>2</sub> capture - SINTEF. <http://www.sintef.no/Home/Materials-and-Chemistry/Process-Technology/CO2-Capture/>. 4
- [3] Per Arild Aarrestad and Jan Ove Gjershaug. Effects on terrestrial vegetation, soil and fauna of amines and possible degradation products relevant for CO<sub>2</sub> capture - a review. Scientific Report OR 3/2009, Norwegian Institute for Air Research (NILU), Kjeller, February 2009. 6
- [4] Young-Ho Ahn. Sustainable nitrogen elimination biotechnologies: A review. *Process Biochemistry*, 41(8):1709–1721, August 2006. 13, 14, 17
- [5] A. C. Anthonisen, R. C. Loehr, T. B. S. Prakasam, and E. G. Srinath. Inhibition of nitrification by ammonia and nitrous acid. *Journal (Water Pollution Control Federation)*, 48(5):835–852, 1976. 16
- [6] H el ene Baribeau, Mary Kay Kozyra, and Beth Behner. Microbiology and isolation of nitrifying bacteria. In American Water Works Association, editor, *Fundamentals and Control of Nitrification in Chloraminated Drinking Water Distribution Systems*, pages 69–94. Glacier Publishing Services, Inc., United States of America, first edition edition, 2006. 12, 15, 16, 17, 18, 20
- [7] B. Beek, Tom Bosma, Hauke Harms, and Alexander Zehnder. Biodegradation of xenobiotics in environment and technosphere. In *Biodegradation and Persistence*, volume 2K of *The Handbook of Environmental Chemistry*, pages 163–202. Springer Berlin / Heidelberg, 2001. 9
- [8] Adeola Bello and Raphael O. Idem. Pathways for the formation of products of the oxidative degradation of CO<sub>2</sub>-loaded concentrated aqueous monoethanolamine solutions during CO<sub>2</sub> absorption from flue gases. *Industrial & Engineering Chemistry Research*, 44(4):945–969, February 2005. 5, 7



- [9] Eberhard Bock, Michael Wagner, Martin Dworkin, Stanley Falkow, Eugene Rosenberg, Karl-Heinz Schleifer, and Erko Stackebrandt. Oxidation of inorganic nitrogen compounds as an energy source. In *The Prokaryotes: Ecophysiology and biochemistry*, volume Vol. 2, pages 457–495. Springer, Liv, 3 edition, 2007. [12](#), [13](#)
- [10] Steven Brooks. The toxicity of selected primary amines and secondary products to aquatic organisms: A review. Scientific Report OR-28285, Norwegian Institute for Water Research (NIVA), Oslo, November 2008. [70](#)
- [11] Geoff Byrns. The fate of xenobiotic organic compounds in wastewater treatment plants. *Water Research*, 35(10):2523–2533, July 2001. [9](#)
- [12] Edward J Calabrese and Linda A Baldwin. Toxicology rethinks its central belief. *Nature*, 421(6924):691–692, February 2003. [67](#), [77](#)
- [13] Lie E. Welander T. Christensson, M. A comparison between ethanol and methanol as carbon sources for denitrification. *Water Science and Technology*, 30(6 pt 6):83–90, 1994. [41](#)
- [14] Ana Borges Colaco. Biological water treatment for removal of ammonia from process water in a CO<sub>2</sub>-capture plant. Master thesis, Instituto Superior Tecnico, Lisboa, 2009. [5](#), [23](#), [25](#), [27](#), [28](#), [29](#), [30](#), [38](#), [41](#), [45](#), [52](#), [69](#), [70](#), [77](#), [97](#)
- [15] Eirik F. da Silva and Hallvard F. Svendsen. Computational chemistry study of reactions, equilibrium and kinetics of chemical CO<sub>2</sub> absorption. *International Journal of Greenhouse Gas Control*, 1(2):151–157, April 2007. [7](#)
- [16] Jason Davis and Gary Rochelle. Thermal degradation of monoethanolamine at stripper conditions. *Energy Procedia*, 1(1):327–333, February 2009. [7](#)
- [17] Ingvild Eide-Haugmo, Odd Gunnar Brakstad, Karl Anders Hoff, Kristin Rist Sørheim, Eirik Falck da Silva, and Hallvard F. Svendsen. Environmental impact of amines. *Energy Procedia*, 1(1):1297–1304, February 2009. [7](#), [70](#), [96](#)
- [18] D.J. Gapes and J. Keller. Impact of oxygen mass transfer on nitrification reactions in suspended carrier reactor biofilms. *Process Biochemistry*, 44(1):43–53, January 2009. [22](#)
- [19] George S. Goff and Gary T. Rochelle. Monoethanolamine degradation: O<sub>2</sub> mass transfer effects under CO<sub>2</sub> capture conditions. *Industrial & Engineering Chemistry Research*, 43(20):6400–6408, 2004. [4](#), [6](#), [7](#)
- [20] Albert Guisasola, Irene Jubany, Juan A Baeza, Julián Carrera, and Javier Lafuente. Respirometric estimation of the oxygen affinity constants for biological ammonium

- and nitrite oxidation. *Journal of Chemical Technology & Biotechnology*, 80(4):388–396, 2005. [17](#)
- [21] Steven B. Hawthorne, Alena Kubátová, John R. Gallagher, James A. Sorensen, and David J. Miller. Persistence and biodegradation of monoethanolamine and 2-Propanolamine at an abandoned industrial site. *Environmental Science & Technology*, 39(10):3639–3645, May 2005. [10](#)
- [22] Mogens Henze, Poul Harremoes, Erik Arvin, and Jes la Cour Jansen. Basic biological processes. In *Wastewater Treatment: Biological and Chemical Processes*, pages 89–108. Springer, Berlin, 3 edition, 2002. [13](#), [16](#), [17](#), [18](#), [19](#), [20](#)
- [23] DuPont Samuel J., Finklea Brent D., Posso Lina M., and Stroot Peter G. High-rate nitrification by CO-sensitive nitrifying bacteria. *Proceedings of the Water Environment Federation*, 11:1627–1637, 2006. [95](#)
- [24] Dong-Jin Kim, Yeseul Lim, Daechul Cho, and In Rhee. Biodegradation of monoethanolamine in aerobic and anoxic conditions. *Korean Journal of Chemical Engineering*, 27(5):1521–1526, September 2010. [11](#), [94](#), [95](#), [97](#)
- [25] D. Kleiner. Bacterial ammonium transport. *FEMS Microbiology Letters*, 32(2):87–100, 1985. [12](#)
- [26] H el ene Lepaumier, Eirik F. da Silva, Aslak Einbu, Andreas Grimstvedt, Jacob N. Knudsen, Kolbj orn Zahlse, and Hallvard F. Svendsen. Comparison of MEA degradation in pilot-scale with lab-scale experiments. *Energy Procedia*, 4:1652–1659, 2011. [55](#)
- [27] A. M Martin. Application of adapted bacterial cultures for the degradation of xenobiotic compounds in industrial waste-waters. In *Biological degradation of wastes*, pages 261–277. Elsevier Applied Science, 1991. [9](#)
- [28] R. Alan May and Keith J. Stevenson. Software review of origin 8. *Journal of the American Chemical Society*, 131(2):872, January 2009. [40](#), [53](#), [61](#)
- [29] V. R Meyer. In *Practical High-Performance Liquid Chromatography*, page 8;112. John Wiley & Sons, 5 edition, 2010. [31](#)
- [30] Ole Mrklas, Angus Chu, Stuart Lunn, and Laurence R. Bentley. Biodegradation of monoethanolamine, ethylene glycol and triethylene glycol in laboratory bioreactors. *Water, Air, & Soil Pollution*, 159(1):249–263, November 2004. [10](#)
- [31] E. Mulkiewicz, B. Jastorff, A.C. Skladanowski, K. Kleszczynski, and P. Stepnowski. Evaluation of the acute toxicity of perfluorinated carboxylic acids using eukaryotic cell

- lines, bacteria and enzymatic assays. *Environmental Toxicology and Pharmacology*, 23(3):279–285, May 2007. 40, 53
- [32] Stuart A. Narrod and William B. Jakoby. Metabolism of ethanolamine. *Journal of Biological Chemistry*, 239(7):2189–2193, July 1964. 10
- [33] OECD. *Test No. 209: Activated Sludge, Respiration Inhibition Test (Carbon and Ammonium Oxidation)*, *OECD Guidelines for the Testing of Chemicals, Section 2: Effects on Biotic Systems*. Organisation for Economic Co-operation and Development, 2010. 40, 53
- [34] Kazuhisa Ohtaguchi, Kozo Koide, and Takahisa Yokoyama. An ecotechnology-integrated MEA process for CO<sub>2</sub>-removal. *Energy Conversion and Management*, 36(6-9):401–404, June 1995. 10, 95
- [35] Satoshi Okabe, Tomonori Kindaichi, and Tsukasa Ito. Fate of <sup>14</sup>C-Labeled microbial products derived from nitrifying bacteria in autotrophic nitrifying biofilms. *Applied and Environmental Microbiology*, 71(7):3987–3994, July 2005. 14, 15
- [36] Satoshi Okabe, Hisashi Satoh, Tsukasa Ito, and Yoshimasa Watanabe. Analysis of microbial community structure and in situ activity of nitrifying biofilms. *Journal of Water and Environment Technology*, 2(2):65–74, 2004. 14, 15, 16, 70
- [37] Y. Z. Peng, Y. Chen, C. Y. Peng, M. Liu, S. Y. Wang, X. Q. Song, and Y. W. Cui. Nitrite accumulation by aeration controlled in sequencing batch reactors treating domestic wastewater. *Water Science & Technology*, 50(10):35–43, 2004. 13
- [38] Yongzhen Peng and Guibing Zhu. Biological nitrogen removal with nitrification and denitrification via nitrite pathway. *Applied Microbiology and Biotechnology*, 73(1):15–26–26, November 2006. 13, 15, 98
- [39] David Perlman. Some problems on the new horizons of applied microbiology. *Journal of Industrial Microbiology & Biotechnology*, 21(4-5):430–438, 1980. 9
- [40] Hans-Jürgen Rehm, Gerald Reed, and Josef Winter. Nitrogen removal during wastewater treatment. In *Environmental Processes I*, volume 1, pages 37–39. WILEY-VCH, Weinheim, 2 edition, 1999. 18
- [41] B. E Rittmann and P. L McCarty. Nitrification. In *Environmental biotechnology: principles and applications*, pages 470–506. McGraw-Hill, 2001. 14, 15, 16, 18
- [42] G. Rothkopf and R. Bartha. Structure-biodegradability correlations among xenobiotic industrial amines. *Journal of the American Oil Chemists' Society*, 61(5):977–980, May 1984. 9, 10

- [43] Bjorn Rusten, Bjørnar Eikebrokk, Yngve Ulgenes, and Eivind Lygren. Design and operations of the kaldnes moving bed biofilm reactors. *Aquacultural Engineering*, 34(3):322–331, May 2006. [22](#), [23](#)
- [44] Alexis Nadine Schafer, Ian Snape, and Steven Douglas Siciliano. Soil biogeochemical toxicity end points for sub-Antarctic islands contaminated with petroleum hydrocarbons. *Environmental Toxicology and Chemistry*, 26(5):890–897, 2007. [40](#), [53](#)
- [45] Renjie Shao and Aage Stangeland. *Amines used in CO<sub>2</sub> capture - Health and environmental impacts*. Bellona Foundation, 2009. [2](#), [3](#), [4](#), [6](#), [7](#), [8](#)
- [46] Julie Anita Skjæran. Biologisk nitrogenfjerning fra prosessvann fra et CO<sub>2</sub>-innfangingsanlegg. Project work, Trondheim, Norway, December 2009. [23](#), [24](#), [25](#), [45](#), [97](#)
- [47] Julie Anita Skjæran. Biologisk nitrogenfjerning fra prosessvann fra et CO<sub>2</sub>-innfangingsanlegg. Master thesis, Norwegian University of Science and Technology, Trondheim, 2010. [v](#), [21](#), [24](#), [25](#), [27](#), [35](#), [38](#), [45](#), [52](#), [68](#), [69](#), [97](#)
- [48] D. Qin M. Manning Z. Chen M. Marquis K.B. Averyt M.Tignor Solomon, S. and H.L. Miller (eds.). Ipc, 2007: Summary for policymakers. in: Climate change 2007: The physical science basis. contribution of working group i to the fourth assessment report of the intergovernmental panel on climate change. Scientific Report Fourth Assessment Report, Intergovernmental Panel on Climate Change, Cambridge University Press, Cambridge, United Kingdom and New York, NY, USA, 2007. [1](#), [2](#)
- [49] Susan Solomon, John S. Daniel, Todd J. Sanford, Daniel M. Murphy, Gian-Kasper Plattner, Reto Knutti, and Pierre Friedlingstein. Persistence of climate changes due to a range of greenhouse gases. *Proceedings of the National Academy of Sciences*, 107(43):18354–18359, October 2010. [2](#), [3](#)
- [50] Brian R. Strazisar, Richard R. Anderson, and Curt M. White. Degradation pathways for monoethanolamine in a CO<sub>2</sub> capture facility. *Energy & Fuels*, 17(4):1034–1039, July 2003. [5](#), [6](#), [55](#)
- [51] Isamu Suzuki, Usha Dular, and S. C Kwok. Ammonia or ammonium ion as substrate for oxidation by nitrosomonas europaea cells and extracts. *Journal of Bacteriology*, 120(1):556–558, 1974. [12](#)
- [52] Karin Veltman, Bhawna Singh, and Edgar G. Hertwich. Human and environmental impact assessment of postcombustion CO<sub>2</sub> capture focusing on emissions from Amine-Based scrubbing solvents to air. *Environmental Science & Technology*, 44(4):1496–1502, February 2010. [5](#)

- 
- [53] W. Verstraete and S. Philips. Nitrification-denitrification processes and technologies in new contexts. *Environmental Pollution*, 102(1, Supplement 1):717–726, 1998. [12](#), [17](#)
- [54] Christian Vogelsang. *Gel entrapment in open systems - nitrification in wastewater treatment*. Promotion, Norwegian University of Science and Technology, Trondheim, 1999. [32](#), [35](#), [46](#)
- [55] Wuncheng Wang. Time response of nitrobacter to toxicity. *Environment International*, 10(1):21–26, 1984. [67](#)
- [56] David M. Whitacre, Guibing Zhu, Yongzhen Peng, Baikun Li, Jianhua Guo, Qing Yang, and Shuying Wang. Biological removal of nitrogen from wastewater. In *Reviews of Environmental Contamination and Toxicology*, volume 192, pages 159–195. Springer New York, 2008. [11](#)
- [57] WG Zumft. Cell biology and molecular basis of denitrification. *Microbiology and Molecular Biology Reviews*, 61(4):533–616, December 1997. [10](#), [18](#), [19](#), [20](#)

# Appendices

## Appendix A

# Biofilm development - Nitrifying activity

The nitrifying activity during the biofilm development is given in Figure A.1.

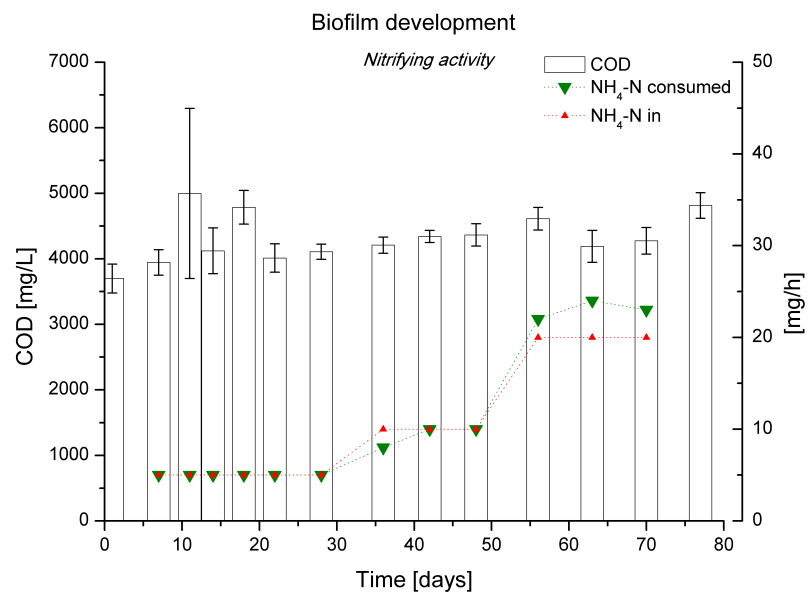


Figure A.1: Nitrifying activity during the biofilm development.

## Appendix B

# Reclaimer waste analysis - LC-MS

The positive and negative LC-MS scan of the reclaimer waste is shown in [Figure B.1](#).



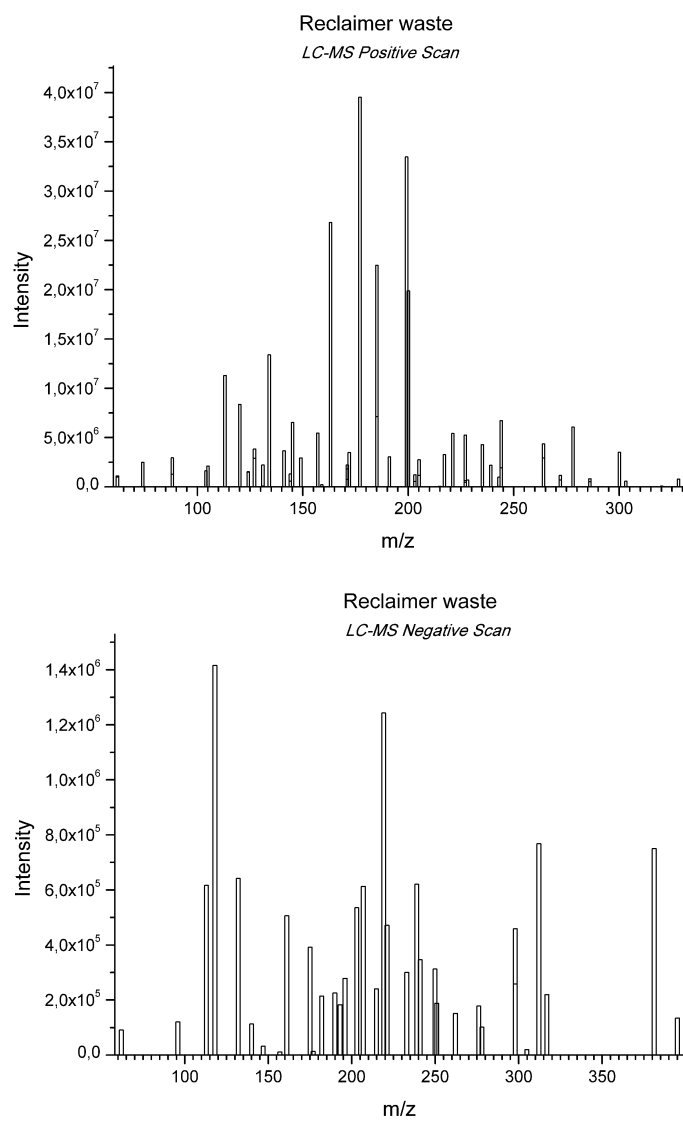


**Figure B.1:** LC-MS analyses of reclaimer waste, as intensity versus mass-charge ratio ( $m/z$ ). The positive LC-MS scan is shown in the upper panel and the negative LC-MS scan in the lower panel.

## Appendix C

# Acute toxicity test - Nitrifying culture

### *Reclaimer waste - Experiment 1:*

For calculating the value of  $EC_{50}$  a three-parameter logarithm model (Equation 2.4) was applied, yielding a corrected R-square of 0.994. The parameters for the model were  $a = 81.50$ ,  $b = 17.27$ , and  $c = -1.64$ , resulting in an  $EC_{50}$  of 8mmol/L for the reclaimer waste, illustrated in Figure C.1.

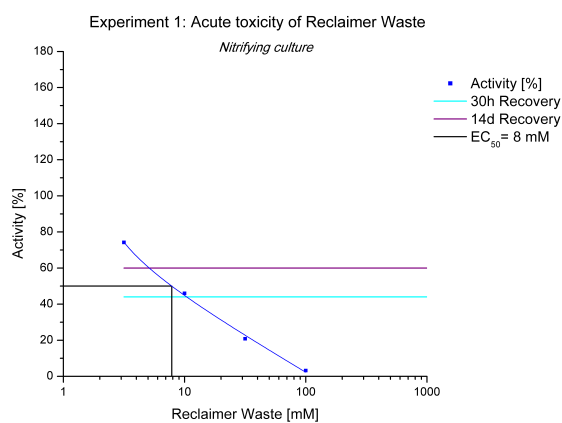


**Figure C.1:** Experiment 1: Effect concentration of the reclaimer waste on the nitrifying culture. The calculation of  $EC_{50}$  is based on a three-parameter logarithm model as described in the section 2.6.6, with a monitoring time range of 3 hours for each concentration.

### Reclaimer waste - Experiment 2:

For calculating the value of  $EC_{50}$  a logistic model (Equation 2.1) was applied, yielding a corrected R-square of 0.854. The parameters for the model were  $A1 = 112.3$ ,  $A2 = 12.58$ ,  $x_0 = 32.26$ , with  $p = 2.28$ . Based on these values an  $EC_{50}$  of 40mmol/L was calculated, illustrated in Figure C.2.

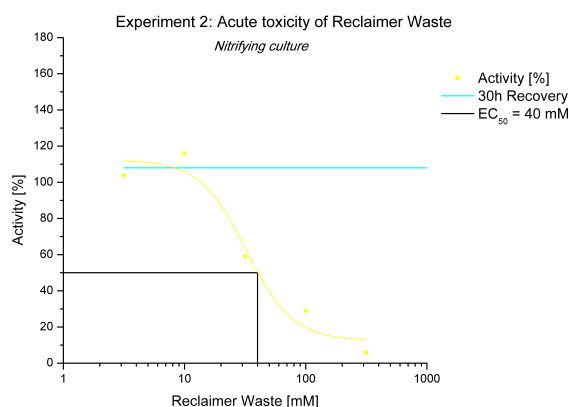


**Figure C.2:** Experiment 2: Effect concentration of the reclaimer waste on the nitrifying culture. The calculation of  $EC_{50}$  is based on a logistic model as described in section 2.4.5, with a monitoring time range of 3 hours for each concentration.

### MEA - Experiment 2:

For the acute toxicity test of MEA, as shown in Figure C.3, the logistic model (Equation 2.1) showed the best fit with a corrected R-square of 0.976. The parameters for the model were  $A1 = 140.06$ ,  $A2 = 23.99$ ,  $x_0 = 35.36$ , with  $p = 1.41$ . Based on these values an  $EC_{50}$  of 86mmol/L was calculated.

### Piperazine - Experiment 3:

The parameters for the logistic model, with a corrected R-square of 0.999, were  $A1 = 218.74$ ,  $A2 = 0.22$ ,  $x_0 = 2.79$ , with  $p = 0.96$ . Based on these values an  $EC_{50}$  of 10mmol/L was calculated for piperazine, illustrated in Figure C.4.

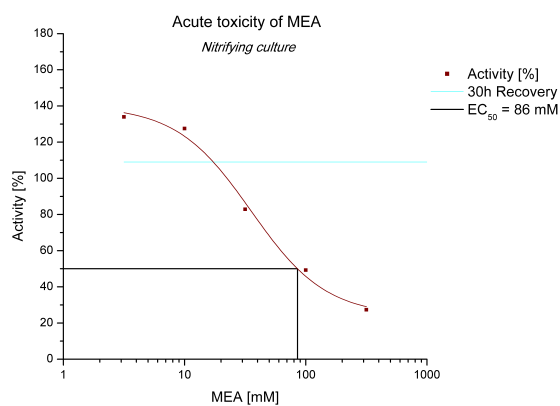


**Figure C.3:** Experiment 2: Effect concentration of MEA on the nitrifying culture. The calculation of  $EC_{50}$  is based on a logistic model as described in section 2.4.5, with a monitoring time range of 3 hours for each concentration.

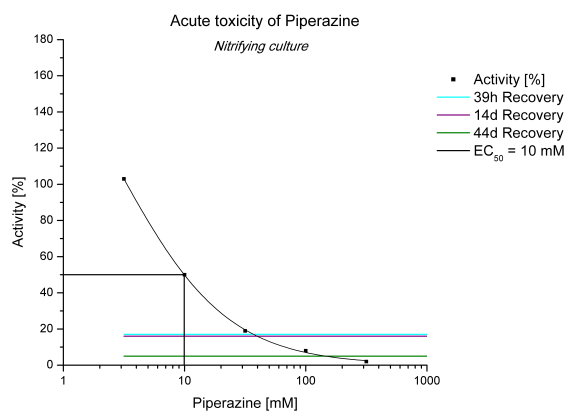


**Figure C.4:** Experiment 3: Effect concentration of piperazine on the nitrifying culture. The calculation of  $EC_{50}$  is based on a logistic model as described in section 2.4.5, with a monitoring time range of 3 hours for each concentration.

*AMP - Experiment 3:*

The parameters for the logistic model, with a corrected R-square of 1.000, were  $A1 = 144.46$ ,  $A2 = -2.7$ ,  $x_0 = 18.51$ , with  $p = 1.21$ . Based on this equation, an  $EC_{50}$  of 30mmol/L was calculated for AMP, illustrated in Figure C.5.

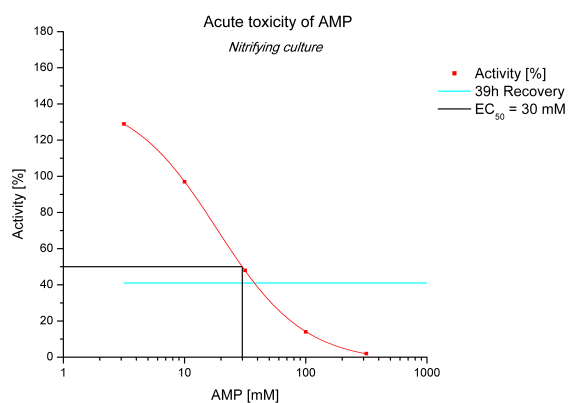


**Figure C.5:** Experiment 3: Effect concentration of AMP on the nitrifying culture. The calculation of  $EC_{50}$  is based on a logistic model as described in section 2.4.5, with a monitoring time range of 3 hours for each concentration.

*DEA - Experiment 3:*

The parameters for the logistic model, with a corrected R-square of 0.986, were  $A1 = 113.54$ ,  $A2 = 6.51$ ,  $x_0 = 14.47$ , with  $p = 2.08$ . Based on this equation, an  $EC_{50}$  of 18mmol/L was calculated for DEA, illustrated in Figure C.6.

*aMDEA - Experiment 3:*

The parameters for the model, with a corrected R-square of 0.991, were  $A1 = 155.11$ ,  $A2 = 5.71$ ,  $x_0 = 25.89$ , with  $p = 2.14$ . Based on this equation, an  $EC_{50}$  of 39mmol/L was calculated for aMDEA, illustrated in Figure C.7.

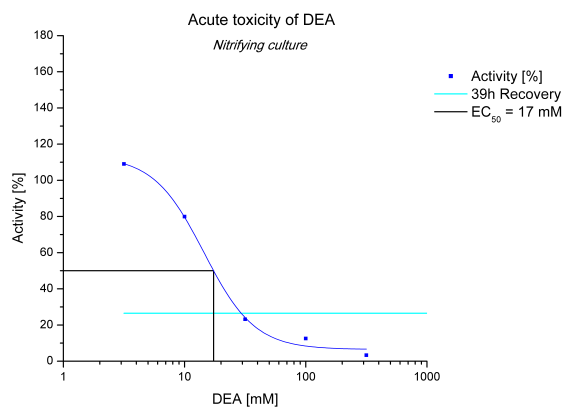


**Figure C.6:** Experiment 3: Effect concentration of DEA on the nitrifying culture. The calculation of EC<sub>50</sub> is based on a logistic model as described in section 2.4.5, with a monitoring time range of 3 hours for each concentration.

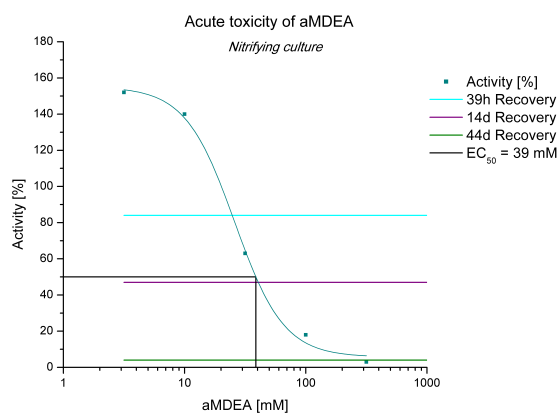


**Figure C.7:** Experiment 3: Effect concentration of aMDEA on the nitrifying culture. The calculation of EC<sub>50</sub> is based on a logistic model as described in section 2.4.5, with a monitoring time range of 3 hours for each concentration.

## Appendix D

# Pre-Denitrification

### D.1 Rawdata

The measured data of the denitrifying reactor is given in Figure D.1 and Figure D.2.

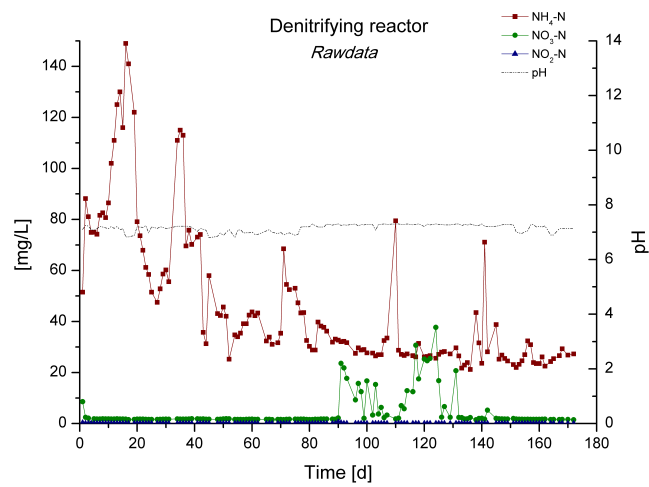


**Figure D.1:** Measured values of ammonium, nitrate, nitrite and pH of the denitrifying reactor.

The measured data of the nitrifying reactor is given in Figure D.3 and Figure D.4.

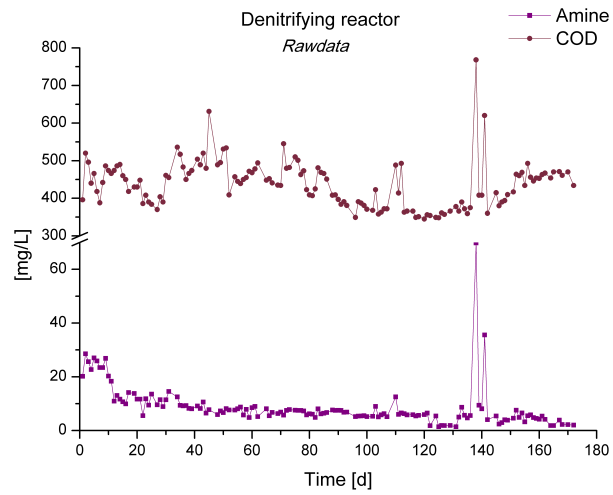


Figure D.2: Measured values of COD and amine (MEA) of the denitrifying reactor.

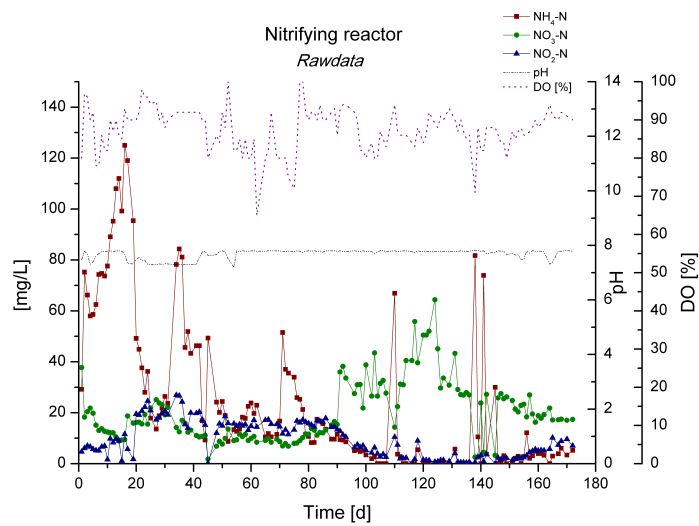


Figure D.3: Measured values of ammonium, nitrate, nitrite, pH and DO of the nitrifying reactor.



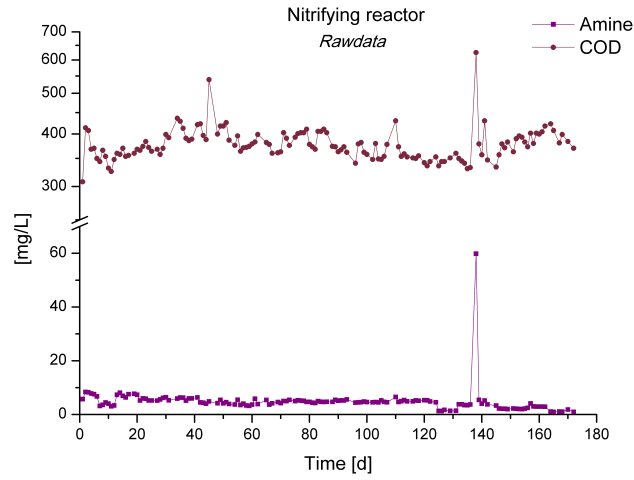


Figure D.4: Measured values of COD and amine (MEA) of the nitrifying reactor.

## D.2 Removal efficiency

The efficiency of the nitrogen removal in %, is calculated as given in Equation D.1. Table D.1 gives the respective average values in [mg/mL] for each regime.

$$\text{Efficiency [\%]} = \frac{\text{total nitrogen in} - \text{total nitrogen out}}{\text{total nitrogen in}} \times 100 \quad (\text{D.1})$$

Table D.1: Average total nitrogen removal efficiency of the pre-denitrification system.

Time	Regime	Total Nitrogen in	Total Nitrogen in - out	Efficiency [%]
d1-41	+50mg/L NH <sub>4</sub> -N	214.2	116.0	54
d42-76		163.4	112.8	69
d77-86	+35mg/L NO <sub>3</sub> -N	153.4	105.7	69
d88-90	+50mg/L NO <sub>3</sub> -N	168.8	124.4	74
d91-132	+75mg/L NO <sub>3</sub> -N	205.1	156.0	76
d133-151	+50mg/L NO <sub>3</sub> -N	191.8	130.1	68
d152-172		121.2	126.6	104

The values for calculating the MEA nitrogen removal efficiency are given in Table D.2.

**Table D.2:** Average MEA nitrogen removal efficiency of the pre-denitrification system.

Time	Regime	MEA Nitrogen in	MEA Nitrogen in - out	Efficiency [%]
d1-41	+50mg/L NH <sub>4</sub> -N	135.0	129.0	96
d42-76		141.8	137.4	97
d77-86	+35mg/L NO <sub>3</sub> -N	113.1	108.3	96
d88-90	+50mg/L NO <sub>3</sub> -N	119.6	114.7	96
d91-132	+75mg/L NO <sub>3</sub> -N	130.8	126.0	97
d133-151	+50mg/L NO <sub>3</sub> -N	138.8	133.7	96
d152-172		119.4	114.8	96

For calculating the COD removal efficiency, Equation D.2 was applied and the respective values are given in Table D.3.

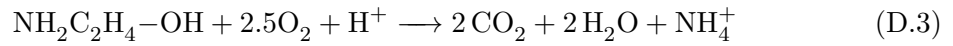
$$\text{Efficiency [\%]} = \frac{\text{COD in} - \text{COD out}}{\text{COD in}} \times 100 \quad (\text{D.2})$$

**Table D.3:** Average COD removal efficiency of the pre-denitrification system.

Time	Regime	COD in	COD in - out	Efficiency [%]
d1-41	+50mg/L NH <sub>4</sub> -N	1230	857	70
d42-76		1245	852	68
d77-86	+35mg/L NO <sub>3</sub> -N	1302	906	70
d88-90	+50mg/L NO <sub>3</sub> -N	1385	1002	72
d91-132	+75mg/L NO <sub>3</sub> -N	1324	966	73
d133-151	+50mg/L NO <sub>3</sub> -N	1300	923	71
d152-172		1365	970	71

### D.3 Calculation of COD

The amount of COD from MEA is based on Equation D.3 and calculated as given by Equation D.5. The molecular weight of MEA is 61.1g/mol and the average concentrations of MEA and COD in the medium were 9.4mmol/L and 1287mg/L, respectively.



$$\begin{aligned} \text{COD} &= \frac{2.5\text{molO}_2}{\text{molMEA}} \\ &= \frac{2.5 \times 32}{61.1} \\ &= 1.309\text{gO}_2/\text{gMEA} \end{aligned} \quad (\text{D.4})$$

$$\begin{aligned} \text{MEA} &= 9.4\text{mmol/L} = 574.3\text{mg/L} = 0.574\text{g/L} \\ &= 0.574\text{g/L} \times 1.309\text{gO}_2/\text{gMEA} \\ &= 0.752\text{gO}_2/\text{L} \\ &= 751.8\text{mgO}_2/\text{L} \end{aligned} \quad (\text{D.5})$$

$$\begin{aligned} 1287\text{mg/L} &= 100\%\text{COD} \\ 752\text{mg/LMEA} &= 58\%\text{COD} \end{aligned} \quad (\text{D.6})$$